

**SOCIAL INFLUENCES AMONG DRUG USERS AND
MEAN FIELD APPROXIMATION OF CELLULAR
AUTOMATA**

by

Afsaneh Bakhtiari

B.Sc., Khayyam Higher Education Center, 2000

A THESIS SUBMITTED IN PARTIAL FULFILLMENT
OF THE REQUIREMENTS FOR THE DEGREE OF
MASTER OF SCIENCE
in the
Department of Mathematics

© Afsaneh Bakhtiari 2009
SIMON FRASER UNIVERSITY
Fall 2009

All rights reserved. However, in accordance with the Copyright Act of Canada, this work may be reproduced, without authorization, under the conditions for Fair Dealing. Therefore, limited reproduction of this work for the purposes of private study, research, criticism, review, and news reporting is likely to be in accordance with the law, particularly if cited appropriately.

APPROVAL

Name: Afsaneh Bakhtiari
Degree: Master of Science
Title of Thesis: Social influences among drug users and mean field approximation of cellular automata

Examining Committee: Dr. Marni Mishna
Chair

Dr. Peter Borwein
Senior Supervisor

Dr. Alexander Rutherford
Supervisor

Dr. Nilima Nigam
SFU Examiner

Date Approved: December 7, 2009



SIMON FRASER UNIVERSITY
LIBRARY

Declaration of Partial Copyright Licence

The author, whose copyright is declared on the title page of this work, has granted to Simon Fraser University the right to lend this thesis, project or extended essay to users of the Simon Fraser University Library, and to make partial or single copies only for such users or in response to a request from the library of any other university, or other educational institution, on its own behalf or for one of its users.

The author has further granted permission to Simon Fraser University to keep or make a digital copy for use in its circulating collection (currently available to the public at the "Institutional Repository" link of the SFU Library website <www.lib.sfu.ca> at: <<http://ir.lib.sfu.ca/handle/1892/112>>) and, without changing the content, to translate the thesis/project or extended essays, if technically possible, to any medium or format for the purpose of preservation of the digital work.

The author has further agreed that permission for multiple copying of this work for scholarly purposes may be granted by either the author or the Dean of Graduate Studies.

It is understood that copying or publication of this work for financial gain shall not be allowed without the author's written permission.

Permission for public performance, or limited permission for private scholarly use, of any multimedia materials forming part of this work, may have been granted by the author. This information may be found on the separately catalogued multimedia material and in the signed Partial Copyright Licence.

While licensing SFU to permit the above uses, the author retains copyright in the thesis, project or extended essays, including the right to change the work for subsequent purposes, including editing and publishing the work in whole or in part, and licensing other parties, as the author may desire.

The original Partial Copyright Licence attesting to these terms, and signed by this author, may be found in the original bound copy of this work, retained in the Simon Fraser University Archive.

Simon Fraser University Library
Burnaby, BC, Canada

Abstract

Street-involved youth have a propensity for illicit drug use and trade. There are approximately one million street-involved youth in the United States and about 150,000 in Canada. The need for a proper intervention and follow-up strategy seems remarkably clear.

A stochastic cellular automata (CA) model of the influences among current and potential illegal drug users and traffickers is presented. Simulation and mean field analysis are used to study the model. The mean field approximation (MFA) and compartmental representation of the model are also studied. The phase plane of the mean field and possible bifurcations of the system are explored. MFA typically provides a good picture of a CA model near a bifurcation. The model allows us to compare the potential effectiveness of different types of responses to the drug epidemic. Both indirect and direct strategies are found effective on their own, but combined strategies proved to be most effective.

*To my dearest parents &
beloved husband, Hamid.*

Acknowledgments

I would like to thank my supervisors Dr. Alexander Rutherford and Dr. Peter Borwein for their teachings and guidance in this thesis. I would also like to thank Dr. Ralf Wittenberg, Dr. Bojan Ramadanovic, and Mr. Laurens Bakker for their useful comments and discussions. I am very thankful to the IRMACS Centre for the administrative and technical support that greatly facilitated this research. Finally, I am grateful to my dearest parents, Hossein and Safieh, and my beloved husband, Hamid, for their care and continual support throughout my graduate studies.

Contents

Approval	ii
Abstract	iii
Dedication	iv
Acknowledgments	v
Contents	vi
List of Tables	x
List of Figures	xi
1 Introduction	1
1.1 Vancouver Downtown East Side	3
1.2 Project Overview	4
2 Literature Review . . .	7
2.1 Compartmental Representations of Models	8
2.2 Compartmental Models	8
2.3 Cellular Automata Models	10

3	Bifurcation Theory of ...	16
3.1	Complex System	16
3.2	Fixed Points	17
3.2.1	Trajectory	17
3.3	Phase plane	17
3.3.1	Stability Language	17
3.4	Fixed Points and Linearization	18
3.4.1	Linearization	18
3.4.2	Linearized System	18
3.5	Classification of Linear System	20
3.6	Classification of Fixed Points	21
3.7	Bifurcation	24
3.7.1	Saddle-node Bifurcation	24
3.7.2	Transcritical Bifurcation	24
4	Cellular Automata & Mean ...	26
4.1	Cellular Automata	26
4.2	History	26
4.2.1	The Cell	27
4.3	One Dimensional Cellular Automata	28
4.4	Two Dimensional Cellular Automata	29
4.4.1	Boundary Condition	29
4.5	Dynamical Rule	30
4.5.1	Legal and Other Forms of Rules	30
4.5.2	Rule Codes	32

4.6	Mean Field Approximation	32
4.7	Mean Field Approximation	33
4.8	MFA for the Two State CA with Elementary Rules	34
4.8.1	Approximating CA by Differential Dynamical Systems	36
4.9	Three State 1-D CA and Outer-Totalistic Rules	37
4.10	Three State 1-D CA and Asymmetrical Rules	41
5	Cellular Automata Model For the DTES	46
5.1	Description of the 1-D CA Model	47
5.2	Social Influence	48
5.3	Transition	49
5.4	Rules for Updating Cells	50
5.5	Parameter and Initial Conditions	50
5.6	Simulation Result for the 1-D PCA Model	51
5.7	The 2-D Cellular Automata Model	53
5.8	Scenario and Simulation Results for 2D PCA Model	54
5.8.1	Phase Diagram for 2-D PCA Model	57
5.9	Simulation Result Comparison Between 1-D and 2-D CA Model	59
6	Mean Field Approximation	62
6.1	MFA for the 1-D PCA Model	62
6.2	Compartmental Representation of the Model	65
6.3	Constant Population Equations	66
6.4	Solutions to the System of Equations	70
6.5	Physical Solutions of the System	71
6.6	Analyzing the fixed points of the system	71

6.6.1	First Fixed Point	72
6.6.2	Second Fixed Point	72
6.6.3	Third Fixed Point	73
6.6.4	Phase Plane of the System	74
6.7	Bifurcations	75
6.7.1	Saddle Node Bifurcation when $\tilde{\alpha}_{em}$ Varies	75
6.7.2	Transcritical Bifurcation when δ Varies	75
6.7.3	When $\delta = \delta_0 = 0$	76
6.7.4	When b varies	76
6.8	Comparison Between Analytical Result and Simulation Result for the PCA model	78
6.9	Totalistic PCA	79
6.10	Generalized Mean Field Approximation for the PCA	81
6.10.1	Binomial Theorem	82
7	Conclusion and Discussion	87
7.1	Future work	89
A	Cellular Automata and Elementary Rules	90
	Bibliography	95

List of Tables

5.1	Definition of the State of the Cells	48
5.2	Rules for Updating the Cells	50
5.3	Parameter and Initial Value	51

List of Figures

1.1	prevalence of drug users world wide [42]	2
1.2	Vancouver Downtown east side [45]	3
2.1	The system dynamic model of the epidemic of problematic drug use in [5]. . .	9
2.2	Model structure in [14].	10
2.3	CA model based on compartmental framework in [22].	11
2.4	The state transition for the SIRS model in [20].	12
2.5	Typical spatial structured model of the two-patch spread of epidemics in [20].	13
3.1	Type and stability of all the different fixed points diagram. [26]	22
3.2	typical phase portrait for star node [26]	23
3.3	typical phase portrait for degenerate node. [26]	23
4.1	A generalized state transition [34].	28
4.2	One Dimensional Cellular Automata	28
4.3	Von Neumann neighborhood	29
4.4	3×3 Moore neighborhood	30
4.5	Two-Dimensional CA [28] <i>left</i> without edges pasted <i>right</i> with edges pasted .	31
4.6	The time evolution of the 1-D CA for rule R90 with random initial condition.	35

4.7	The time evolution of the 1-D CA for rule R90 , an initial state with of a single nonzero value.	35
4.8	Simulation result for the exact limiting density of 1s applying R90	37
4.9	The time evolution of the 1-D CA for Outer-totalistic rule 4.7, an initial state with of a single nonzero value.	38
4.10	The time evolution of the 1-D CA for outer-totalistic rule 4.7, with random initial condition.	39
4.11	Phase Portrait of the system of differential equations 4.11 and the stable fixed point $[q = 0, p = 0.618]$	40
4.12	Simulation result for the exact limiting densities of 1s & 2s using the Outer-totalistic 4.7.	41
4.13	Phase Portrait of the system of differential equations 4.18 and the stable fixed point $[q = 0.33, p = 0.33]$	43
4.14	The time evolution of the 1-D CA for the rule 4.12, an initial state with of a single nonzero value.	43
4.15	The time evolution of the 1-D CA for rule 4.12 with random initial condition.	44
4.16	Simulation result for the exact limiting densities of 1s & 2s using the rule 4.12.	44
5.1	Model structure	47
5.2	Phase diagram of the mean prevalence of dealers for the 2-D CA model . . .	52
5.3	Rotated phase diagram for the 1-D CA model	52
5.4	Contour plots for the phase diagram in 1-D CA model	53
5.5	The bifurcation curve for the 1-D PCA model	54
5.6	Mean prevalence of dealers in the 2-D CA model	55
5.7	Time evolution (month) of the 2-D CA, with no influences from dealer on susceptibles	56
5.8	Time evolution (month) of the 2-D CA model, with no influences from dealers on light users	56

5.9	Time evolution (month) of the 2-D CA model, when social influences on both susceptibles and drug users are included	57
5.10	Phase diagram of the mean prevalence of dealers for the 2-D CA model	58
5.11	Rotated phase diagram for the 2-D CA model	58
5.12	Contour plots for the phase diagram	59
5.13	The bifurcation curve for the 2-D PCA model	60
5.14	Phase diagram for the drug use epidemic, for 1-D CA with $N = 2$ neighbors (red curve) and 2-D CA with $N = 4$ neighbors (blue curve).	61
5.15	Time evolution (month) of the impact of social interaction on the spread of drug use, for the neighborhood sizes of $N = 2$ and $N = 4$	61
6.1	Model of the social influences Among Community of Drug Users	66
6.2	The Phase Portrait of the System	74
6.3	Saddle-node Bifurcation. Trivial fixed point is the only stable fixed point.	76
6.4	The fixed point $[x_2 = 0, y_2 = 0]$ is stable.	77
6.5	Bifurcation Curve	78
6.6	Simulation result and the mean field approximation (red dashed line) for 1-D PCA	79
6.7	Simulation result and the mean field approximation (red dashed line) for 2-D PCA	80
7.1	The effect of combined strategies	88
A.1	Space-time pattern of a few elementary legal rules for $k = 2, r = 1$, an initial state with of a single nonzero value.	91
A.2	Space-time pattern of a few totalistic rules for $k = 2, r = 1$, an initial state with of a single nonzero value.	92
A.3	Space-time pattern of a few elementary legal rules for $k = 2, r = 1$, with random initial condition.	93

A.4 Space-time pattern of a few totalistic rules for $k = 2$, $r = 2$, with random initial condition.	94
---	----

Chapter 1

Introduction

Many of the social issues of the 21st century are being studied through collaborations between social and mathematical scientists [36]. Interdisciplinary research that targets these issues can have a profound impact on the quality of life for everyone involved by reducing crime [15], reducing harm and addiction [14], and enhancing safety and security [50], all while maintaining privacy and improving health and welfare [49].

In the past, much of the quantitative research in criminology, health science, and urban dynamics focused on applying statistical techniques to determine relationships. Although these studies provide insight into social issues, they are limited in their ability to model complicated dynamics, because they are unable to capture the qualitative dynamics and the effect of relations in the system. This restricts somewhat the applicability to policy analysis.

Mathematical modeling is a tool that can be used for answering many questions brought up by various disciplines. It provides a better understanding of complicated dynamics that arise from the overlap between social issues and the dynamic nature of social interactions. Mathematical models can take many forms, including but not limited to dynamical system models, statistical models and differential equations models. Different types of models can be combined to determine the expected response of any social system to social policies.

We have developed a mathematical model to understand the impact of social influence

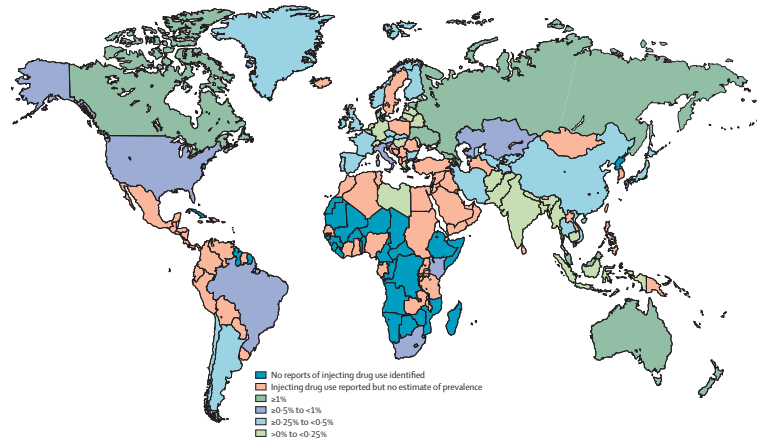


Figure 1.1: prevalence of drug users world wide [42]

among drug user and traffickers within a community. We seek to answer questions such as: who are the drug users and traffickers; why do they persist and what are the possibilities for more effective action to control drug use and drug trade. Can mathematical modeling help us understand the impact of specific types of intervention on drug trafficking organization?

In 1993, UNICEF estimated that over 100 million youth lived or worked on the street world wide. This includes 40 million youth in Latin America, 25 to 30 million in Asia, 20 million in Europe, and over 10 million in Africa [3]. The United Nations Office on Drugs and Crime (UNODC) reported in 2004 that approximately three percent of the world population, 185 million people, abused drugs during the year 2003 [37]. In Canada illicit drug use increased substantially in just one year across the country between 1993 and 1994 [38]. Currently there are approximately 150,000 street-involved youth living in Canada, and 1 million such youth in the United States ([10, 2]), who are involved in the illicit drug use and trade [4].

Illicit drugs cause harm indirectly as well as directly. The indirect negative effects of drug use are drug related criminality, loss of productivity, infectious diseases (HIV/AIDS and hepatitis) and mortality. In fact, indirect negative effects of drug use are amplified disproportionately and far outweigh direct negative effects [38]. The most direct harm occur in high-risk populations such as injecting drug users, street youth, the inner-city poor, and aboriginals. There have been a number of studies to explore the risk of a future rise of HIV prevalence and preventing HIV infection among injection drug users. [40, 41, 43]



Figure 1.2: Vancouver Downtown east side [45]

1.1 Vancouver Downtown East Side

The Downtown east side of Vancouver is the poorest postal code in Canada [14]. It has the highest HIV infection rate in North America, affecting 30 per cent of the local population, most of whom are women. The homeless population continues to grow, with an estimated 2000 homeless people, a population that has doubled since 2002 [45]. Cohort studies undertaken in Vancouver Downtown east side showed that street-involved youth are frequently involved in illicit drug use and trade. In addition, they often poor and homeless [4, 21].

The need for a proper intervention and a follow-up strategy as well as evaluating the results of such strategy seem remarkably clear. However, a good implementation of a strategy requires an understanding of both the drug problem phenomenon and the effect of the social interactions in the communities. Mathematical models help us to understand the problem and implement an intervention.

The major goal of this thesis is to understand the complicated dynamics of the drug trade and to study the social interactions that are responsible for the drug use spread within drug users community [14]. We construct a mathematical model to study the impact of social influence among drug users. We use cellular automata (CA) model to study the interactions among individuals in drug users community and perform mean field approximation for the CA model to explore some properties of the CA model.

We consider three types of individuals in the CA model and describe them as follow:

- **Susceptible** : Individuals who have a potential to become a drug user by a contact with dealers. Susceptible can stay susceptible or make a transition and become drug users.
- **Light Users**: Individuals who have already initiated some form of drug use. Light users are at risk of becoming dealers through contacts with a pusher operating in the black market of drugs. A light user can either stop using drugs or start a drug dealing career.
- **Drug Traffickers (Dealers)**: Individuals who are involved in the importation, manufacturing, distribution, and/or sale of illicit drugs [39]. Dealers are assumed to constantly employ drug users, who are in need to generate income to pay for their own drug use. Drug dependency is the main motivation for users to participate in the illicit drug trade and become drug dealers [4, 44].

1.2 Project Overview

We present a mathematical model of the social influence within the drug users community. More specifically, we study the impact of social interaction on the spread of drug use in the community of drug users. This model is motivated by *Werb et al* [4] and *Carla Rossi's* [5] models (see Chapter 2 for more details). The model shows how individuals can become drug users and start a drug trading career of their own. Our model is a Stochastic cellular automata (CA) model which can be used to point out the importance of social influences in spreading drug use behavior.

The following is an overview for the main chapters of this project:

In this project, we first provide some background information on the bifurcation theory of differential dynamical systems and a review on the basic concepts of Cellular Automata (see Chapters 3 and 4).

In Chapter 5, we develop the stochastic cellular automata (CA) model to study the effect of the social interactions within a drug users community. Cellular automata (CA) can be

used to study the effects of social interactions at the individual level, on the evolution of an epidemic at the population level [28]. Due to their flexibility, cellular automata can serve as virtual laboratories for testing a numerous number of social scenarios. We choose a Mover-Stayer-type model as the basic framework, since it has been used previously to represent the spread of drug use as an epidemic [5, 14]. To address individual variation in behavior we study the phase diagram of the (CA) model using both simulation and mean field approximation.

Mean field approximation (MFA) for the CA model is the main focus of Chapter 6. We perform MFA (described in [24]) with different neighborhood sizes of $N = 2$, and $N = 4$. MFA provides an estimation on the density and other properties of the CA model. As the model is general, we expand the MFA results for $N = 2$, and $N = 4$ to suit the case when $N = n$. Thus, the mean field approximation for the CA model with total number of $N = n$ neighbors is also performed (see Section 6.10). Interestingly, the approximation up to second degree in densities reproduces the scaled constant population equations which correspond to the compartmental model.

The compartmental representation of the model divides the population in to three compartments: susceptibles, light users and dealers. Once the population has been split into relevant compartments, we describe the dynamics in terms of system of differential equations (see Section 6.3). The mean field analysis of the system of differential equations, has unique stable points and unstable equilibrium solutions. However, the interesting bifurcations happen as a result of parameter variations (“what if ” analysis). The compartmental model usually provides a good approximation of the CA model near the bifurcation, thus the appearance of the phase portrait and the bifurcation curve are as expected. The bulk of Section 6.6 is mainly about changes in social influences affecting the stability of the fixed points and possible bifurcations.

In Section 6.8, MFA is used as a point of comparison for the CA model. The comparison is between the analytical results from MFA and simulation results for the CA model. The comparison shows how accurate the MFA estimates the CA model behavior near the bifurcation.

The model described above, allows us to compare the potential effectiveness of different types of responses to the drug epidemic. In this model we mostly refer to the “Primary Prevention Intervention” as advertising, e.g. health promotions towards susceptible. A “Secondary Prevention Intervention” includes law enforcement towards drug users/dealers, e.g. police involvement. We find that both prevention interventions are effective on their own, but combined interventions proved to be most effective, when taking into account the sensitivity analysis of the parameters in the model.

Next chapter is a brief review on literatures that use ODE’s (compartmental) and CA models to target the complex social system issues.

Chapter 2

Literature Review of Modeling Complex Systems

In the past, compartmental models have been used in the area of the spread of “drug use” and associated diseases. For example, compartmental models were used as a tool for understanding the drug problem, designing a proper intervention, evaluating the result of the intervention and making social policies [5, 14]. The majority of approaches have used ordinary and partial differential equations (ODE’s and PDE’s) and probabilistic methods to seek answers to a number of questions concerning drug use.

Recently, cellular automata (CA) models are mostly used to model the complex social systems in order to target the social issues such as homelessness, crime and drug use problem [15, 14]. CA is a mathematical method which can effectively be used to model the social interaction among individuals in a community. CA models allows us to study the impact of social interaction among individuals in the transmission of infectious disease, drug use and drug trade behavior.

We examine both theses approaches by developing a Cellular Automata (CA) model which is based on compartmental framework. In addition, we perform the mean field approximation followed by the bifurcation analysis for the CA model for drug use problem in DTES Vancouver.

2.1 Compartmental Representations of Models

In mathematical modeling compartmental models represent a powerful and well-established mathematical tool. Compartmental models generally help to study the spread of diseases in a population. As Rossi stated in [5] “ There is evidence that drug use spreads as an infectious disease, i.e. the rate of new cases depends bilinearly on the number of existing cases and on the number of susceptibles” [5]. So the spread of drug use can be treated as an infectious disease in mathematical modeling perspective.

Compartmental models provide a framework in which numbers of people in different compartments, the relationships between compartments and the spread of the disease in the population can be expressed in differential equations [5].

Two main classes of mathematical models commonly used to describe the spread of diseases are deterministic models and stochastic models. They are described as follow:

- **Deterministic Models:** Changes in the size of each compartments over time is expressed in terms of systems of differential or difference equations.
- **Stochastic Models:** Changes in the size of each compartments over time is expressed in terms of a stochastic equation which is a differential equation in which one or more of the terms is a stochastic process.

2.2 Compartmental Models

It is common practice in mathematical modeling to use compartmental models, as Carla Rossi uses such a model in [5] to understand the epidemic of problematic drug use in Italy. She performs scenario analyses, for the heroin (by injection) epidemic which has been taken place in the past 20 years (beginning around 1980, with the epidemic peak in 1990 - 91). She designs a mathematical model that treats the spread of problematic drug use as an infectious disease.

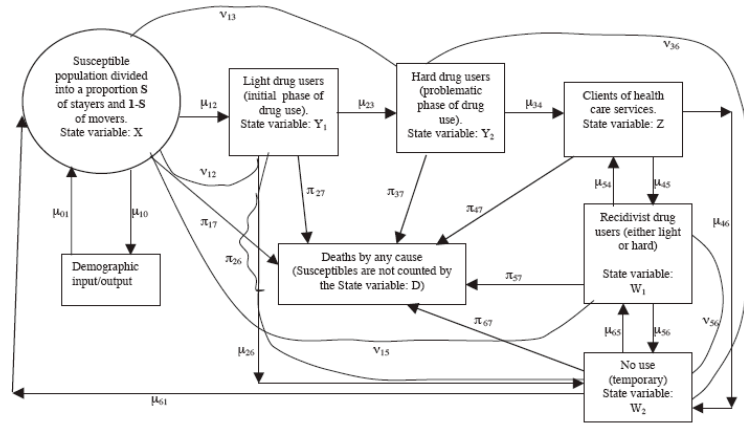


Figure 2.1: The system dynamic model of the epidemic of problematic drug use in [5].

Carla Rossi develops a compartmental Mover-Stayer model for the epidemic of problematic drug use (see Fig 2.1). She considers the susceptible population as subdivided into two main groups: the group of stayers, that is, the group of individuals who are considered not at risk of infection, and the group of movers (divided into sub-groups with different risk behavior) who are at risk of infection. Due to the interactions between infectious individuals and the susceptibles, some individuals may pass to the drug user compartments and begin a drug user career. Rossi uses the mean field analysis which corresponds to the compartmental model to analyzes the epidemic and evaluates the impact of interventions towards susceptibles and drug users. She shows how primary prevention intervention is the most effective strategy to control drug use in Italy .

A cohort study by Werb *et al* in [4] conduct an investigation of the factors associated with drug use and drug trade involvement among street-based youth in Vancouver, Canada. The method used to examine those factors among the participants is logistics regression analysis. They find that over half of the street-involved youth participating in the study reported involvement in illicit drug trade. Among individuals who reported drug dealing, the vast majority reported doing so in order to pay for their personal drug use. The authors observe a strong association between homelessness and drug dealing which points out the fact that street-involved youth who deal drugs are often marked by extreme poverty and drug dependency [4].

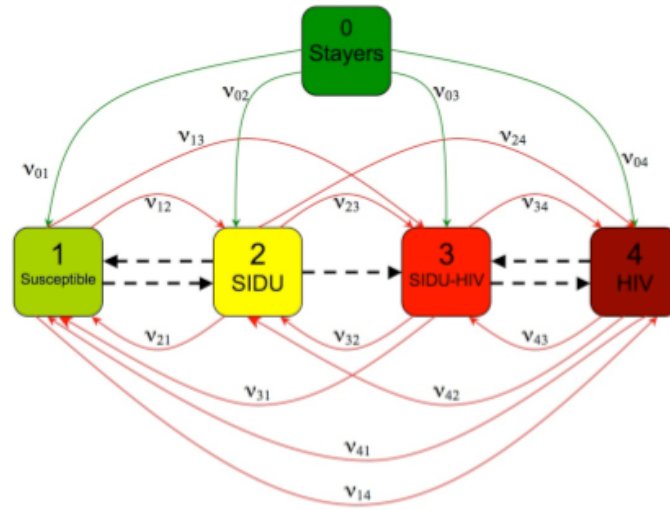


Figure 2.2: Model structure in [14].

2.3 Cellular Automata Models

More recently, there has been an increased interest in modeling interactions between individuals located on networks with a mixture of local and global interactions using CA models. The following is a brief description of the literature using CA models to target the complex social system issues.

Dabbaghian *et al* in [14] construct a cellular automaton model to study the dynamics of the HIV epidemic in an IDU community, in the presence of social influences (see Fig 2.2). The authors consider two types of influences in the model. An individual can influence neighbors by discouraging (α) or encouraging (β) them to share needles. Each cell has a social counter link to it which records and accumulates influences from neighboring cells at each time step. Cells are updated according to the rules which concern the cell's life spans and the values of the counters.

The authors investigate the epidemic behaviour of the model without social influences, with 10% initial HIV prevalence, and α and β at 0, interestingly HIV prevalence rises sharply and crashes within a short period of time. The epidemic becomes self-sustaining once social influence is included in the model. But the epidemic is not self-sustaining always where

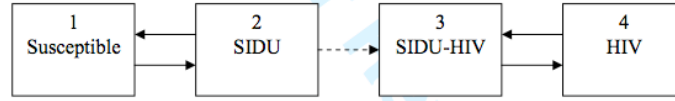


Figure 2.3: CA model based on compartmental framework in [22].

social influence is in the model. The authors conclude that a threshold value exists at which the epidemic crashes. Thus complex social context plays a crucial role in determining HIV risk behaviour among IDU. The authors validate the model for the Downtown Eastside (DTES) HIV epidemic in Vancouver which is the poorest neighborhood in Canada.

Eslahchi *et al* in [22] examine the concurrent spread of hard drug consumption and criminal behavior using cellular automata. The authors describe a stochastic model based on the compartmental framework (see Fig 2.3) for the spread of HIV infection among IDU's within a community. The model is constructed in the presence of influences that promote, α , or discourage, β , sharing used needles.

The model employs a stochastic (a discrete Markov chain) approach by defining a transition matrix to represent the effect of social relationships among IDUs.

$$A = \begin{pmatrix} 1 - \beta & \beta & 0 & 0 \\ \alpha(1 - p) & (1 - \alpha)(1 - p) & p & 0 \\ 0 & 0 & 1 - \alpha & \alpha \\ 0 & 0 & \beta & 1 - \beta \end{pmatrix} \quad (2.1)$$

As the authors point out, it can be seen from the transition matrix (2.1) that the class of transient states is $T = 1, 2$ and the class of recurrent states is $R = 3, 4$ (see Fig 2.3). Eslahchi *et al.* also define $f^k(\alpha, \beta)$ as being the probability that an individual moving from state 2 to state 3 after k units of times. and they prove that for all α and β the probability $f^k(\alpha, \beta)$ tends to a fixed value.

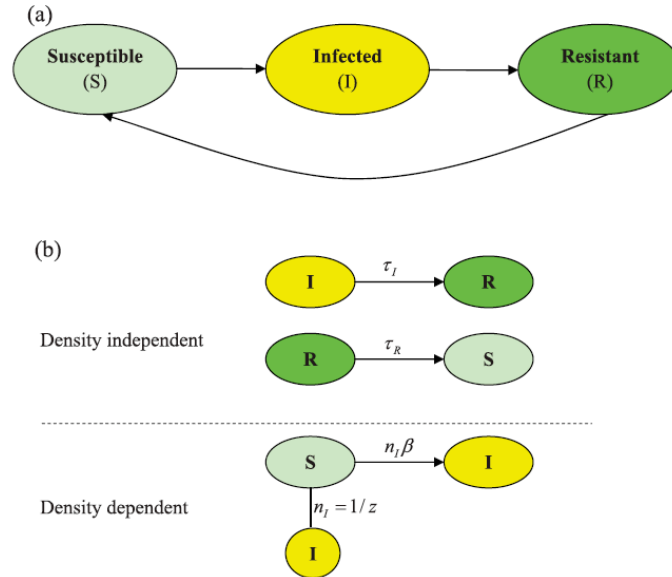


Figure 2.4: The state transition for the SIRS model in [20].

Eslahchi *et al.* [22], had to rely on simulations to represent the proportion of the population that gets infected with HIV at each time step. They show for any fixed β , $f^{1000}(\alpha, \beta)$ is a decreasing function of α . This means that increases in the positive social effects, α , decreases the number of individuals becoming HIV positive. However, it tends to a certain threshold. In other words, if $\beta > 0$ then for every p (probability of HIV transmission) a certain number of individuals become HIV positive.

Another CA model is introduced by van Ballegooijen and Boerlijst in [19] (vBB). They consider three types of spatial patterns in a spatial susceptible–infected–resistant (SIR) model for disease dynamics using a cellular automata model. Liu *et al* in [20] take the framework proposed by vBB as starting point and use a spatial SIRS model with N individuals categorized, according to their infection status (see Fig 2.4). They develop a model which can investigate what enables a disease to persist while others become extinct. Liu *et al* also use the model to understand the change of such effect in combination with individuals mobility within multi patches.

In Fig 2.4, each arrow show a possible transition between two states in Liu *et al.*'s model.

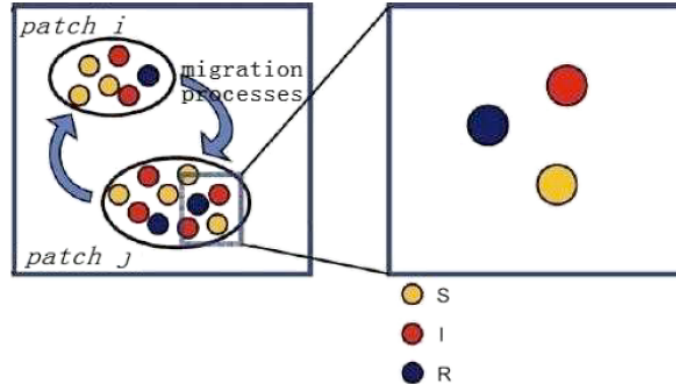


Figure 2.5: Typical spatial structured model of the two-patch spread of epidemics in [20].

Transition probabilities are shown for transitions between different states. The third transition shown is from a susceptible site that has one infected neighbor (local infected occupied $n_I = \frac{1}{z}$; smaller circle, z is the number of the cells neighborhood) to an infected cell.

They perform mean field approximation which corresponds to the SIRS model (2.2), measure the phase transition between the global extinction and the persistence of the epidemic and the effect of individuals movements on the epidemic.

$$\begin{aligned} \frac{dS}{dt} &= -\beta SI + \tau_R R, \\ \frac{dI}{dt} &= -\beta SI + \tau_I I, \end{aligned} \quad (2.2)$$

They also analyze the relationship of infection rate and infection period for the phase transition within a single patch and multiple patches, using simulation. Liu *et al*, in [20] show that the infection rate is limited by an upper bound.

In Fig 2.5, the two patches i and j are connected by migration processes. Each patch contains a population of individuals who are characterized with respect to their stage of the disease. Liu *et al*, in [20] find that higher migration can promote the persistence of the spread of epidemics and so they observe a phase transition occurs from the extinction domain to the persistence domain.

Another cellular automata model applied to infection diseases is that of Benyoussef *et al.* [21]. The authors model the immune cells in the blood by a two-dimensional CA. Then, consider the group of white blood cells (Lymphocytes T), which have the protein marker CD_+^4 . The model contains both the non-infected (T) and infected (T_i) CD_+^4 cells, and the population of plasma virus (V) is included.

The obtained results show the existence of four different behaviors in the plane of death rate of virus-death rate of infected T cell. These regions meet at a critical point, where the virus density and the infected T cell density remain invariant during the evolution of disease. They also introduce two kinds of treatments in order to study their effects on the evolution of HIV infection. Other interesting CA models can be also found in [15, 16, 17].

Due to the complexities that arise in analyzing dynamical systems (such as diseases epidemics) with multiple interacting compartments, the study of infection diseases has mainly been done by simulation.

Closely related to ODE and PDE models are those using mean field approximation (MFA) for the CA models. The MFA ignores space dependence and neglects local correlations in a CA and estimates the density and other properties of the CA (see Chapter 4).

Kleczkowski *et al* in [32] proposed an epidemic model using MFA examining the spread of childhood measles. Noting that MFA neglect localized correlations, it appears meaningless to compare them with CA models because CA models focus on the contact between individuals. However, the authors in [32] mentions that MFA and CA models converge when the MFA mixing parameter tends to infinity that is, when the world contains more disorder than correlation. This convergence is analogous to the situation where differential equation and CA models converge when population size tends to infinity [34]. As the size of CA gets bigger the local effects matters less and less to the overall behavior of the CA. So the average behavior of the CA becomes dominant.

Many groups [29, 30, 31] have used MFA as a point of comparison with the CA models they develop particularly models investigating the effect of host (infected cell) motion.

As can be seen, the increase of cellular automata in modeling the complex social systems is growing. This is because scientists and policy makers are gaining awareness of the advantages of studying the local and global interactions within communities. However, literature in which cellular automata used to investigate drug trafficking is rarer due to the complexity of the system. In such cases, mathematicians often rely on both data simulations and analytical methods to obtain much more detail about the behavior of the system. We perform MFA for the CA model and various simulations. We then use mean field approximation results as a point of comparison for the behavior of the CA model.

In the next chapter, we review the knowledge background for the bifurcation theory of differential dynamical systems.

Chapter 3

Bifurcation Theory of Differential Dynamical System

Before delving into the details of the model in the next couple of chapters, it is worth to review the concepts that are used to analyze the model. The theory in this chapter is developed systematically for the nonlinear systems starting with definition of a fixed point, linearization technique, classification of fixed points and their geometric intuitions and bifurcations. The background given on bifurcation theory of differential dynamical system, helps to better understand *analytical results* and visualize the possible outcome of a dynamical system.

The material explained in this chapter is based on the book “Nonlinear Dynamics and Chaos” by *Steven H. Strogatz*.

3.1 Complex System

A complex system is any dynamical system that consist of more than a few-typically nonlinearly- interacting parts [24]. Perhaps the most familiar example of a complex system is the human brain, which, consisting of something on the order of 10^{10} neurons with $10^3 - 10^4$ connections per neuron. The human brain is arguably the most complex system on this planet.

3.2 Fixed Points

In terms of the differential equation, $\dot{x} = f(x)$, x^* represents the fixed point and satisfies $f(x^*) = 0$. Fixed points are sometimes called equilibrium solutions or steady states since if $x = x^*$ initially, then $x(t) = x^*$ for all t .

3.2.1 Trajectory

As times goes on, a phase point at x_0 moves along x -axis according to some function $x(t)$ which is called the *trajectory* based at x_0 . It represents the solution of differential equation starting from the initial condition x_0 .

3.3 Phase plane

The general form of a vector field on the phase plane is

$$\begin{aligned}\dot{x} &= f(x, y) \\ \dot{y} &= g(x, y)\end{aligned}$$

where f and g are given functions. This system can be written more generally in vector notation as

$$(\dot{x}, \dot{y}) = (f(x, y), g(x, y)),$$

Here (x, y) represents a point in the phase plan, and (\dot{x}, \dot{y}) is the velocity vector at that point. By following along the vector field, a phase point traces out a solution $(x(t), y(t))$, corresponding to a trajectory winding through the phase plane. Furthermore, the entire phase plane is filled with trajectories, since each can play the role of an initial condition. *Phase portrait* shows all the qualitatively different trajectories of the system.

3.3.1 Stability Language

We say $\mathbf{x}^* = \mathbf{0}$ is an attracting fixed point, if all the trajectories that start near \mathbf{x}^* approach it as $t \rightarrow \infty$. If x^* attracts all trajectories in the phase plane, it is called *globally attracting*.

We say that a fixed point x^* is *Liapunov stable* if all trajectories that start sufficiently close to x^* remain close to it for all times. So if the fixed point is both Liapunov stable and attracting, we will call it *stable*. Finally x^* is *unstable* if it is neither attracting nor Liapunov stable.

3.4 Fixed Points and Linearization

Once the fixed points are found, one would like to have a quantitative measure of quantities, such as the rate of decay or growth to a stable or unstable fixed point. This sort of information can be obtained by *linearizing* about the fixed points. The hope is that we can approximate the phase portrait near the fixed points by that of a corresponding linear system.

3.4.1 Linearization

In this section we focus on the *linearization* technique for two-dimensional systems. The hope is that we can approximate the phase portrait near the fixed point.

3.4.2 Linearized System

Consider the system

$$\begin{aligned}\dot{x} &= f(x, y) \\ \dot{y} &= g(x, y)\end{aligned}$$

and suppose that (x^*, y^*) is a fixed point, i.e.,

$$f(x^*, y^*) = 0, \quad g(x^*, y^*) = 0$$

Let

$$u = x - x^*, \quad v = y - y^*$$

denote the components of a small disturbance from the fixed point. To see whether the disturbance grows or decays, we need to derive differential equation for u and v . Let us do

the u -equation first:

$$\begin{aligned}
 \dot{u} &= \dot{x} && \text{(since } x^* \text{ is a constant)} \\
 &= f(x^* + u, y^* + v) && \text{(by substitution)} \\
 &= f(x^*, y^*) + u \frac{\partial f}{\partial x} + v \frac{\partial f}{\partial y} + \mathcal{O}(u^2, v^2, uv) && \text{(Taylor series expansion)} \\
 &= u \frac{\partial f}{\partial x} + v \frac{\partial f}{\partial y} + \mathcal{O}(u^2, v^2, uv) && \text{(since } f(x^*, y^*) = 0 \text{ is a constant)}
 \end{aligned}$$

To simplify the notation, we have written $\frac{\partial f}{\partial x}$ and $\frac{\partial f}{\partial y}$, but remember that these partial derivatives are to be evaluated at the fixed points (x^*, y^*) ; thus they are numbers, not functions. Also the shorthand notation $\mathcal{O}(u^2, v^2, uv)$ is a remainder term, denoting the difference between the Taylor polynomial of degree n and the original function. The remainder term $\mathcal{O}(u^2, v^2, uv)$ depends on (x, y) and is small if (x, y) is close enough to (x^*, y^*) under the hypothesis that $f(x, y)$ is a function which is 1 time continuously differentiable on the closed interval $[(x^*, y^*), (x, y)]$ and 2 times differentiable on the open interval $((x^*, y^*), (x, y))$.

Similarly we find:

$$\dot{v} = u \frac{\partial g}{\partial x} + v \frac{\partial g}{\partial y} + \mathcal{O}(u^2, v^2, uv)$$

Hence the disturbance (u, v) evolves according to

$$\begin{pmatrix} \dot{u} \\ \dot{v} \end{pmatrix} = \begin{pmatrix} \frac{\partial f}{\partial x} & \frac{\partial f}{\partial y} \\ \frac{\partial g}{\partial x} & \frac{\partial g}{\partial y} \end{pmatrix} \cdot \begin{pmatrix} u \\ v \end{pmatrix} + \text{quadratic terms}, \quad (3.1)$$

The matrix

$$\begin{pmatrix} \frac{\partial f}{\partial x} & \frac{\partial f}{\partial y} \\ \frac{\partial g}{\partial x} & \frac{\partial g}{\partial y} \end{pmatrix}_{(x^*, y^*)}$$

is called the *Jacobian matrix* at the fixed point (x^*, y^*) . It is the multivariable analog of the derivatives $f'(x^*)$. Now since the quadratic terms in (3.1) are small, it's tempting to

neglect them altogether. if we do that, we obtain the *linearized system*

$$\begin{pmatrix} \dot{u} \\ \dot{v} \end{pmatrix} = \begin{pmatrix} \frac{\partial f}{\partial x} & \frac{\partial f}{\partial y} \\ \frac{\partial g}{\partial x} & \frac{\partial g}{\partial y} \end{pmatrix} \cdot \begin{pmatrix} u \\ v \end{pmatrix} \quad (3.2)$$

whose dynamics can be analyzed by the methods explain below:

3.5 Classification of Linear System

We study general case of an arbitrary 2×2 matrix, with the aim of classifying all the possible phase portraits that can occur. For the general case, we would like to find the trajectories starting on one of the coordinate axes and exhibit simple exponential growth or decay along it . That is, we seek trajectories of the form

$$\mathbf{x}(\mathbf{t}) = e^{\lambda \mathbf{t}} \mathbf{v}, \quad (3.3)$$

where \mathbf{v} is some fixed vector to be determined, and λ is a growth rate, also to be determined. If such solutions exist, they correspond to exponential motion along the line spanned by the vector \mathbf{v} .

To find the condition on \mathbf{v} and λ , we substitute $\mathbf{x}(\mathbf{t}) = e^{\lambda \mathbf{t}} \mathbf{v}$ in to $\dot{\mathbf{x}} = A\mathbf{x}$, and obtain $\lambda e^{\lambda \mathbf{t}} \mathbf{v} = e^{\lambda \mathbf{t}} A\mathbf{v}$. Canceling the nonzero scalar factor $e^{\lambda \mathbf{t}}$ yields:

$$A\mathbf{v} = \lambda \mathbf{v}, \quad (3.4)$$

which says that the desired straight line solutions exist if \mathbf{v} is an *eigenvector* of A with corresponding *eigenvalue* λ . In this case we call the solution (3.3) an *eigensolution*. In general the eigenvalues of a matrix A are given by the *characteristic equation* $\det(A - \lambda \mathbf{I} = 0)$, where \mathbf{I} is the identity matrix. For a 2×2 matrix

$$A = \begin{pmatrix} a & b \\ c & d \end{pmatrix},$$

the characteristic equation becomes,

$$\det \begin{pmatrix} a - \lambda & b \\ c & d - \lambda \end{pmatrix}. \text{ Expanding the determinant yields:}$$

$$\lambda^2 - \tau\lambda + \Delta = 0 \quad (3.5)$$

where

$$\begin{aligned}\tau &= \text{trac}(A) = a + d, \\ \Delta &= \det(A) = ad - bc.\end{aligned}$$

Then,

$$\lambda_1 = \frac{\tau + \sqrt{\tau^2 - 4\Delta}}{2} \quad \lambda_2 = \frac{\tau - \sqrt{\tau^2 - 4\Delta}}{2}$$

are the solution of the quadratic equation (3.5). In other words, the eigenvalues depend only on the trace and determinant of the matrix A in Section 3.5.

The generic situation is for the eigenvalues to be distinct : $\lambda_1 \neq \lambda_2$. In this case, a theorem of linear algebra states that the corresponding eigenvectors v_1 and v_2 are linearly independent, and hence span the entire plane. In particular, any initial condition x_0 can be written as a linear combination of eigenvectors, say $x_0 = c_1 \mathbf{v}_1 + c_2 \mathbf{v}_2$.

This observation allows us to write the general solution for $\mathbf{x}(t)$. It is simply

$$\mathbf{x}(t) = c_1 e^{\lambda_1 t} \mathbf{v}_1 + c_2 e^{\lambda_2 t} \mathbf{v}_2$$

This is a general solution because it is a linear combination of solution to $\dot{\mathbf{x}} = A\mathbf{x}$, and hence is itself a solution. It satisfies the initial condition $\mathbf{x}(0) = \mathbf{x}_0$ and so by the existence and uniqueness theorem, it is the *only* solution.

3.6 Classification of Fixed Points

The eigenvectors and eigenvalues of the Jacobian matrix A , can roughly predict the type and stability of the fixed points. In general, the signs of the eigenvalues indicate the growth or decay and the eigenvectors provide the direction of the solution near the fixed point. Once we have the information above, we can classify the type and stability of the fixed point. The following is a classification scheme for types and stabilities of the fixed points. (see Figure 3.1).

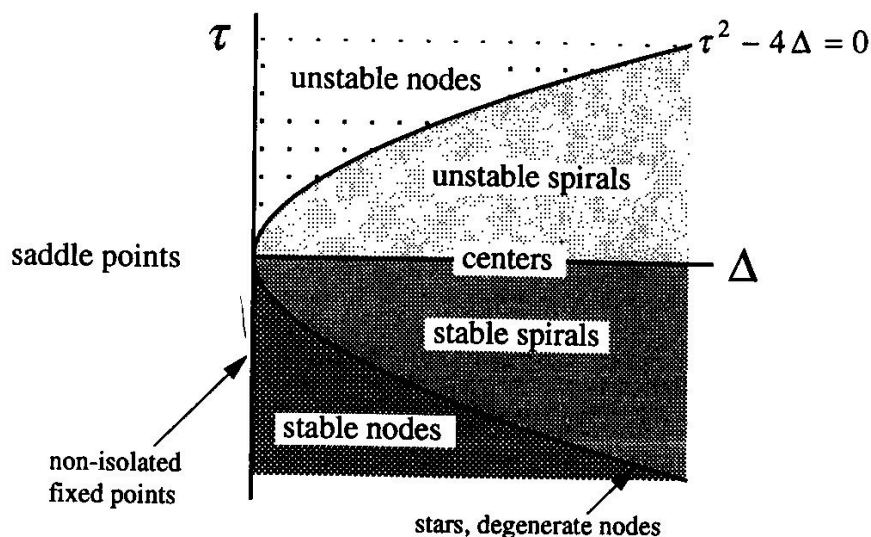


Figure 3.1: Type and stability of all the different fixed points diagram. [26]

We classify fixed points using the trace τ and the determinant Δ of the matrix A (*Jacobian*). The axes in the diagram 3.1 are the trace τ and the determinant Δ . All of the information in the diagram is implied by the following formulas for the 2×2 systems:

$$\lambda_1 = \frac{\tau \pm \sqrt{\tau^2 - 4\Delta}}{2}, \quad \Delta = \lambda_1 \lambda_2, \quad \tau = \lambda_1 + \lambda_2$$

- If $\Delta < 0$ the eigenvalues are real and have opposite sign then the fixed point is a *saddle point*.
- If $\Delta > 0$, the eigenvalues are either real with the same sign (*nodes*), or complex conjugate (*spirals* and *centers*). Thus, nodes satisfy $\tau^2 - 4\Delta > 0$ and spirals satisfy $\tau^2 - 4\Delta < 0$. The parabola $\tau^2 - 4\Delta = 0$ is the borderline between nodes and spirals; star nodes and degenerate nodes lie on this parabola.
- The stability of the nodes and spirals is determined by τ .
 - When $\tau < 0$, both eigenvalues have negative real parts so the fixed point is stable.
 - Unstable spirals and nodes have $\tau > 0$.

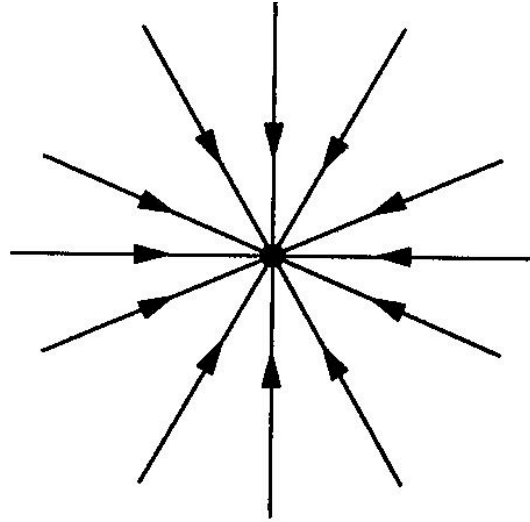


Figure 3.2: typical phase portrait for star node [26]

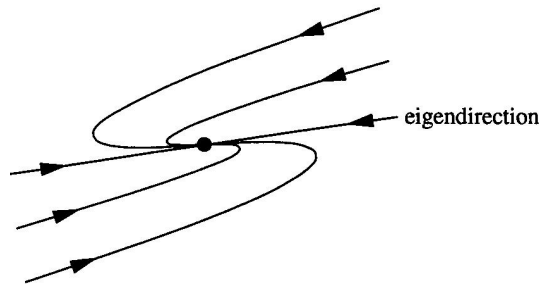


Figure 3.3: typical phase portrait for degenerate node. [26]

- Neutrally stable center live on the borderline τ , where the eigenvalues are purely imaginary.

Note that $\tau^2 - 4\Delta = 0$ if and only if there is only one eigenvalue. Now, if there are two independent eigenvectors then the fixed point is called a *star node* (see Figure 3.2). However, if there is only one eigenvector then the fixed point is called *degenerate* (see Figure 3.3).

A good way to think about the degenerate node is to imagine it has been created by deforming an ordinary node. Realize that the degenerate node is on the *borderline between a spiral and a node* where trajectories are trying to wind around in a spiral, but they do not quite make it. The borderline cases such as degenerate node are very delicate and can

be altered by small nonlinear terms.

The Effect of Small Nonlinear Terms

A linearized system give a quantitatively correct picture of the phase portrait near a fixed point (x^*, y^*) As long as the *the fixed point for the linearized system is not one of the border line cases*, mentioned above.

The borderline cases (center, degenerate nodes, stars, or nonisolated fixed points) are much more delicate. They must be analyzed by looking at higher order terms .

3.7 Bifurcation

If the phase portrait changes its topological structure as a parameter is varied we say that a **bifurcation** has occurred. Example includes changes in the number or stability of the fixed points.

3.7.1 Saddle-node Bifurcation

The saddle-node bifurcation is the basic mechanism by which fixed points are *created and destroyed*. As a parameter is varied, two fixed points move toward each other, collide, and mutually annihilate.

3.7.2 Transcritical Bifurcation

There are certain scientific situations where a fixed point must exist for all values of a parameter and can never be destroyed. For example, in the logistic equation and other simple models for the growth of a single species, there is a fixed point at zero population, regardless of the value of the growth rate. However, such a fixed point may *change its stability* as the parameter is varied. The *transcritical bifurcation* happens when two fixed points with different stability approach together, coalesce and finally *exchange stabilities* as a parameter is varied.

This chapter helps to refresh our knowledge about the dynamics of nonlinear systems. We use this knowledge in Chapter 5 where we develop a Cellular Automata (CA) model and perform the mean field approximation (MFA) for the model. The mean field approximation of the model gives a nonlinear system of differential equations. We then find the fixed points and perform stability analysis, followed by bifurcation analysis for the system (see Chapter 6).

Chapter 4

Cellular Automata & Mean Field Approximation

4.1 Cellular Automata

Cellular Automata (CA) are the simplest mathematical representations of large complex systems [24]. Typically, a cellular automaton is a discrete model composed of an array or grid of cells that evolve over discrete time. This grid can be any finite number of dimensions, but is usually one or two dimensional. This chapter provides an overview of CA and their inherently simple nature, given their complex behavior.

The material explained in this chapter is based on the book “Cellular Automata: A Discrete Universe” by *Andrew Ilachinski*.

4.2 History

The dynamical behavior of many real complex systems have been described by using CA. For example physical fluids, neural networks, molecular dynamical system, natural ecologies, military command and control networks, and the economy, among many others [24]. Three persons had the most contributions to development of this field: Alan Turing, John von Neumann and Stephen Wolfram. In addition, Stanislaw Ulam and John Conway each

made specific, original contributions as well. In the early 1950s Von Neumann followed a suggestion by Ulam to use discrete rather than continuous dynamics modeling, and constructed a two dimensional automaton capable of self-reproducing. Twenty years later, the mathematician John Conway introduced his well-known *Game of Life* [52], which is the best-known example of a cellular automaton.

CA have intuitively used by researchers from diverse fields. They have used CA to understand the dynamic of the problems in their own fields. For example, CA have been used to model biological systems from the level of intracellular activity to the levels of clusters of cells, and population of organisms. CA have been used to model the kinetics of molecular systems and crystal growth in chemistry [46]. In physics, the applications cover the study of dynamical systems starting from the interaction of particles to the clustering of galaxies [47]. In the field of computer science, cellular automata based methods have been employed to model the von Neumann (self-reproducing) machines as well as the parallel processing computer architecture. Beyond the domain of science, CA have also been used to study other diverse fields - as diverse as whether the membership of NATO should be more restricted or not [48].

4.2.1 The Cell

The most basic component in a CA is the cell. Traditionally, all the cells in a CA are equivalent (Homogeneity). Each cell takes on one a finite number of possible discrete states. A cell interacts only with cells that are in its local neighborhood. At each discrete unit time, each cells updates its current state according to transition rule taking into account the states of cells in it's neighborhood (discrete dynamics). Generally, the next state of a cell is a function of its present state and the current states of it's neighbors as shown in Figure 4.1.

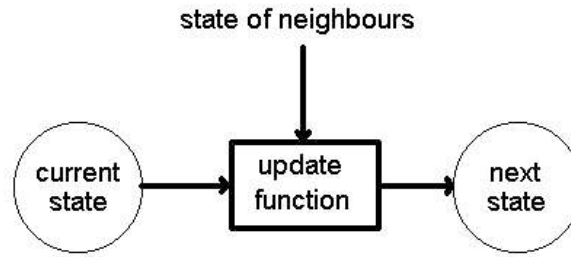


Figure 4.1: A generalized state transition [34].

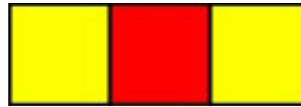


Figure 4.2: One Dimensional Cellular Automata

4.3 One Dimensional Cellular Automata

The general form of a one-dimensional CA (4.2) is given by:

$$\sigma_i(t+1) = \phi(\sigma_{i-r}(t), \sigma_{i-r+1}(t), \dots, \sigma_{i+r-1}(t), \sigma_{i+r}(t)), \quad \phi : S^{2r+1} \rightarrow S.$$

when $\sigma_i \in \{0, 1, \dots, k-1\}$, ' r ' neighborhood radius and ' k ' is the number of states. The rule, ϕ , is explicitly defined by assigning values to each of the k^{2r+1} possible neighborhood and S is the state space (see Figure 4.2).

For example, let $k = 2$ and $\sigma_i \in \{0, 1\}$ we define the rule $\phi : \{0, 1\}^3 \rightarrow \{0, 1\}$ as:

$$\phi(\sigma_{i-1}(t), \sigma_i(t), \sigma_{i+1}(t)) = \sigma_{i-1}(t) \oplus_2 \sigma_{i+1}(t),$$

where ' \oplus ' is addition mod 2.

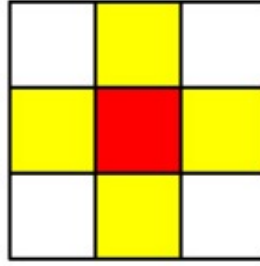


Figure 4.3: Von Neumann neighborhood

4.4 Two Dimensional Cellular Automata

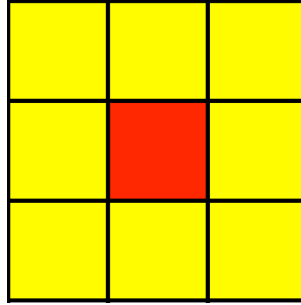
The *von Neumann* neighborhood consists of the four cells which are horizontally and vertically adjacent to the center cell of interest (see Figure 4.3), and the *Moore* neighborhood consists of all eight cells which are adjacent to the center site (see Figure 4.4). The middle red represents the target cell and the yellow cells are its neighbors. Their explicit forms are given as follow:

$$\text{von - Neumann } : \sigma_{i,j}^{(t+1)} = \phi(\sigma_{i,j}^{(t)}, \sigma_{i-1,j}^{(t)}, \sigma_{i+1,j}^{(t)}, \sigma_{i,j-1}^{(t)}, \sigma_{i,j+1}^{(t)})$$

$$\text{Moore } : \sigma_{i,j}^{(t+1)} = \phi(\sigma_{i-1,j-1}^{(t)}, \sigma_{i,j-1}^{(t)}, \sigma_{i+1,j-1}^{(t)}, \sigma_{i-1,j}^{(t)}, \sigma_{i,j}^{(t)}, \sigma_{i+1,j}^{(t)}, \sigma_{i-1,j+1}^{(t)}, \sigma_{i,j+1}^{(t)}, \sigma_{i+1,j+1}^{(t)})$$

4.4.1 Boundary Condition

Although CA are assumed to live on infinitely large lattices, computer simulations must necessarily be run on finite sets. We let $\sigma_{\vec{i}}$ be the value of the \vec{i}^{th} cell at time t . For a one dimensional lattice with N cells, it is common to use *periodic boundary conditions*, in which σ_{N+1} is identified with σ_1 . Similarly, in two dimensions, it is usual to have the dynamics

Figure 4.4: 3×3 Moore neighborhood

take place on a *torus*, in which $\sigma_{i,M+1} = \sigma_{i,1}$ and $\sigma_{N+1,j} = \sigma_{1,j}$ (see Figure 4.5). Boundary conditions often plays an important rule in shaping of the resulting dynamics when the size of CA is small.

4.5 Dynamical Rule

Individual cells evolve iteratively according to a fixed, either deterministic or stochastic, function (update rule). The next state of a cell is a function of its current state and its neighboring cells. One *iteration* of the dynamical evolution is achieved after the simultaneous application of the rule ϕ to each cell in the lattice. Defining $N\{\vec{i}\}$ to be the neighborhood about cell \vec{i} , the transition rule is most generally written as:

$$\sigma_{\vec{i}}(t+1) = \phi(\sigma_{\vec{j}} \in N\{\vec{i}\}),$$

This implies that state transitions are *local* in both space and time.

4.5.1 Legal and Other Forms of Rules

Because of the rather large total number of $k^{k^{2r+1}}$ possible for a given ‘ k ’ and ‘ r ’, it is frequently convenient to deal with some restricted classes, such as:

Legal Rules: Legal rules are those for which the following two properties hold:

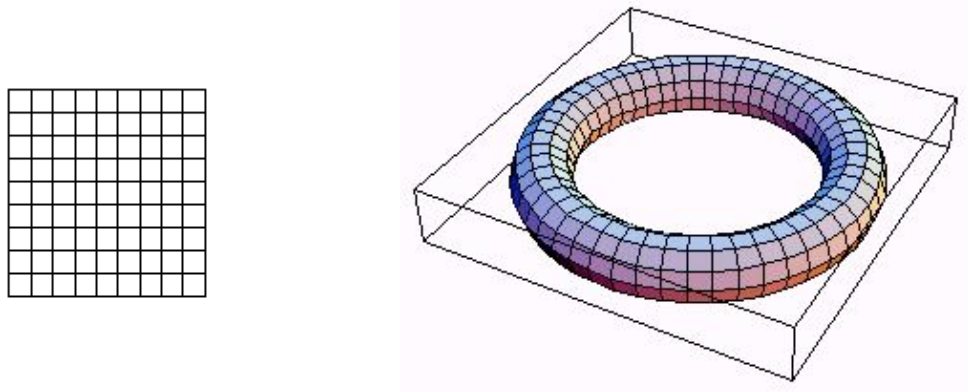


Figure 4.5: Two-Dimensional CA [28] *left* without edges pasted *right* with edges pasted

Null state quiescence: $\phi(0, 0, \dots, 0) = 0$

Reflection Symmetry: $\phi(\sigma_{i-r}, \dots, \sigma_{i+r}) = \phi(\sigma_{i+r}, \dots, \sigma_{i-r})$

Totalistic Rules: Totalistic T rules, ϕ_{tot} , are functions of the sums of the values of all sites in a particular neighborhood: $\phi_{tot} = \phi_{tot}(\sum_{j=-r}^r \sigma_{i+j})$.

Outer-Totalistic Rules: Outer-totalistic (OT) rules, $\phi_{out-tot}$, are function of both the value of a given site and the sum of values of all *remaining* sites in the neighborhood of that site. Therefore, $\phi_{out-tot} = \phi_{out-tot}(\sigma_i, \sum_{j=-r}^r \sigma_{i+j} - \sigma_i)$.

Additive Rules: Rules belonging to the special class of *additive rules*, ' ϕ_{add} ', are linear function of the sum neighborhood sites:

$$\phi_{add} = \sum_{j=-r}^r \alpha_j \sigma_{i+j} \bmod k, \quad \alpha_j \in S.$$

The eight additive $r = 1$, $k = 2$ rules, for example, are of the general form

111	110	101	100	011	010	001	000
↓	↓	↓	↓	↓	↓	↓	↓
a	b	0	c	b	a	c	0

Where $a, b, c \in \{0, 1\}$ and $c = (a + b) \bmod 2$

4.5.2 Rule Codes

The rules are conventionally identified by a compact *code* rather than by lengthy explicit listings of their local actions. For example the bottom eight binary digits (01011010) are interpreted as the binary representation of a decimal number **90** which is given by base 2 equivalent.

111	110	101	100	011	010	001	000
↓	↓	↓	↓	↓	↓	↓	↓
0	1	0	1	1	0	1	0

$$R[\phi] = 0 \cdot 2^0 + 1 \cdot 2^1 + 0 \cdot 2^2 + 1 \cdot 2^3 + 1 \cdot 2^4 + 0 \cdot 2^5 + 1 \cdot 2^6 + 0 \cdot 2^7 = \mathbf{90}.$$

We refer to this rule in the text as **R90**.

4.6 Mean Field Approximation

We consider 1-D CA whose site variables take on only one of two values and evolve according to rules. Rules often depend only on the previous values of a given site and those of its immediate left and right neighbors.

$$\sigma_i(t+1) = \phi(\sigma_{i-1}(t), \sigma_i(t), \sigma_{i+1}(t)), \quad \sigma \in \{0, 1\}. \quad (4.1)$$

For general rules, a first order statistical approximation for limiting densities of the CA, defined in (4.1), can be obtained by the *mean field approximation*.

Definition of the Mean Field Approximation

A many-body system with interactions is generally very difficult to solve exactly, except for extremely simple cases (Gaussian field theory, 1D Ising model). The Mean Field Approximation (MFA) replaces an n -body problem with a chosen external field, ignoring space dependence and neglects local correlations. The external field replaces the interaction of all the other particles to an arbitrary particle [33].

MFA provides a good approximation near the bifurcation for CA models. This is because the cells are highly correlated near the bifurcation and the global effects dominate over the local effects. Thus, MFA can provide a good approximation for the behavior of the system.

MFA estimates the density and other properties of CA. One way to get an estimation is to make the assumption that the value of a given site at each time step is completely random. And with this assumption, if the overall density of sites with value ‘1’ at the particular step is p , then each site at that step should independently have probability p of having value ‘1’. This means that the probability to find a site with value ‘1’ followed by two zero sites is $p(1-p)^2$ in 1-D CA. In general, the probabilities for all possible configuration of n neighborhood are found and in terms of these probabilities, the density at the next step in the evolution of CA is estimated [25] .

The differences between mean field estimation and exact limiting densities can be expected because of the presence of correlations in actual CA. The mean field approximation typically estimates the exact limiting density within 10 – 20% error [24].

4.7 Mean Field Approximation

As a first order approximation, we will ignore all correlations between values at different sites and parametrize configuration purely in terms of the average density at time ‘t’, ρ . The time evolution of ρ under an arbitrary rule ‘ ϕ ’ is then given by the master equation:

$$\frac{d\rho}{dt} = f_{0 \rightarrow 1} - f_{1 \rightarrow 0} \tag{4.2}$$

where $f_{0 \rightarrow 1}$ and $f_{1 \rightarrow 0}$ are the average fraction of sites whose value changed from $\sigma = 0$ to $\sigma = 1$ and vice versa. An explicit for these fractions is obtained by observing that the probability ‘ P ’ of having the 3-tuple $\vec{\sigma} = \langle \sigma_1, \sigma_2, \sigma_3 \rangle$ appear in a neighborhood is:

$$P(\sigma_1, \sigma_2, \sigma_3) = p^{\#_1(\vec{\sigma})} (1 - p)^{3 - \#_1(\vec{\sigma})} \tag{4.3}$$

where $\#_1(\vec{\sigma})$ is the number of times ‘1’ appears in the string $\vec{\sigma}$. Thus,

$$\begin{aligned} f_{0 \rightarrow 1} &= \sum_{\{\vec{\sigma} | \sigma_2=0\}} \phi(\sigma_1, \sigma_2, \sigma_3) P(\sigma_1, \sigma_2, \sigma_3), \\ f_{1 \rightarrow 0} &= \sum_{\{\vec{\sigma} | \sigma_2=1\}} [1 - \phi(\sigma_1, \sigma_2, \sigma_3)] P(\sigma_1, \sigma_2, \sigma_3). \end{aligned} \tag{4.4}$$

The equilibrium, or *steady state* density $\rho(t \rightarrow \infty)$ is achieved when

$$\frac{d\rho}{dt} = 0 \tag{4.5}$$

4.8 MFA for the Two State CA with Elementary Rules

We use MFA to estimate the density of ones in the time evolution of CA with two state $k = 2$, (0 and 1), with the elementary rule **R90** (see Section 4.5.2) and neighborhood radius $r = 1$. Note that we have $k^{2r+1} = 2^3$ possible neighborhood (see section 4.3 for the possible number of neighborhood) and the resulting state for the middle site under the rule **R90** are given by:

111	110	101	100	011	010	001	000
↓	↓	↓	↓	↓	↓	↓	↓
0	1	0	1	1	0	1	0

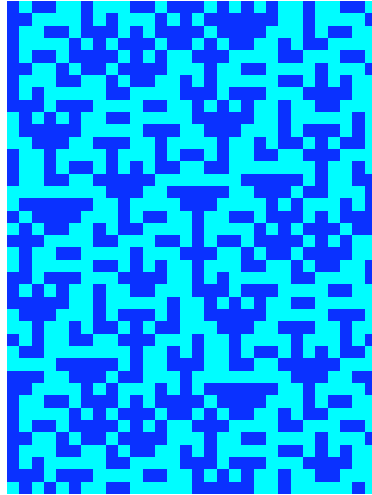


Figure 4.6: The time evolution of the 1-D CA for rule **R90** with random initial condition.

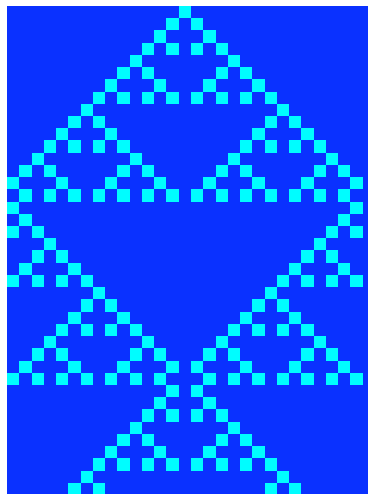


Figure 4.7: The time evolution of the 1-D CA for rule **R90**, an initial state with of a single nonzero value.

We let p be the probability of a site with value ‘1’ at time ‘ t ’ and describe configurations (using 4.3) in terms of the average density of ones, ρ . Then we calculate the average fraction of the sites whose value changes from ‘1’ to ‘0’ or vice versa (see equations in 4.4):

$$\begin{aligned} f_{0 \rightarrow 1} &= P(0, 0, 1) + P(1, 0, 0) = 2(1 - p)^2 p, \\ f_{1 \rightarrow 0} &= P(0, 1, 0) + P(1, 1, 1) = (1 - p)^2 p + p^3. \end{aligned}$$

Thus change in density of ones, under the rule **R90**, over time is given by differential equation 4.2:

$$\frac{d\rho}{dt} = 2(1 - p)^2 p - (1 - p)^2 p + p^3, \quad (4.6)$$

So $\frac{d\rho}{dt}$ becomes:

$$\frac{d\rho}{dt} = (1 - 2p).$$

So the equilibrium density, $\rho_1(t \rightarrow \infty)$, is achieved when: $\frac{d\rho}{dt} = 0 \implies p(1 - 2p) = 0$

which has a solutions $p^* = 0$ (or the null state) and $p^* = \frac{1}{2}$. Using linear stability analysis for the fixed points (see Chapter 3) we linearize the system about the fixed points and let $f(p) = p(1 - 2p)$. Since $f'(p^*) > 0$ for $p^* = 0$ and $f'(p^*) < 0$ thus $p^* = \frac{1}{2}$ we conclude a nonzero fixed point $p^* = \frac{1}{2}$ is a stable fixed point, which is the most likely state for the system to be in. The MFA estimates that the half of the sites in CA are ones. The simulation result is consistent with the mean field approximation as the histogram in Figure 4.8 shows: the exact limiting density is 0.5.

4.8.1 Approximating CA by Differential Dynamical Systems

We performed the mean field approximation for an elementary rule in Section 4.8. We observed that the MFA of the CA yields the system of differential equations in (4.6). This is because differential dynamical system can approximate the behavior of the CA. Furthermore, changes in densities and other property of the CA can be well expressed in terms of differential equations. Therefore, the bifurcation theory of differential dynamical system

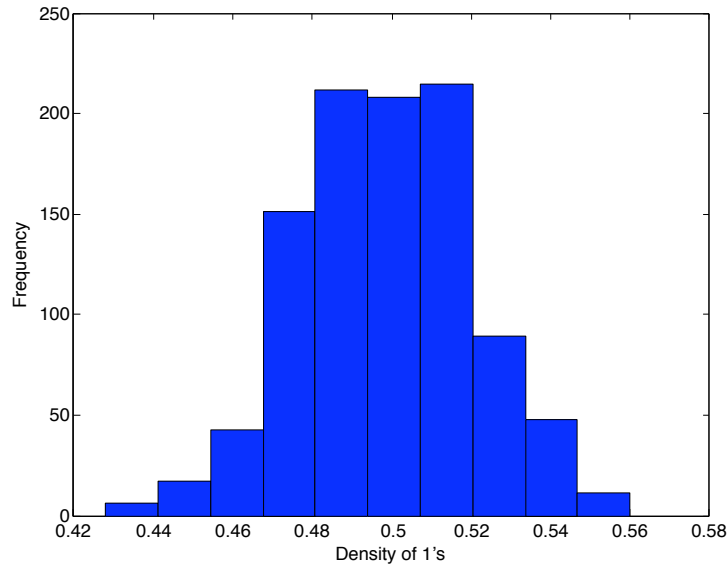


Figure 4.8: Simulation result for the exact limiting density of 1s applying **R90**

(reviewed in chapter 3) can be used to determine the steady state and estimate the time evolution of average densities of the CA.

We continue with more complicated examples in the next sections. As the MFA works for the general rules, so we use it to estimate the density and other properties of a three state CA under an Outer-Totalistic rule in the following section:

4.9 Three State 1-D CA and Outer-Totalistic Rules

We perform the MFA for a three states, $k = 3$, CA with a neighborhood of radius of $r = 1$, $(\sigma_{i-1}, \sigma_i, \sigma_{i+1})$, under an Outer-Totalistic rule (see definition in section 4.5.1). We would like to understand the changes in densities and approximate the behavior of a CA under this rule. We also examine the consistency of the MFA and simulation result for an Outer-Totalistic given as:

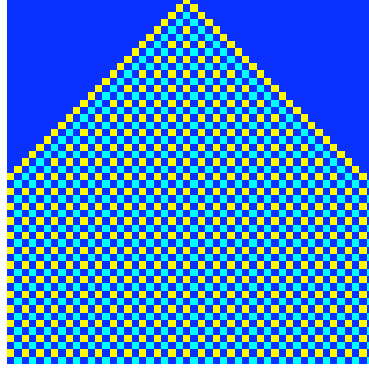


Figure 4.9: The time evolution of the 1-D CA for Outer-totalistic rule 4.7, an initial state with of a single nonzero value.

$$\sigma_i(t+1) = \begin{cases} \sigma_{i-1}(t) + \sigma_{i+1}(t) & \text{if } \sigma_{i-1}(t) + \sigma_{i+1}(t) \leq 2, \\ 1 & \text{otherwise.} \end{cases} \quad (4.7)$$

We let q , p and $(1-p-q)$ be the probability of a site being in state 0, 1 and 2, respectively. We also let the average densities of 0, 1 and 2 at time 't', be μ, ρ, ζ . The time evolution of μ and ρ under the defined Outer-totalistic rule are given by system of differential equations:

$$\begin{aligned} \frac{d\mu}{dt} &= (f_{1 \rightarrow 0} + f_{2 \rightarrow 0}) - (f_{0 \rightarrow 1} + f_{0 \rightarrow 2}), \\ \frac{d\rho}{dt} &= (f_{0 \rightarrow 1} + f_{2 \rightarrow 1}) - (f_{1 \rightarrow 0} + f_{1 \rightarrow 2}). \end{aligned} \quad (4.8)$$

where, $(f_{1 \rightarrow 0} + f_{2 \rightarrow 0})$ and $(f_{0 \rightarrow 1} + f_{0 \rightarrow 2})$ are:

$$\begin{aligned} f_{1 \rightarrow 0} + f_{2 \rightarrow 0} &= pq^2 + q^2(1-p-q), \\ f_{0 \rightarrow 1} + f_{0 \rightarrow 2} &= 2pq^2 + 2pq(1-p-q) + q(1-p-q)^2 + q^2(1-p-q) + \\ &\quad p^2q + q^2(1-p-q). \end{aligned} \quad (4.9)$$

and $(f_{0 \rightarrow 1} + f_{2 \rightarrow 1})$ and $(f_{1 \rightarrow 0} + f_{1 \rightarrow 2})$ are:

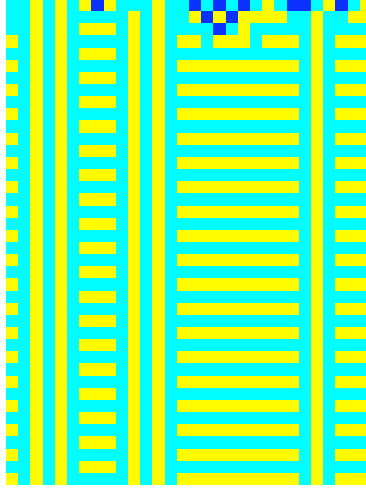


Figure 4.10: The time evolution of the 1-D CA for outer-totalistic rule 4.7, with random initial condition.

$$\begin{aligned}
 f_{0 \rightarrow 1} + f_{2 \rightarrow 1} &= 2pq^2 + 2pq(1-p-q) + q(1-p-q)^2 & (4.10) \\
 &+ 2pq(1-p-q) + 2p(1-p-q)^2 + (1-p-q)^3, \\
 f_{1 \rightarrow 0} + f_{1 \rightarrow 2} &= pq^2 + pq(1-p-q) + p^3 + pq(1-p-q).
 \end{aligned}$$

We simplify equations 4.9 and 4.10 and substitute them for $(\frac{d\mu}{dt}, \frac{d\rho}{dt})$ in equations 4.8. So we have:

$$\begin{aligned}
 \frac{d\mu}{dt} &= q^2 - q, & (4.11) \\
 \frac{d\rho}{dt} &= 1 - p - 2q + 2pq + q^2 - p^2.
 \end{aligned}$$

We solve the system of equation $(\frac{d\mu}{dt} = 0, \frac{d\rho}{dt} = 0)$ for $[q, p]$. There are two physical solutions for this system $[q = 0, p = 0.618]$ and $[q = 1, p = 0]$.

We linearize the system around the fixed points (see Section 3.4.2) and let λ_1 and λ_2 denote the eigenvalues of the *Jacobian* (matrix A'), respectively.

$$A' = \begin{pmatrix} 2q - 1 & 0 \\ -2 + 2p + 2q & -1 + 2q - 2p \end{pmatrix}$$

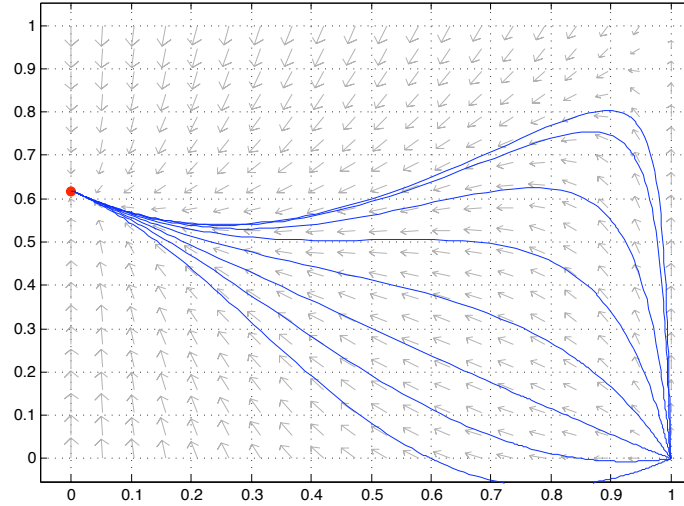


Figure 4.11: Phase Portrait of the system of differential equations 4.11 and the stable fixed point $[q = 0, p = 0.618]$.

There are two eigenvalues: $\lambda_1 = 2q - 1$ and $\lambda_2 = -1 + 2q - 2p$. The corresponding eigenvectors are:

$$\begin{pmatrix} \frac{p}{-1+p+q} \\ 1 \end{pmatrix}, \begin{pmatrix} 0 \\ 1 \end{pmatrix}$$

Note that the eigensolutions decay exponentially for $[q = 0, p = 0.618]$ and grow for $[q = 1, p = 0]$. So according to stability analysis and classification of the fixed points, they are stable node and saddle point, respectively (see Figure 4.11). Now that we have the analytical result we compare it to the simulations result.

The time evolution of the CA in Figure 4.10 shows how the zeros die out in the early steps and iteration continues with ones and twos. Figure 4.12 shows the simulation result for the exact limiting density of ones in blue which is around 0.575. Note that this value is very close to the the value that the mean field calculation estimates for p (density of ons) which is 0.618.

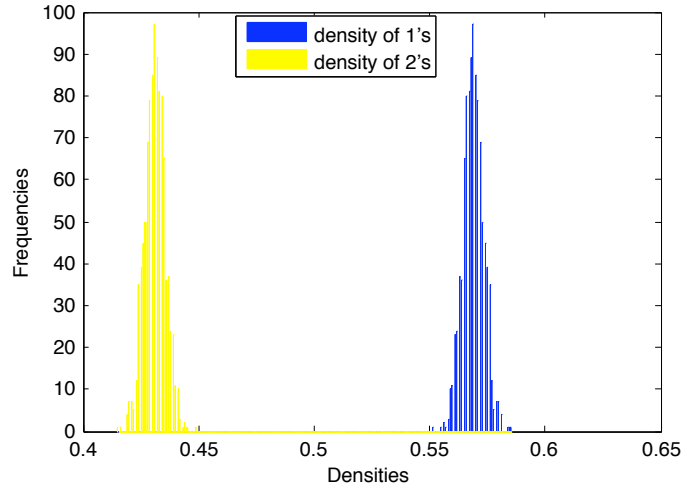


Figure 4.12: Simulation result for the exact limiting densities of 1s & 2s using the Outer-totalistic 4.7.

4.10 Three State 1-D CA and Asymmetrical Rules

All the rules we used in the previous examples were the legal rules (symmetric) (see definition in 4.5.1). For those types of rules, configuration of local states for the adjacent cells at time ' t ' makes no difference to the resulting state at time ' $t + 1$ '. Given that the mean field approximation neglects the configuration, we would like to examine the accuracy of the mean field approximation for an asymmetrical rule.

We consider the three states, $k = 3$ which are 0, 1 and 2, CA with the neighborhood radius of $r = 1$, $(\sigma_{i-1}, \sigma_i, \sigma_{i+1})$. We define the asymmetric rule as follow:

$$\sigma_i(t+1) = \begin{cases} 0, & \text{if } \sigma_{i-1}(t) < \sigma_{i+1}(t) \\ 1, & \text{if } \sigma_{i-1}(t) = \sigma_{i+1}(t) \\ 2, & \text{if } \sigma_{i-1}(t) > \sigma_{i+1}(t) \end{cases} \quad (4.12)$$

We let q, p and $1-p-q$ be the probability of a site being in state 0, 1 and 2, respectively. We also let the average densities of 0, 1 and 2 at time ' t ', be μ, ρ, ζ . We estimate the densities of ones and zeros using MFA. So we have:

$$\begin{aligned}\frac{d\mu}{dt} &= (f_{1\rightarrow 0} + f_{2\rightarrow 0}) - (f_{0\rightarrow 1} + f_{0\rightarrow 2}), \\ \frac{d\rho}{dt} &= (f_{0\rightarrow 1} + f_{2\rightarrow 1}) - (f_{1\rightarrow 0} + f_{1\rightarrow 2}).\end{aligned}\tag{4.13}$$

where, $(f_{1\rightarrow 0} + f_{2\rightarrow 0})$ and $(f_{0\rightarrow 1} + f_{0\rightarrow 2})$ are:

$$\begin{aligned}f_{1\rightarrow 0} + f_{2\rightarrow 0} &= qp^2 + pq(1 - p - q) + p^2(1 - p - q) + pq(1 - p - q) + \\ &\quad q(1 - p - q)^2 + p(1 - p - q)^2,\end{aligned}\tag{4.14}$$

$$\begin{aligned}f_{0\rightarrow 1} + f_{0\rightarrow 2} &= q^3 + p^2q + q(1 - p - q)^2 + pq^2 + (1 - p - q)q^2 + \\ &\quad (1 - p - q)pq.\end{aligned}\tag{4.15}$$

and $(f_{0\rightarrow 1} + f_{2\rightarrow 1})$ and $(f_{1\rightarrow 0} + f_{1\rightarrow 2})$ are:

$$\begin{aligned}f_{0\rightarrow 1} + f_{2\rightarrow 1} &= q^3 + p^2q + q(1 - p - q)^2 + q^2(1 - p - q) + \\ &\quad p^2(1 - p - q) + (1 - p - q)^3,\end{aligned}\tag{4.16}$$

$$\begin{aligned}f_{1\rightarrow 0} + f_{1\rightarrow 2} &= qp^2 + pq(1 - p - q) + p^2(1 - p - q) + p^2q + \\ &\quad (1 - p - q)pq + (1 - p - q)p^2.\end{aligned}\tag{4.17}$$

We simplify equations 4.14 and 4.16 and substitute them for $(\frac{d\mu}{dt}, \frac{d\rho}{dt})$ in equations 4.13. So we have:

$$\begin{aligned}\frac{d\mu}{dt} &= -q^2 - pq - p^2 + p, \\ \frac{d\rho}{dt} &= 1 - 2q - 3p + 2pq + 2p^2 + 2q^2.\end{aligned}\tag{4.18}$$

The solution to $(\frac{d\mu}{dt} = 0, \frac{d\rho}{dt} = 0)$ for $[q, p]$ are $[q = 0, p = 1]$ and $[q = 0.33, p = 0.33]$. The fixed points are saddle point and stable node respectively (see Figure 4.13).

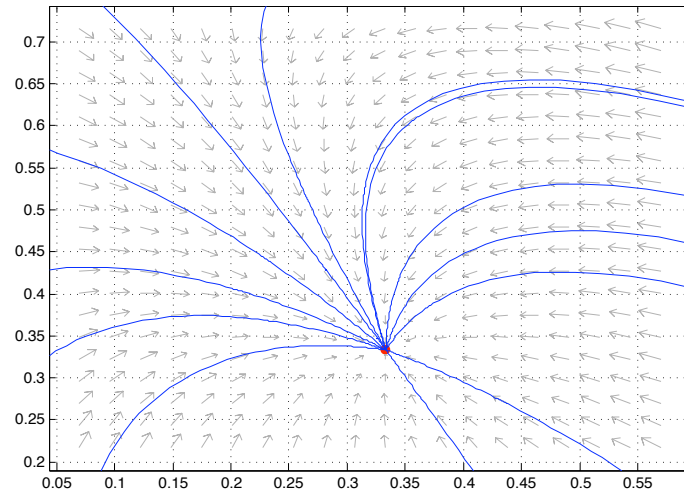


Figure 4.13: Phase Portrait of the system of differential equations 4.18 and the stable fixed point $[q = 0.33, p = 0.33]$.

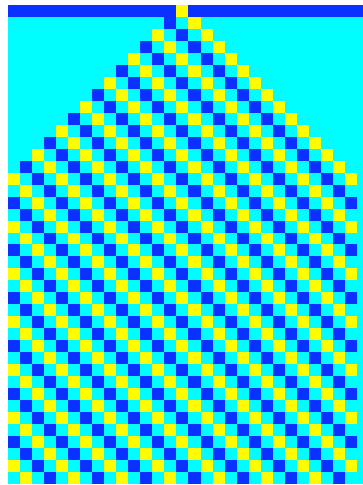


Figure 4.14: The time evolution of the 1-D CA for the rule 4.12, an initial state with of a single nonzero value.

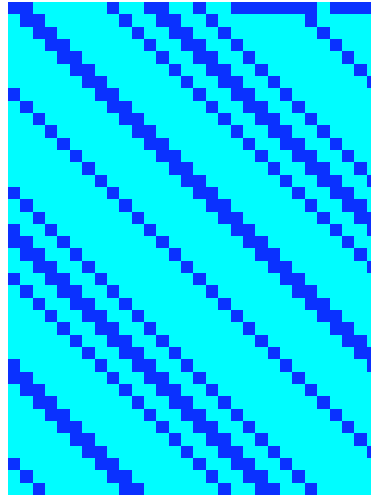


Figure 4.15: The time evolution of the 1-D CA for rule 4.12 with random initial condition.

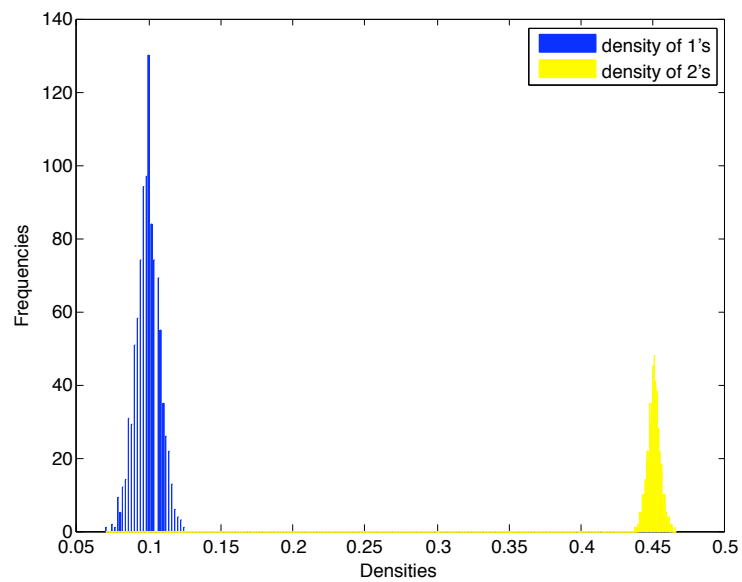


Figure 4.16: Simulation result for the exact limiting densities of 1s & 2s using the rule 4.12.

The mean field approximation predicts that the system will most likely be in the state $[q = 0.33, p = 0.33]$ (stable fixed point). However, the simulation result in Figure 4.16 shows different limiting densities. It shows that the probability of a random cell being in state '1' is 0.1.

We have found an example for which the mean field approximation can not estimate the exact limiting densities correctly. This inaccuracy is likely being caused by the fact that the mean field approximation neglects the configuration of the adjacent cells. If the rule is asymmetric, then some more information about the CA is lost and this may effect the ability of the MFA to estimate steady state densities.

Chapter 5

Cellular Automata Model For the DTES

Cellular automata (CA) can be used to illustrate the effects of social influences on individuals located on networks with a mixture of local and global interactions. Furthermore, a CA model can assist in improving our understanding of the complex social system issues and related processes tied to the cause of those issues such as disease transmission, drug addiction patterns and behavior modification among the individuals with high - risk behavior [15].

In this chapter, we present both one and two dimensional Probabilistic Cellular Automata (PCA) model to study the effect of social influence on the spread of drug use/trade in the drug user community in Vancouver Down Town East Side (DTES). The CA model is based on an epidemic compartmental framework. Compartmental models employ differential equations and define groups of individuals of different types (in this models defined as susceptible, light users and dealers). The model is motivated by a paper by Dabbaghian et al [14] and has additional functionalities such as probabilistic interaction rules and updating cells as well as ability to approximate the global behavior of the PCA (see Chapter 6).

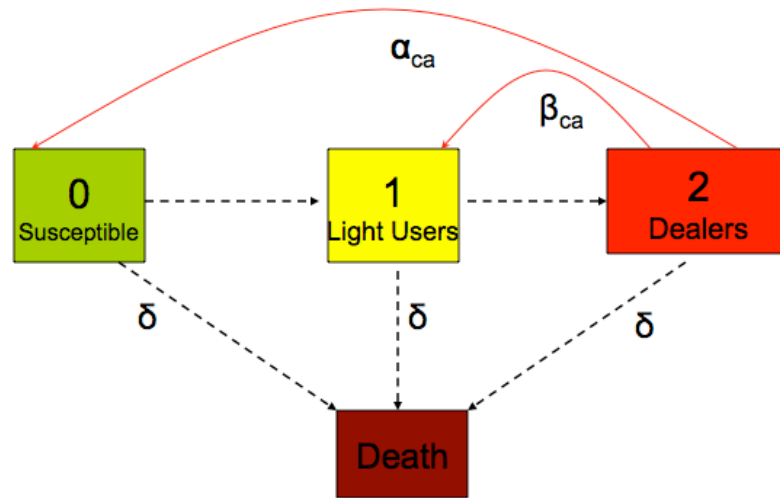


Figure 5.1: Model structure

5.1 Description of the 1-D CA Model

To model the interaction among drug users and the spread of drug use in a community, we use a three-state cellular automaton. Figure 5.1 shows the two type of interactions in the model, *social influences* and *transitions*, with solid curve and dashed, straight arrows, respectively. Boxes 0, 1 and 2 represents groups of susceptible, light Users and dealer respectively.

This probabilistic cellular automata model mimics the spread of drug use in a community. Our PCA is a discrete model composed of a large grid of cells (the grid can be any finite dimensions). Each one of cells can be in one of a finite number of states 0, 1 or 2 which are correspond to the three defined types. The three states that used in the CA model are defined in the Table 5.1. Each cell represents an individual interacting with its neighbors and identified as a member of a compartment. The model is run for a certain number of time steps, with the grid being updated at every time step τ . Each cell “interacts” with other cells in the neighborhood and is updated according to interaction rules.

We define two things for each cell. First of all, we define each cells *neighborhood*. A neighborhood is simply a list of cells that a given cell will interact with, and will typically be the

Table 5.1: Definition of the State of the Cells

0 Susceptible	Either a non users or can become a users. Can make a transition to light users state
1 Light Users	A user which can make a transition to dealer state
2 Dealers	No transition

cells immediately surrounding the given cell. We define each individuals neighbors to be those within the individuals *1-D neighborhood* (see Figure 4.2) where the number of nearest neighbors is $N = 2$.

Secondly, we assign a *rule* for updating the cells. A *rule* will consider some or all of the interactions of a given cell at a time step, and will either change the state of the given cell or leave the given cell in the same state, depending on these interactions. In most cellular automata models, the rule does not change over time and is the same for each cell. Moreover, it is usually applied to the entire grid at once.

5.2 Social Influence

Two types of social influence are possible in this model. An individual can influence others by encouraging drug use through α_{ca} and drug dealing through β_{ca} .

For the group of Susceptibles, social influence is interpreted slightly differently. Susceptibles must first become a drug user before they engage in any drug dealing career. Social influences on susceptible clearly refers to drug user behavior only. Only dealers can influences their neighbors and all can receive social influence from their neighbors.

This model employs a novel approach to represent the effect of prolonged social relationships between members of a community where dealing drug is prevalent. In such an environment, a person is more likely to experiment drug use if in a lengthy relationship with at least one dealer. In the model, dealers in the neighborhood can act independently with certain probability to convince a susceptible or a light user to use or deal drugs, respectively.

The probability of an independent event is obtained by using the *binomial distribution*. The binomial distribution function generates random numbers with a parameter α_{ca} or β_{ca} is being specified. We use the binomial distribution to model the number of successes in a sample of size one. Here, success interpreted as convincing an individual to become a user/dealer under the influence of neighbors. Equations for the independent probabilistic events of type 0 becoming type 1, and type 1 becoming type 2 are as follow:

$$\begin{aligned} C_0(t, \alpha_{ca}) &= \text{binornd}(\#R_2, \alpha_{ca}) \\ C_1(t, \beta_{ca}) &= \text{binornd}(\#R_2, \beta_{ca}) \end{aligned} \tag{5.1}$$

$\#R_2$ is the number of type 2 neighbors in the neighborhood. Thus, the change in states is given by a binomial random variable x with number of trail $\#R_2$ with probability success α_{ca} or β_{ca} . Where $C_0(t, \alpha_{ca})$ denotes the change in states for an individual of type 0 at time t under the influences of a dealer.

$C_0(t, \alpha_{ca})$ is given by a random variable x with number of trail $\#R_2$ with probability success α_{ca} . Similarly, $C_1(t, \beta_{ca})$ is given by random variable x with number of trail $\#R_2$ with probability success β_{ca} . we let β_{ca} be the probability that an individual of type 1 changes his/her behavior and become a type 2 after a lengthy friendship with a type 2 in one unit of time. Furthermore, Influences are considered (encouraging using/dealing drugs) with value in the interval (0,1).

5.3 Transition

Since the spread of the drug use is linked to drug dealing involvement, the model represents two linked epidemics. An individual makes a transition from type 0 to 1 or from 1 to 2 with the fixed probability either α_{ca} or β_{ca} at each time step, if and only if there exists a dealer in the neighborhood. Dealers can act independently with certain probability either α_{ca} or β_{ca} to convince an individual to use or deal drugs, respectively (see Section 5.2).

Table 5.2: Rules for Updating the Cells

<p>0 Suspetible</p> <p>a). Dies after τ_0 time steps.</p> <p>b). If not dead and $C_0(t) > 0$ then transition Light User</p>
<p>1 Light Users</p> <p>a). Dies after τ_1 time steps.</p> <p>b). If not dead and $C_1(t) > 0$ then transition to Dealers</p>
<p>2 Dealers</p> <p>a). Dies after τ_2 time steps.</p>

5.4 Rules for Updating Cells

Cells are updated according to the probabilistic rules in (5.1) and the rules described in Table (5.2). At each time step, all cells in the lattice are updated simultaneously. If the probability of change is zero then the individual can not be convinced by any of his neighbors to start using/dealing and the state of that cell remains unchanged. On the other hand, if it is not zero then the individual is recruited in the drug use or deal career. If it returns 1 then that means one of the neighbors has succeed to convince the individual and so on. The parameters τ_i denote the life expectancy of an individual of type i for $i = 0 \dots 2$. We have considered the same life expectancy for all three groups. At each time step, a dead cell of any type gets replaced with a susceptible so the size of population remains unchanged.

5.5 Parameter and Initial Conditions

The model is constructed with inner-city neighborhoods of numerous large urban centers in mind that currently experience epidemics of drug use. Some parameters were initially defined based on the estimates in the literature in [14] and then we run the model for all the values in the range $[0, 0.05]$. Parameter and initial conditions are listed in Table 5.3.

Table 5.3: Parameter and Initial Value

Parameter	Value
Life Expectancy	
Susceptibles	50 years
Light users	50 years
Dealers	50 years
Initial Population	
Susceptibles (0)	30%
Light users (1)	35%
Dealers (2)	35%

5.6 Simulation Result for the 1-D PCA Model

To understand the global behavior of the 1-D CA model we constructed a $(\alpha_{ca}, \beta_{ca})$ parameter space of the ranges $(0 \dots 0.05)$. The average prevalence for dealers is determined by simulating 70×70 cell lattices with ten independent runs. The lattice is initially set with random occupation by 35% drug users. Figure 5.2 which is the phase diagram shows how the system makes a big leap from one steady state (dark blue), the drug free state, to another steady state (red) where the mean prevalence of 80% dealers is observed. This suggests the dependence of average prevalence of dealers on the parameters.

Figure 5.2 consists of all the curves composed of different combinations of $(\alpha_{ca}, \beta_{ca})$ which result in different mean prevalences for dealers. The curves in which the prevalence fall between (0-15%) are densely packed and represent the phase transition of the system. The steady state (flat regions) on two sides of these curves correspond to extinct and endemic states.

We also construct the projection of the mean prevalences of dealers on the α_{ca} and β_{ca} plane (see Figure 5.3). Note that the blue and red region are divided by a curve which is called the *Bifurcation Curve*. The points below the curve are the combinations of α_{ca} 's and β_{ca} 's that drive the number of dealers to extinction (0%-10%) whereas the points above the curve correspond to the states in which the prevalence is highest.

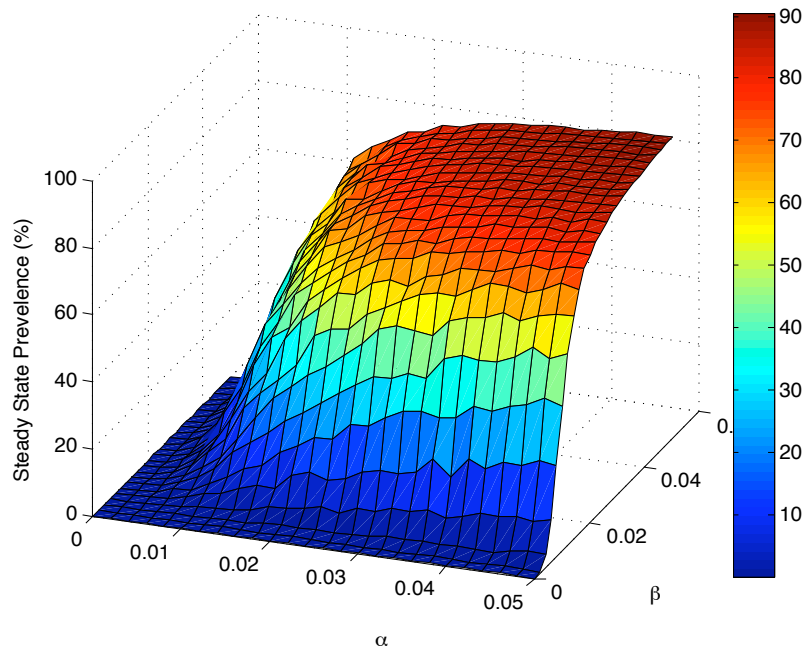


Figure 5.2: Phase diagram of the mean prevalence of dealers for the 2-D CA model

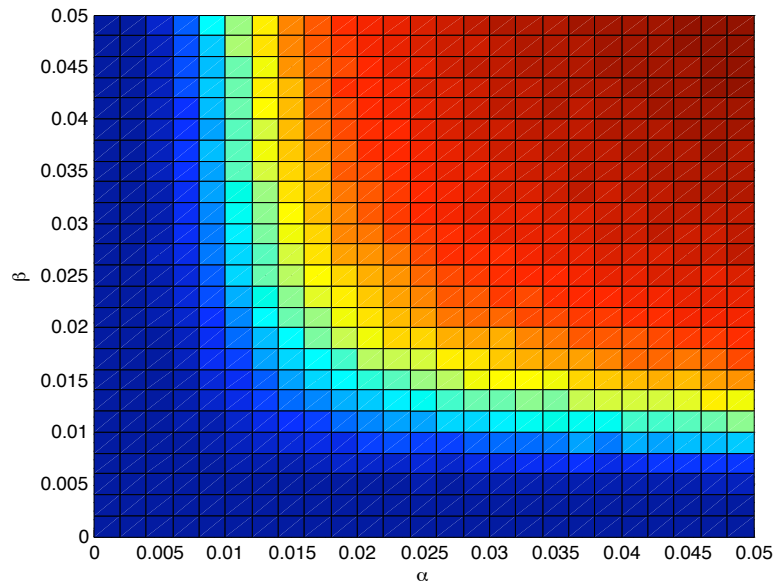


Figure 5.3: Rotated phase diagram for the 1-D CA model

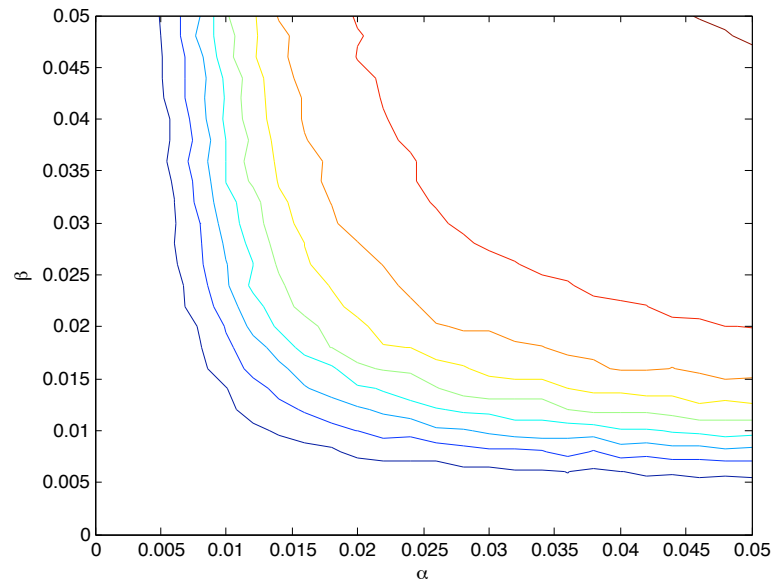


Figure 5.4: Contour plots for the phase diagram in 1-D CA model

Figure 5.4 consists of all the curves composed of different combinations of $(\alpha_{ca}, \beta_{ca})$ which result in different mean prevalences for dealers. We find the $(\alpha_{ca}, \beta_{ca})$ points that correspond to the mean prevalence of dealers in the range (35%-40%) and give a sketch of the *bifurcation curve* for 1-D CA in the Figure 5.5.

5.7 The 2-D Cellular Automata Model

We use the model description that was introduced in Section 5.1 to simulate the 2-D CA model. However, we apply the *von Neumann neighborhood* (see Figure 4.3) to produce the results in two dimension. Von Neumann neighborhood is a diamond-shaped neighborhood on a square grid and the smallest symmetric two dimensional neighborhood. This neighborhood contains the north, south, east and west neighbors. We consider the same social influence and transitions rules explained in pervious sections (5.2 and 5.3). However, we use various scenarios to perform further analysis for the 2-D PCA model. Parameters and initial conditions remain unchanged and cells get updated according to the rules shown in the Table 5.2.

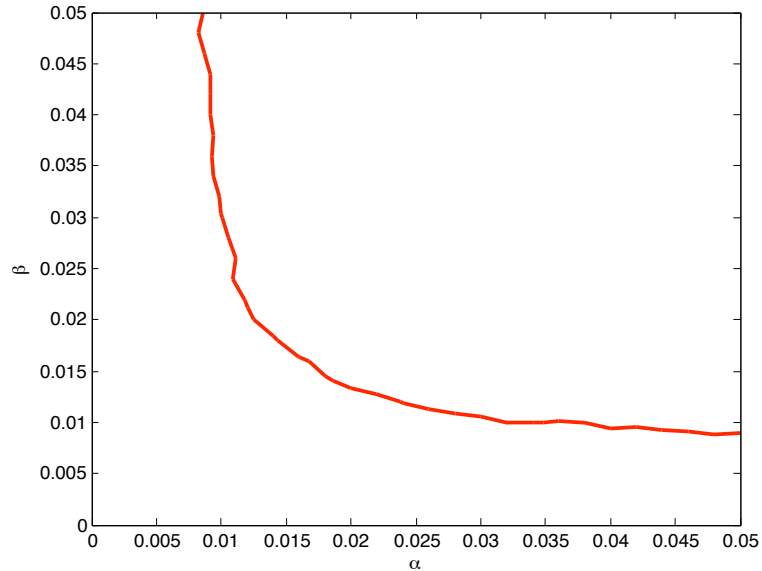


Figure 5.5: The bifurcation curve for the 1-D PCA model

The following sections mostly focus on the simulation result with different scenarios for the 2-D PCA mode. Later, we compare the simulation results between the 1-D and 2-D PCA model for further analysis.

5.8 Scenario and Simulation Results for 2D PCA Model

We begin with investigating a scenario where we fix (α_{ca}) and increase the influence on drug users (β), in small steps ($\Delta\beta = 0.005$) in a 70×70 grid lattice. We run the model for 3000 iteration and compute the mean prevalence of dealers over the last 1000 runs. The mean prevalence of dealers where $\alpha_{ca} = 0.01$ for the range of $\beta_{ca} = (0.25...0.05)$ is roughly 30% (see Figure 5.6).

We then set the social influences of dealers on susceptibles to zero, ($\alpha_{ca} = 0$), to investigate the scenario when susceptible receive no influence from their neighbors. As expected, the mean prevalence of Light users (yellow) and eventually drug dealers (red) fall sharply and the number of Susceptibles (green) rise very fast. Since no new dealer can be recruited without the social influences α_{ca} , the prevalence of dealers can not sustain itself (see Figure 5.7).

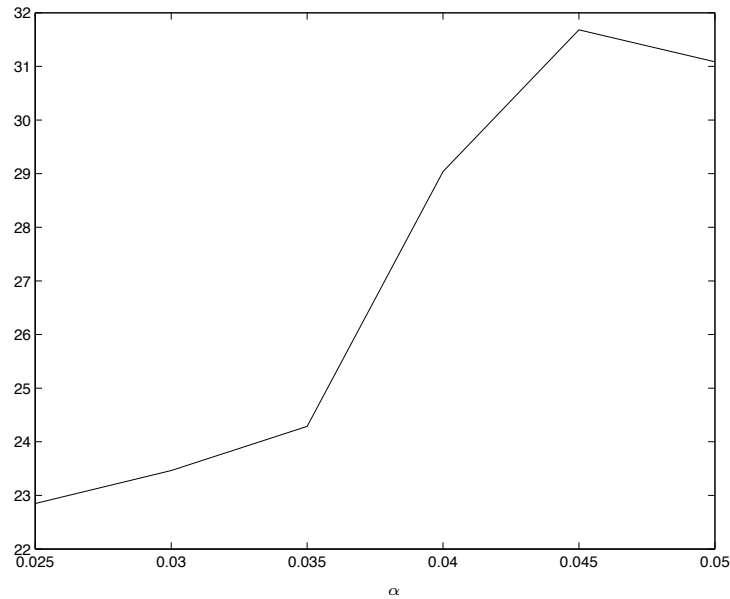


Figure 5.6: Mean prevalence of dealers in the 2-D CA model

We then set $\beta_{ca} = 0$ which represents no encouragement for drug dealing in the model. The mean prevalence of drug dealers (red) falls over the time evolution, since there are no influences from dealers on drug users. Note that the mean prevalence for light users (yellow) sustains as ($\alpha_{ca} \neq 0$) thus some transitions happen from susceptible to light users through the social influence α_{ca} (see Figure 5.8).

We also investigate a scenario when both the social influences (α_{ca} and β_{ca}) is included, where the drug using/dealing encouragement is prevalent. As its been shown in Figure 5.9 the mean prevalences of drug users and dealers are self-sustain. Figure 5.9 shows the time evolution of the CA model when $\alpha_{ca} = 0.01$ and $\beta_{ca} = 0.03$.

So far we have found the combination of $\alpha_{ca} = 0.01$ and $\beta_{ca} = 0.03$ such that the mean prevalence for dealer has become lowered with respect to the two other prevalence. These values for α_{ca} and β_{ca} were obtained through trial and error. In the next Section 5.8.1 we explore the phase diagram of the 2D CA model which is a systematical way to find all the

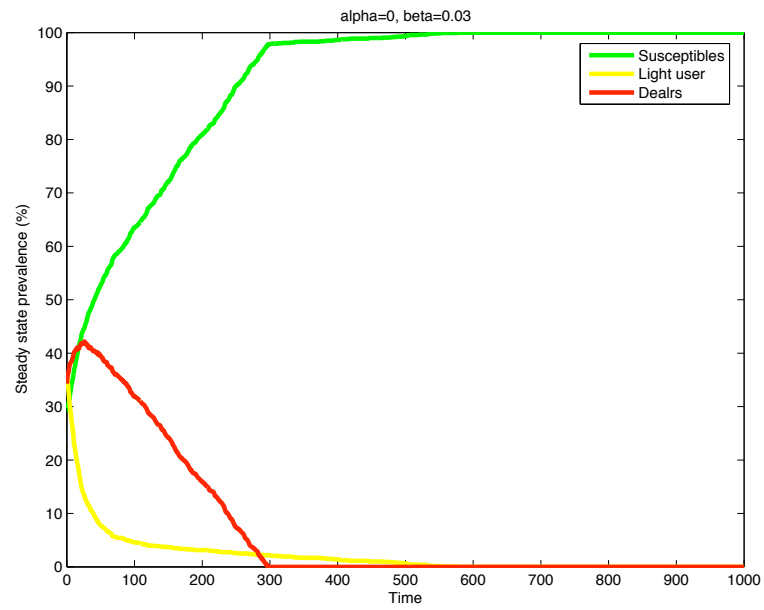


Figure 5.7: Time evolution (month) of the 2-D CA, with no influences from dealer on susceptibles

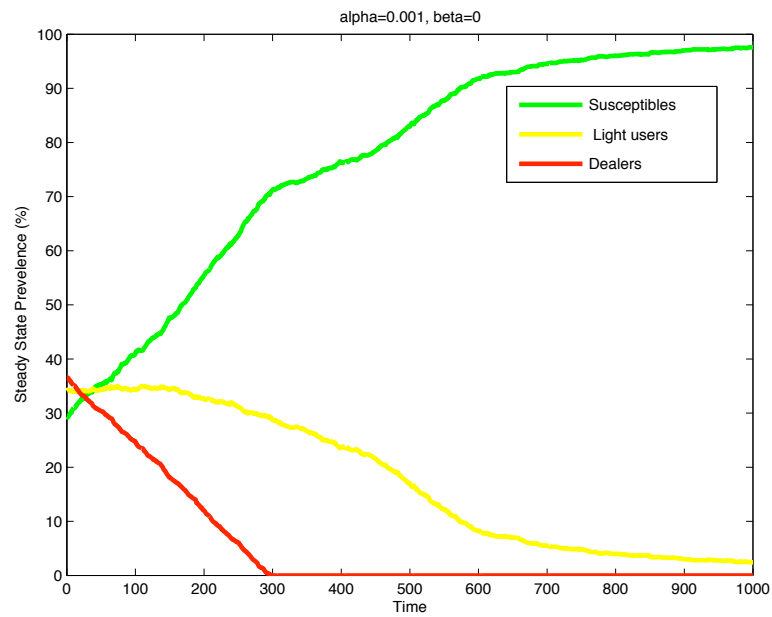


Figure 5.8: Time evolution (month) of the 2-D CA model, with no influences from dealers on light users

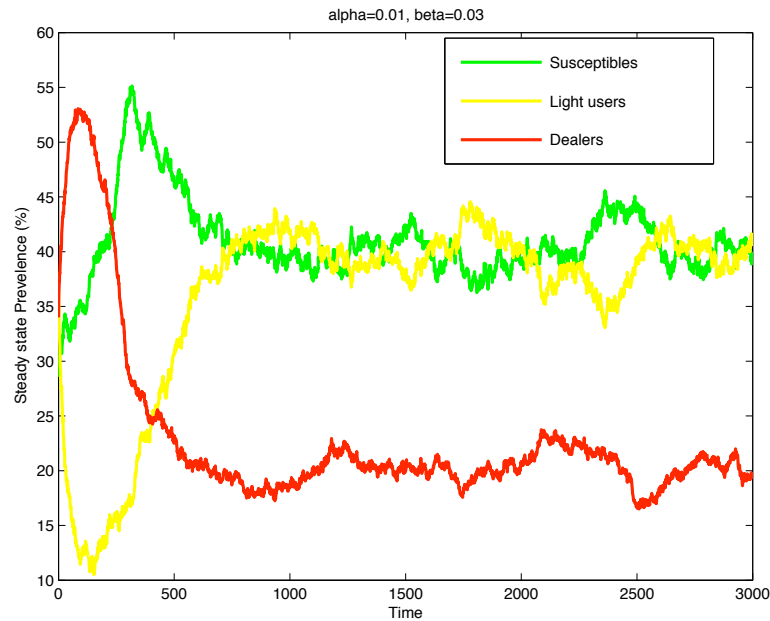


Figure 5.9: Time evolution (month) of the 2-D CA model, when social influences on both susceptibles and drug users are included

combination of $(\alpha_{ca}, \beta_{ca})$ point which drives the number of dealers to an extinction.

5.8.1 Phase Diagram for 2-D PCA Model

We construct a three dimension phase diagram for the same range value of α_{ca} and β_{ca} that was used in the simulation of the 1-D CA model (see Figure 5.10). The projection of the mean prevalences of dealers on the α_{ca} and β_{ca} is also presented in Figure 5.11. Note that the blue and red region are divided by a curve which is the *Bifurcation Curve* for the 2-D CA model.

The points below the curve are the combinations of α_{ca} 's and β_{ca} 's that drive the prevalence of dealers to an extinction state (0%-30%) in which above that the mean prevalence is highest. This means for those $(\alpha_{ca}, \beta_{ca})$ points below the curve drug problem can be eliminated. Note that α_{ca} and β_{ca} are the probability that dealers in the neighborhood act independently to convince an individual to use or deal drugs respectively, (see Section 5.2).

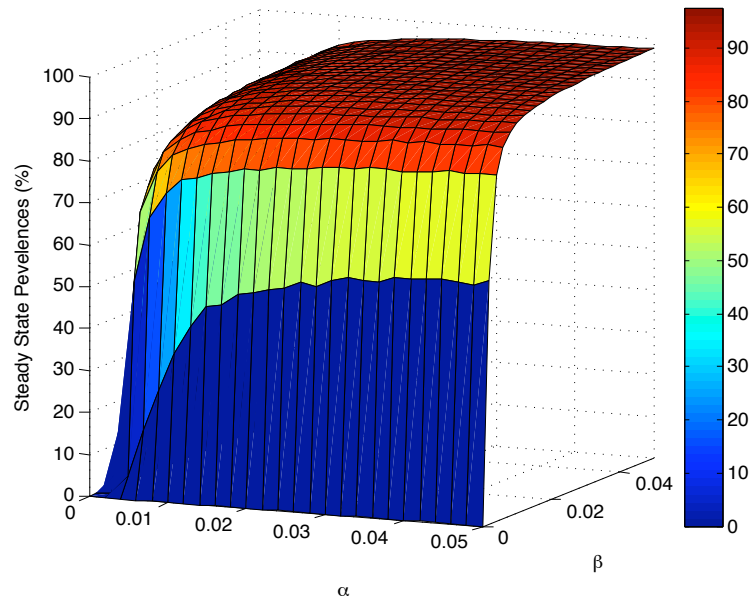


Figure 5.10: Phase diagram of the mean prevalence of dealers for the 2-D CA model

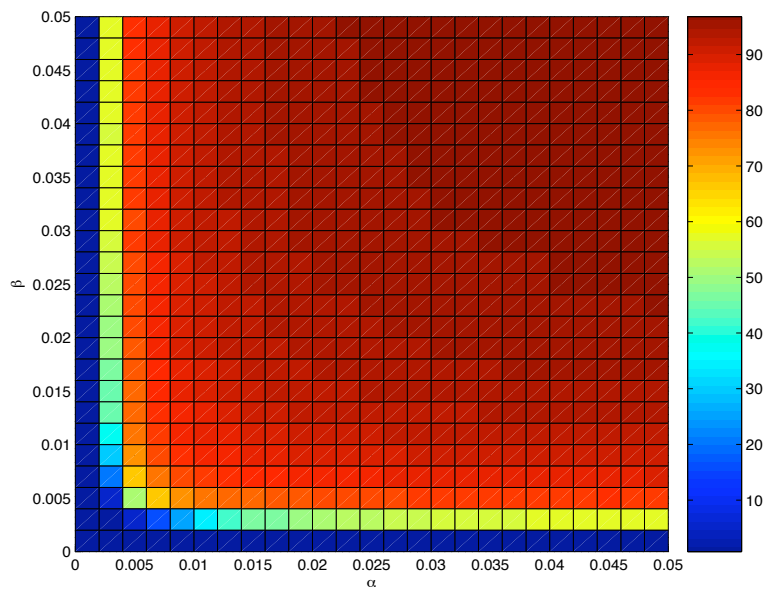


Figure 5.11: Rotated phase diagram for the 2-D CA model

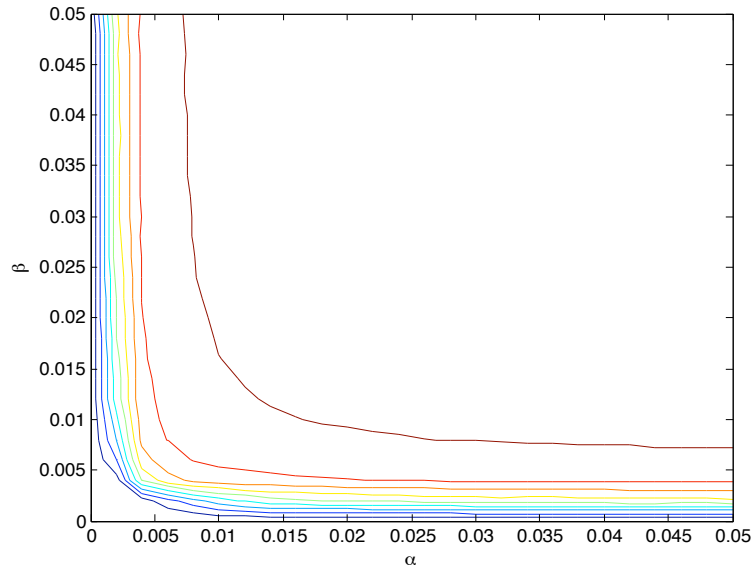


Figure 5.12: Contour plots for the phase diagram

We find the $(\alpha_{ca}, \beta_{ca})$ points that correspond to the mean prevalence of dealers in the range (35%-40%) in Figure 5.12 and we sketch the bifurcation curve for the 2-D PCA model (see Figure 5.13).

5.9 Simulation Result Comparison Between 1-D and 2-D CA Model

A comparison between the result for 1-D and 2-D case shows the importance role of the social influences in spreading drug using/ dealing behavior in a community. To show this we compare the bifurcation curves and the time evaluation of the PCA model to understand the impact of the social influence on spreading drug use.

We compare the bifurcation curves for 1-D and 2-D CA models which we obtained in previous sections. Figure 5.14 shows both bifurcation curves for 1-D and 2-D models in one plot for a better visualization. The red and blue curves correspond to the bifurcation curves for the $N = 2$ and $N = 4$ neighborhood sizes. Note that less reduction for α_{ca} and β_{ca} is required to reach to the bifurcation curve for the 1-D (red curve) than the 2-D CA model.

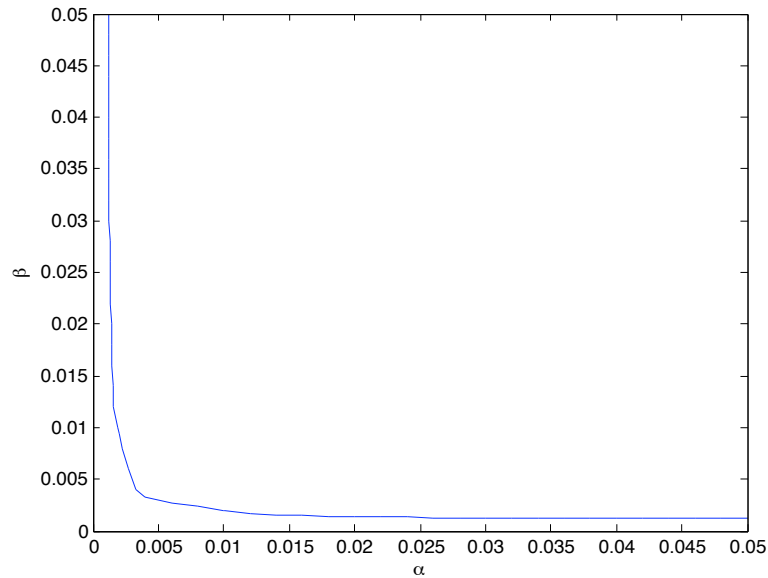


Figure 5.13: The bifurcation curve for the 2-D PCA model

Reduction for α_{ca} and β_{ca} can be viewed as primary prevention intervention and secondary prevention intervention, respectively. So, the less social influences in smaller neighborhood will result in a lower need for intervention.

The simulation result also shows that a person who has more dealers in the neighborhood is more likely to experiment drug use. Figure 5.15 is the time evolutions of 1-D and 2-D CA models for the neighborhood sizes of $N = 2$ and $N = 4$, respectively. The time evolution of CA model has obtained for the range of $\alpha_{ca} = 0 \cdots 0.5$ and $\beta_{ca} = 0 \cdots 0.5$ and neighborhood sizes of $N = 2$ and $N = 4$. Note that the mean prevalence of dealers (red curves) reaches to approximately 90% for the neighborhood sizes of $N = 2$ and to 100% for $N = 4$.

Its worth mentioning that, the mean prevalence of dealers increases by 10% when the size of neighborhood becomes larger, $N = 4$. This means, the mean prevalence of dealers changes as a function of the neighborhood size.

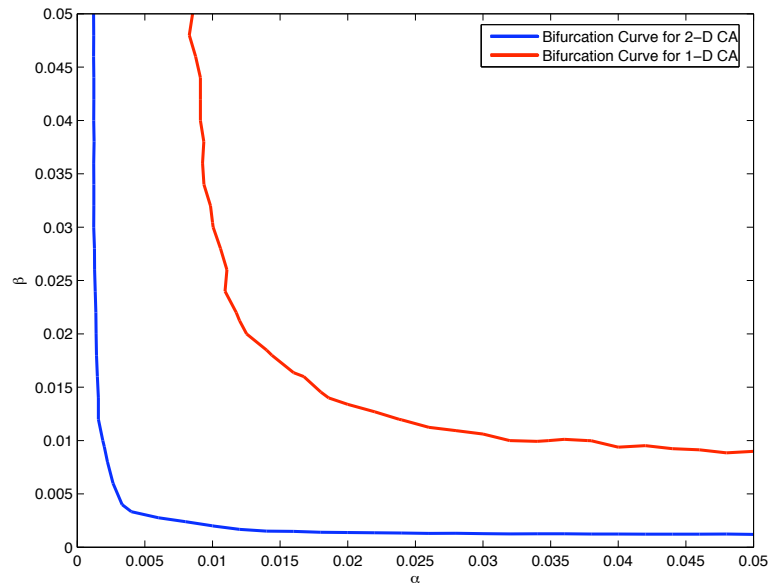


Figure 5.14: Phase diagram for the drug use epidemic, for 1-D CA with $N = 2$ neighbors (red curve) and 2-D CA with $N = 4$ neighbors (blue curve).

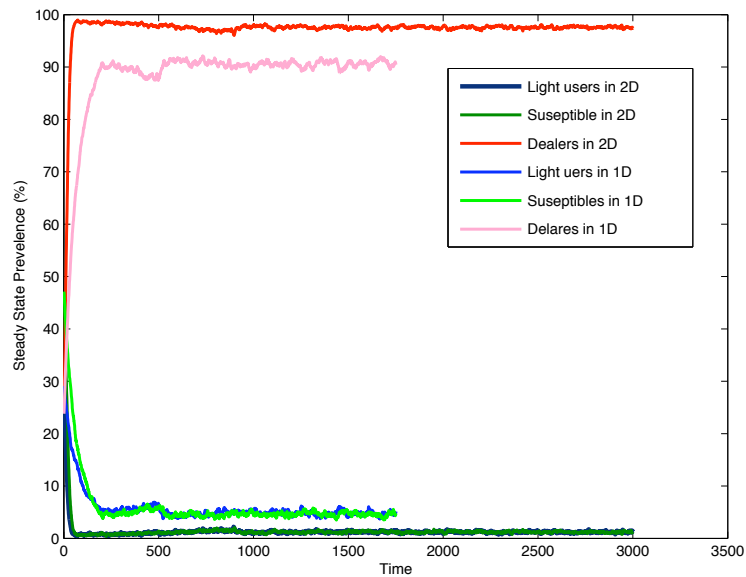


Figure 5.15: Time evolution (month) of the impact of social interaction on the spread of drug use, for the neighborhood sizes of $N = 2$ and $N = 4$.

Chapter 6

Mean Field Approximation

The Probabilistic Cellular Automata (PCA) model developed in Chapter 5, was used to evaluate the impact of social influences in the spread of drug use behavior in down town east side (DTES) Vancouver. We studied personal interactions among drug users/dealers at the micro level. The simulation presented in Chapter 5 demonstrated the importance of social factors in driving the problematic drug users/trade to the various states.

In this chapter we first perform the mean field approximation for the 1-D and 2-D PCA model. Then we generalize the result for the higher dimension and larger neighborhood configurations of the same model.

Interestingly, the approximation up to 2nd order in densities reproduces the scaled constant population equations which corresponds to the compartmental model (6.13).

6.1 MFA for the 1-D PCA Model

Recall the probabilistic CA model for the drug users community in Chapter 5. The model is a three states, $k = 3$, CA where the states 0,1, and 2 refers to susceptibles, light users and dealers, respectively. Two types of interaction exist in the model such as *social influence* and *transitions*. We let α_{ca} and β_{ca} to be the probabilities that a susceptible become a users

and a light user become a dealer after a lengthy relationship with a dealer. We also defined δ_{ca} be the death rate for all three groups. In the PCA model cells were updated according to the rules ϕ (defined in Chapter 5.4).

Here we perform MFA for 1-D (see Section 4.3) PCA model with three states, $k = 3$ which are 0, 1 and 2, and radius neighborhood of $r = 1$ with neighborhood size of $N = 2$. We let q , p and $(1 - p - q)$ be the probability that of a random given site being in state 0, 1 and 2, respectively. The goal is to compute the densities and approximate the highest probability that the system will most likely be in.

First we consider the average prevalence of the three groups. These prevalences are given in Tabel 5.3. This means we no longer assume that every site is only interacting with the four nearest neighbors defined in *von Neumann* neighborhood. We assume that sites in CA are interacting with the average prevalence in CA. In another words we replace the CA with an external background field.

Next, we describe the $k^{2r+1} = 3^3 = 27$ (see Section 4.7) possible neighborhood by the average densities of 0, 1 and 2's at time ' t ', μ, ρ, ζ . The time evolution of μ and ρ under the rule ' ϕ ' (defined in the Section 5.4) are given by the system of equations:

$$\begin{aligned} \frac{d\mu}{dt} &= (f_{1 \rightarrow 0} + f_{2 \rightarrow 0}) - (f_{0 \rightarrow 1} + f_{0 \rightarrow 2}) \\ \frac{d\rho}{dt} &= (f_{0 \rightarrow 1} + f_{2 \rightarrow 1}) - (f_{1 \rightarrow 0} + f_{1 \rightarrow 2}) \end{aligned} \quad (6.1)$$

Note that the equalities in the system of equations (6.1) hold only when the size of CA is large. In this case change in densities is equal to change in probability transitions.

$f_{i \rightarrow j}$'s are the probability transitioning of sites from $\sigma = i$ to $\sigma = j$. These probabilities are obtained by observing the probability ' P ' of having the 3-tuple $\vec{\sigma} = \langle \sigma_1, \sigma_2, \sigma_3 \rangle$ appear in a neighborhood:

$$P(\vec{\sigma}) = (p^{\#_0(\sigma)})(q^{\#_1(\sigma)})(1 - p - q)^{\#_2(\sigma)}$$

where $\#_0(\sigma), \#_1(\sigma), \#_2(\sigma)$ is the number of occurrences of the digit $\{0, \dots, 2\}$ in the neighborhood.

$$\begin{aligned} f_{i \rightarrow j} &= \sum_{\{\vec{\sigma} | \sigma_2 = i, \phi(\sigma_1, \sigma_2, \sigma_3) = j\}} P(\sigma_1, \sigma_2, \sigma_3), \\ f_{j \rightarrow i} &= \sum_{\{\vec{\sigma} | \sigma_2 = j, \phi(\sigma_1, \sigma_2, \sigma_3) = i\}} P(\sigma_1, \sigma_2, \sigma_3). \end{aligned} \quad (6.2)$$

We obtain average fractions using the equations (6.2) and substitute them in to the system of equations in (6.1) in order to estimate the changes in densities.

Note that $f_{2 \rightarrow 1} = 0$ and $f_{0 \rightarrow 2} = 0$ due to definition of the PCA model in Chapter 5 which are the probability transition from dealer to light users and susceptible to dealers. So the equations become:

$$\begin{aligned} \frac{d\mu}{dt} &= (f_{1 \rightarrow 0} + f_{2 \rightarrow 0}) - (f_{0 \rightarrow 1}) \\ \frac{d\rho}{dt} &= (f_{0 \rightarrow 1}) - (f_{1 \rightarrow 0} + f_{1 \rightarrow 2}) \end{aligned} \quad (6.3)$$

Recall that in the PCA model described in Chapter 5 every dead cell is replaced by a susceptible. So the only way for the cells transition back to be susceptible is by death. Here we define δ_{ca} as the probability that a dealer or a light user being in state 0. for example, $f_{1 \rightarrow 0} = \delta_{ca}p$, where δ_{ca} is defined the death rate for each group in the model.

$$f_{1 \rightarrow 0} = \delta_{ca}p \quad (6.4)$$

$$f_{2 \rightarrow 0} = \delta_{ca}(1 - p - q) \quad (6.5)$$

Notice that how the probability transitioning from state 0 to 1 is a multiple of the probabilities. More specifically, this probability is given by the probability that a person is a susceptible who survives $(1 - \delta_{ca})$, and has at least a dealer neighbor in the neighborhood $(1 - p - q)$. The same scenario holds for the probability transition from state 1 to 2 as well. After simplification the probability transitions are given by:

$$\begin{aligned}
f_{0 \rightarrow 1} &= (1 - \delta_{ca})\alpha_{ca}q(1 - p - q)(2 - \alpha_{ca}(1 - p - q)) \\
f_{1 \rightarrow 2} &= (1 - \delta_{ca})\beta_{ca}p(1 - p - q)(2 - \beta_{ca}(1 - p - q))
\end{aligned} \tag{6.6}$$

So, we substitute the probability transitions in (6.3):

$$\begin{aligned}
\frac{d\mu}{dt} &= \delta_{ca}p + \delta_{ca}(1 - p - q) - (1 - \delta_{ca})\alpha_{ca}q(1 - p - q)(2 - \alpha_{ca}(1 - p - q)), \\
\frac{d\rho}{dt} &= 2(1 - \delta_{ca})\alpha_{ca}q(1 - p - q) - \delta_{ca}p - (1 - \delta_{ca})\beta_{ca}p(1 - p - q)(2 - \beta_{ca}(1 - p - q))
\end{aligned} \tag{6.7}$$

We simplify and expand the equations in (6.7) and we get:

$$\begin{aligned}
\frac{d\mu}{dt} &= \delta_{ca}p + \delta_{ca}(1 - p - q) - 2(1 - \delta_{ca})\alpha_{ca}q(1 - p - q) + (1 - \delta_{ca})\alpha_{ca}^2q(1 - p - q)^2, \\
\frac{d\rho}{dt} &= -\delta_{ca}p + 2(1 - \delta_{ca})(\alpha_{ca}q - \beta_{ca}p)(1 - p - q) + (1 - \delta_{ca})\beta_{ca}^2p(1 - p - q)^2.
\end{aligned} \tag{6.8}$$

The system of equations in (6.14) are the mean field approximation (MFA) for the 1-D PCA model.

Next, we aim for the compartmental representation of the PCA model which is defined as a system of differential equations. We perform further analysis on the mean field equations which include finding the number of equilibriums and performing stability analysis using the bifurcation theory of differential dynamical system explained in Chapter 3.

6.2 Compartmental Representation of the Model

The presented compartmental model is motivated by Werb et al in [4]. According to their findings dealers are constantly encouraging street-involved youth to use/trade drugs. Most of street-involved youth are convinced to do so as they need to generate income to pay for their own personal drug use. The mathematical model we have developed models how a susceptible can move from/to a compartment and start a drug user/trade career, after a

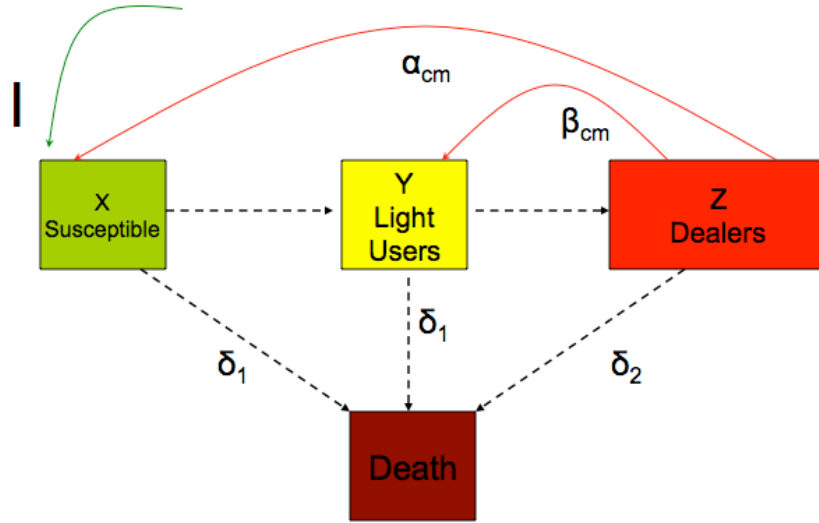


Figure 6.1: Model of the social influences Among Community of Drug Users

lengthly relation with dealers.

In order to write the deterministic equations, we introduce some known and unknown parameters. First we assume the change in the population is zero and the death rate δ_1 is the same for susceptible and light users. However, dealers are known to have a higher death rate, δ_2 . The parameter α_{cm} and β_{cm} is defined as the interaction between dealers with susceptible and light users, respectively.

6.3 Constant Population Equations

We set the total population to be, N , constant and we assume the rate of change in the population is zero $\frac{d}{dt}(x + y + z) = 0$. So the nonlinear system of constant population equations are as follows:

$$\begin{aligned}
 \frac{dX}{dt} &= I - \delta_1 X - \alpha_{cm} X Z \\
 \frac{dY}{dt} &= -\beta_{cm} Y Z + \alpha_{cm} X Z - \delta_1 Y \\
 \frac{dZ}{dt} &= \beta_{cm} Y Z - \delta_2 Z
 \end{aligned} \tag{6.9}$$

So, the unknowns are X , Y and Z which are in order the number of Susceptibles, Light users and Dealers. Note that *demographic input* is $I = \delta_1(X + Y) + \delta_2Z$ so we substitute it in to the equation(6.9).We also let $\delta_1 = \delta_2 = \delta$ for simplicity and further analysis.

$$\begin{aligned}\frac{dX}{dt} &= \delta Y + \delta Z - \alpha_{\text{cm}} X Z \\ \frac{dY}{dt} &= -\beta_{\text{cm}} Y Z + \alpha_{\text{cm}} X Z - \delta Y \\ \frac{dZ}{dt} &= \beta_{\text{cm}} Y Z - \delta Z\end{aligned}\tag{6.10}$$

Then we scale the system of equations (6.10) by dividing it by N (total population) and let $x = \frac{X}{N}$, $y = \frac{Y}{N}$, $\tilde{\alpha}_{\text{cm}} = \alpha_{\text{cm}}N$, and $\tilde{\beta}_{\text{cm}} = \beta_{\text{cm}}N$. So the system of equations become:

$$\begin{aligned}\frac{dx}{dt} &= \delta y + \delta z - \tilde{\alpha}_{\text{cm}} x z \\ \frac{dy}{dt} &= -\tilde{\beta}_{\text{cm}} y z + \tilde{\alpha}_{\text{cm}} x z - \delta y \\ \frac{dz}{dt} &= \tilde{\beta}_{\text{cm}} y z - \delta z\end{aligned}$$

Since $\frac{d}{dt}(x + y + z) = 0$ we can consider the first two equations only with the constraint $x + y + z = 1$. So the system of equation becomes:

$$\frac{dx}{dt} = \delta y + \delta z - \tilde{\alpha}_{\text{cm}} x z\tag{6.11}$$

$$\frac{dy}{dt} = -\tilde{\beta}_{\text{cm}} y z + \tilde{\alpha}_{\text{cm}} x z - \delta y\tag{6.12}$$

$$x + y + z = 1$$

We solve for z and substitute $z = 1 - x - y$ in to the equations (6.11) and (6.12). After simplification we obtain the compartmental model equations:

$$\begin{aligned}\frac{dx}{dt} &= \delta - (\delta + \tilde{\alpha}_{\text{cm}})x + \tilde{\alpha}_{\text{cm}}xy + \tilde{\alpha}_{\text{cm}}x^2 \\ \frac{dy}{dt} &= \tilde{\alpha}_{\text{cm}}x - (\tilde{\beta}_{\text{cm}} + \delta)y - \tilde{\alpha}_{\text{cm}}x^2 + \tilde{\beta}_{\text{cm}}y^2 + (\tilde{\beta}_{\text{cm}} - \tilde{\alpha}_{\text{cm}})xy\end{aligned}\tag{6.13}$$

Note that x, y are densities of susceptibles and light users in the compartmental model. Consider the mean field approximation (MFA) equations we obtained in Section 6.1 when

$p, q, (1-p-q)$ are also densities of susceptibles and light users and dealers in the CA model.

$$\begin{aligned}\frac{d\mu}{dt} &= \delta_{ca}p + \delta_{ca}(1-p-q) - 2(1-\delta_{ca})\alpha_{ca}q(1-p-q) + (1-\delta_{ca})\alpha_{ca}^2q(1-p-q)^2, \\ \frac{d\rho}{dt} &= -\delta_{ca}p + 2(1-\delta_{ca})(\alpha_{ca}q - \beta_{ca}p)(1-p-q) + (1-\delta_{ca})\beta_{ca}^2p(1-p-q)^2.\end{aligned}\quad (6.14)$$

We neglect the third or higher order terms in densities in the system of equations (6.14) and we get:

Hence, we have:

$$\begin{aligned}\frac{d\mu}{dt} &= \delta_{ca}p + \delta_{ca}(1-p-q) - 2(1-\delta_{ca})\alpha_{ca}q(1-p-q), \\ \frac{d\rho}{dt} &= -\delta_{ca}p + 2(1-\delta_{ca})(\alpha_{ca}q - \beta_{ca}p)(1-p-q).\end{aligned}\quad (6.15)$$

We expand the equations in (6.15):

$$\begin{aligned}\frac{d\mu}{dt} &= \delta_{ca}(1-q) - 2(\alpha_{ca}(1-\delta_{ca})(q-pq-q^2)), \\ \frac{d\rho}{dt} &= 2(\alpha_{ca}(1-\delta_{ca})(q-pq-q^2)) - \delta_{ca}p - 2(\beta_{ca}(1-\delta_{ca})(p-p^2-pq))\end{aligned}\quad (6.16)$$

So we collect terms in the equations (6.16). Hence, we have:

$$\begin{aligned}\frac{d\mu}{dt} &= \delta_{ca} - (\delta_{ca} + 2(1-\delta_{ca})\alpha_{ca})q + (2(1-\delta_{ca})\alpha_{ca})q^2 + (2(1-\delta_{ca})\alpha_{ca})pq, \\ \frac{d\rho}{dt} &= (2\alpha_{ca}(1-\delta_{ca}))q + (-\delta_{ca} - 2\beta_{ca}(1-\delta_{ca}))p - (2\alpha_{ca}(1-\delta_{ca}) - 2\beta_{ca}(1-\delta_{ca}))pq \\ &\quad - (2\alpha_{ca}(1-\delta_{ca}))q^2 + (2\beta_{ca}(1-\delta_{ca}))p^2\end{aligned}\quad (6.17)$$

Now, we let $\tilde{\delta}_{ca} = \delta_{ca}$, $\tilde{\alpha}_{ca} = 2\alpha_{ca}(1-\delta_{ca})$ and $\tilde{\beta}_{ca} = 2\beta_{ca}(1-\delta_{ca})$. So the system of equations become:

$$\begin{aligned}\frac{d\mu}{dt} &= \tilde{\delta}_{ca} - (\tilde{\delta}_{ca} + \tilde{\alpha}_{ca})q + \tilde{\alpha}_{ca}pq + \tilde{\alpha}_{ca}q^2 \\ \frac{d\rho}{dt} &= \tilde{\alpha}_{ca}q - (\tilde{\delta}_{ca} + \tilde{\beta}_{ca})p - \tilde{\alpha}_{ca}q^2 + \tilde{\beta}_{ca}p^2 + (\tilde{\beta}_{ca} - \tilde{\alpha}_{ca})pq\end{aligned}\tag{6.18}$$

Remark 1. *The compartmental model equations in (6.13) are the same as the mean field approximation equations in (6.18) provided that we drop third or higher order terms in densities. We then make the following identifications: $x \leftrightarrow \mu$, $y \leftrightarrow \rho$, $\delta = \delta_{ca}$, $\tilde{\alpha}_{cm} = 2\alpha_{ca}(1 - \delta_{ca})$, and $\tilde{\beta}_{cm} = 2\beta_{ca}(1 - \delta_{ca})$.*

So, we have proved the following theorems:

Theorem 6.3.1. *Compartmental model equations are the same as the mean field approximation for the 1-D CA provided that we do the followings:*

(i) *Drop terms of 3nd or higher order in densities.*

(ii) *Equate the function of the coefficients:*

- $x \leftrightarrow \mu$, $y \leftrightarrow \rho$, and $\delta = \delta_{ca}$,
- $\tilde{\alpha}_{cm} = 2\alpha_{ca}(1 - \delta_{ca})$ and $\tilde{\beta}_{cm} = 2\beta_{ca}(1 - \delta_{ca})$.

Theorem 6.3.2. *Compartmental model equations are the same as the mean field approximation for the 2-D CA provided that we do the followings:*

(i) *Drop terms of 3nd or higher order in densities.*

(ii) *Equate the function of the coefficients:*

- $x \leftrightarrow \mu$, $y \leftrightarrow \rho$, and $\delta = \delta_{ca}$,
- $\tilde{\alpha}_{cm} = 4\alpha_{ca}(1 - \delta_{ca})$ and $\tilde{\beta}_{cm} = 4\beta_{ca}(1 - \delta_{ca})$.

6.4 Solutions to the System of Equations

We solve the system of equations in (6.13) where we set $[\frac{dx}{dt} = 0, \frac{dy}{dt} = 0]$. Note that We obtained the same equations from the MFA for the 1-D CA model in (6.18). Thus, solutions for the system of equations (6.13) are also solutions for the equations (6.18). The solutions for the system of equations (6.13) are as follow:

Clearly, $[x_1 = 1, y_1 = 0]$ is a trivial solution of the above system. Let $a := \tilde{\beta}_{\text{cm}}\tilde{\alpha}_{\text{cm}} - \delta\tilde{\alpha}_{\text{cm}} + \tilde{\beta}_{\text{cm}}\delta$. Then the two other nontrivial solutions are as follows:

$$[x_2 = \frac{a + \sqrt{a^2 - 4\tilde{\beta}_{\text{cm}}^2\tilde{\alpha}_{\text{cm}}\delta}}{2\tilde{\beta}_{\text{cm}}\tilde{\alpha}_{\text{cm}}}, \quad y_2 = \frac{\delta}{\tilde{\beta}_{\text{cm}}}] \quad \text{and} \quad [x_3 = \frac{a - \sqrt{a^2 - 4\tilde{\beta}_{\text{cm}}^2\tilde{\alpha}_{\text{cm}}\delta}}{2\tilde{\beta}_{\text{cm}}\tilde{\alpha}_{\text{cm}}}, \quad y_3 = \frac{\delta}{\tilde{\beta}_{\text{cm}}}]. \quad (6.19)$$

Note that the second and third solutions exist if and only if:

$$\tilde{\alpha}_{\text{cm}}^2(\tilde{\beta}_{\text{cm}} - \delta)^2 - 2\tilde{\alpha}_{\text{cm}}(\tilde{\beta}_{\text{cm}}^2\delta - \delta^2\tilde{\beta}_{\text{cm}}) + \tilde{\beta}_{\text{cm}}^2\delta^2 \geq 0.$$

Consider the following equation:

$$\tilde{\alpha}_{\text{cm}}^2(\tilde{\beta}_{\text{cm}} - \delta)^2 - 2\tilde{\alpha}_{\text{cm}}(\tilde{\beta}_{\text{cm}}^2\delta - \delta^2\tilde{\beta}_{\text{cm}}) + \tilde{\beta}_{\text{cm}}^2\delta^2 = 0,$$

which is a parabola in α_{cm} with positive coefficient for quadratic term. Solving the quadratic equation above for α_{cm} yields:

$$\tilde{\alpha}_{\text{cm},1} = \frac{(\delta + \tilde{\beta}_{\text{cm}} + 2\sqrt{\tilde{\beta}_{\text{cm}}\delta})\delta\tilde{\beta}_{\text{cm}}}{\tilde{\beta}_{\text{cm}}^2 - 2\tilde{\beta}_{\text{cm}}\delta + \delta^2}, \quad \text{and} \quad \tilde{\alpha}_{\text{cm},2} = -\frac{(-\delta - \tilde{\beta}_{\text{cm}} + 2\sqrt{\tilde{\beta}_{\text{cm}}\delta})\delta\tilde{\beta}_{\text{cm}}}{\tilde{\beta}_{\text{cm}}^2 - 2\tilde{\beta}_{\text{cm}}\delta + \delta^2}.$$

Physical Solutions:

Note that in the most logistic equations where we look at the growth of a group in the population, the fixed point has to be positive real and it can be at most the total population. If a fixed point has this criteria, we call the fixed point a *Physical Solution*. Now that we have found the real solutions for this system, we can discuss the positivity of these solutions. Since the denominator of the non-trivial solutions (6.19) is positive, we only need to check the sign of the numerator for these solutions:

- If $a > 0$, then $a + \sqrt{a^2 - 4\tilde{\beta}_{\text{cm}}^2 \tilde{\alpha}_{\text{cm}} \delta} > 0$ and If $a < 0$, then $a + \sqrt{a^2 - 4\tilde{\beta}_{\text{cm}}^2 \tilde{\alpha}_{\text{cm}} \delta} < 0$.
- If $a > 0$, then $a - \sqrt{a^2 - 4\tilde{\beta}_{\text{cm}}^2 \tilde{\alpha}_{\text{cm}} \delta} > 0$ and If $a < 0$, then $a - \sqrt{a^2 - 4\tilde{\beta}_{\text{cm}}^2 \tilde{\alpha}_{\text{cm}} \delta} < 0$.

So, if $a > 0$, then $x_2, x_3 > 0$ and if $a < 0$ then $x_2, x_3 < 0$.

6.5 Physical Solutions of the System

1. If $\tilde{\alpha}_{\text{cm},1} < \tilde{\alpha}_{\text{cm}} < \tilde{\alpha}_{\text{cm},2}$ or if $a < 0$, then system has only one physical solution which is the trivial solution $[x = 1, y = 0]$.
2. if $\tilde{\alpha}_{\text{cm}} > \tilde{\alpha}_{\text{cm},1}$ or $\tilde{\alpha}_{\text{cm}} < \tilde{\alpha}_{\text{cm},2}$ and if $a > 0$, then system has three physical solutions:
 - (a) $[x_1 = 1, y_1 = 0]$,
 - (b) $[x_2 = \frac{a + \sqrt{a^2 - 4\tilde{\beta}_{\text{cm}}^2 \tilde{\alpha}_{\text{cm}} \delta}}{2\tilde{\beta}_{\text{cm}} \tilde{\alpha}_{\text{cm}}}, y_2 = \frac{\delta}{\tilde{\beta}_{\text{cm}}}]$, and
 - (c) $[x_3 = \frac{a - \sqrt{a^2 - 4\tilde{\beta}_{\text{cm}}^2 \tilde{\alpha}_{\text{cm}} \delta}}{2\tilde{\beta}_{\text{cm}} \tilde{\alpha}_{\text{cm}}}, y_3 = \frac{\delta}{\tilde{\beta}_{\text{cm}}}]$.
3. if $\tilde{\alpha}_{\text{cm}} > \tilde{\alpha}_{\text{cm},1}$ or $\tilde{\alpha}_{\text{cm}} < \tilde{\alpha}_{\text{cm},2}$ and if $a = 0$, then system has one physical solution $[x_1 = 1, y_1 = 0]$.
4. if $\tilde{\alpha}_{\text{cm}} = \tilde{\alpha}_{\text{cm},1}$ or $\tilde{\alpha}_{\text{cm}} = \tilde{\alpha}_{\text{cm},2}$ and if $a > 0$ then system have two positive real solutions:
 - (a) $[x = 1, y = 0]$,
 - (b) $[x = \frac{a}{2\tilde{\beta}_{\text{cm}} \tilde{\alpha}_{\text{cm}}}, y = \frac{\delta}{\tilde{\beta}_{\text{cm}}}]$.

6.6 Analyzing the fixed points of the system

Once the fixed points are found, one would like to have a quantitative measure of stabilities, such as the rate of decay or grow to a stable or unstable fixed point. This sort of information can be obtained by *linearizing* about the fixed points using *Jacobian* of the system of equation in (6.13). The hope is that we can approximate the *phase portrait* near the fixed points by that of a corresponding linear system.

We linearize the system using Jacobian around the fixed points (see Section 3.4.2). Let Δ and τ denote the determinant and trace of the *Jacobian* evaluated at a fixed point, respectively.

6.6.1 First Fixed Point

Now we linearize the system in (6.13) around the fixed point $[x = 1, y = 0]$. The Jacobin at this point is:

$$\begin{pmatrix} -\delta + \alpha_{\text{cm}} & \alpha_{\text{cm}} \\ -\alpha_{\text{cm}} & -\alpha_{\text{cm}} - \delta \end{pmatrix}$$

There is one eigenvalue of multiplicity 2: $\lambda_1 = \lambda_2 = -\delta$. The corresponding eigenvector is:

$$\begin{pmatrix} 1 \\ -1 \end{pmatrix}.$$

Note that the eigensolution decays exponentially. So the fixed point is stable. Since there is only one eigendirection, the fixed point is a degenerate node. (see Figure 3.3.) So to analyze the nonlinear system we use the numerical method. If $\alpha_{\text{cm}} < \alpha_{\text{cm},1}$ then $[x = 1, y = 0]$ is a stable node and If $\alpha_{\text{cm}} > \alpha_{\text{cm},2}$ then this fixed point is a stable spiral.

It is easy to see that the fixed point can not be stable spiral just because in order for trajectories to wind around the fixed point $[x = 1, y = 0]$ they have to pass though negative plane $y < 0$ and that can not happen in this model so the fixed point must be a *stable node*.

6.6.2 Second Fixed Point

We linearize the system using Jacobian around $[x_2 = \frac{a + \sqrt{a^2 - 4\tilde{\beta}_{\text{cm}}^2 \tilde{\alpha}_{\text{cm}} \delta}}{2\tilde{\beta}_{\text{cm}} \tilde{\alpha}_{\text{cm}}}, y_2 = \frac{\delta}{\tilde{\beta}_{\text{cm}}}]$

Let $b = \tilde{\beta}_{\text{cm}} \tilde{\alpha}_{\text{cm}} - \delta \tilde{\alpha}_{\text{cm}} - \tilde{\beta}_{\text{cm}} \delta$. The determinant of the Jacobin matrix is:

$$\Delta = \frac{-1}{2\tilde{\alpha}_{\text{cm}} \tilde{\beta}_{\text{cm}}} (\sqrt{b^2 - 4\delta^2 \tilde{\alpha}_{\text{cm}} \tilde{\beta}_{\text{cm}}} (b - \sqrt{b^2 - 4\delta^2 \tilde{\alpha}_{\text{cm}} \tilde{\beta}_{\text{cm}}}))$$

- If $b > 0$ then $b - \sqrt{b^2 - 4\delta^2 \tilde{\alpha}_{\text{cm}} \tilde{\beta}_{\text{cm}}} > 0$. So, $\Delta < 0$. This might suggest that the fixed point is a saddle.

- If $b < 0$ then $b - \sqrt{b^2 - 4\delta^2\tilde{\alpha}_{cm}\tilde{\beta}_{cm}} < 0$. So, $\Delta > 0$. In this case we need to further investigate τ , trace of the matrix. We have

$$\tau = -\tilde{\alpha}_{cm} + \frac{\tilde{\alpha}_{cm}\delta}{\tilde{\beta}_{cm}} + \frac{a + \sqrt{a^2 - 4\tilde{\beta}_{cm}^2\tilde{\alpha}_{cm}\delta}}{\tilde{\beta}_{cm}} - \tilde{\beta}_{cm} + \frac{1}{2}(\tilde{\beta}_{cm} - \tilde{\alpha}_{cm}) \frac{a + \sqrt{a^2 - 4\tilde{\beta}_{cm}^2\tilde{\alpha}_{cm}\delta}}{\tilde{\beta}_{cm}\tilde{\alpha}_{cm}}.$$

Let $\omega = \frac{a + \sqrt{a^2 - 4\tilde{\beta}_{cm}^2\tilde{\alpha}_{cm}\delta}}{\tilde{\beta}_{cm}}$. Notice that $\frac{\omega}{2\tilde{\alpha}_{cm}} = x_2$ and $\frac{\tilde{\alpha}_{cm}\delta}{\tilde{\beta}_{cm}} = \tilde{\alpha}_{cm}y_2$ in the expression above. So, $\tau = -(\tilde{\alpha}_{cm} + \tilde{\beta}_{cm}) + \tilde{\alpha}_{cm}y_2 + \omega + (\tilde{\beta}_{cm} - \tilde{\alpha}_{cm})(x_2)$. Since x_2 and y_2 are the proportion of the population, they are small numbers. Thus $\tau < 0$. In this case $\tau^2 - 4\Delta > 0$ and the fixed point is a stable node (see Figure 3.1).

6.6.3 Third Fixed Point

The analysis of this case is very similar to the previous case. We linearize the system using Jacobian around $[x_3 = \frac{a - \sqrt{a^2 - 4\tilde{\beta}_{cm}^2\tilde{\alpha}_{cm}\delta}}{2\tilde{\beta}_{cm}\tilde{\alpha}_{cm}}, y_3 = \frac{\delta}{\tilde{\beta}_{cm}}]$. Again, we let $b = \tilde{\beta}_{cm}\tilde{\alpha}_{cm} - \delta\tilde{\alpha}_{cm} - \tilde{\beta}_{cm}\delta$. The determinant of the Jacobin matrix evaluated at this fixed point is:

$$\Delta = \frac{1}{2\tilde{\alpha}_{cm}\tilde{\beta}_{cm}} (\sqrt{b^2 - 4\delta^2\tilde{\alpha}_{cm}\tilde{\beta}_{cm}}(b + \sqrt{b^2 - 4\delta^2\tilde{\alpha}_{cm}\tilde{\beta}_{cm}})).$$

- If $b > 0$ then $b - \sqrt{b^2 - 4\delta^2\tilde{\alpha}_{cm}\tilde{\beta}_{cm}} > 0$. So, $\Delta > 0$. Now, we need to look at the trace of the matrix evaluated at this fixed point. We have:

$$\tau = -\tilde{\alpha}_{cm} + \frac{\tilde{\alpha}_{cm}\delta}{\tilde{\beta}_{cm}} - \frac{-a + \sqrt{a^2 - 4\tilde{\beta}_{cm}^2\tilde{\alpha}_{cm}\delta}}{\tilde{\beta}_{cm}} - \tilde{\beta}_{cm} - \frac{1}{2}(\tilde{\beta}_{cm} - \tilde{\alpha}_{cm}) \frac{-a + \sqrt{a^2 - 4\tilde{\beta}_{cm}^2\tilde{\alpha}_{cm}\delta}}{\tilde{\beta}_{cm}\tilde{\alpha}_{cm}}.$$

Let $\omega = \frac{a - \sqrt{a^2 - 4\tilde{\beta}_{cm}^2\tilde{\alpha}_{cm}\delta}}{\tilde{\beta}_{cm}}$. Notice that $\frac{1}{2\tilde{\alpha}_{cm}}(\omega) = x_3$ and $\frac{\tilde{\alpha}_{cm}\delta}{\tilde{\beta}_{cm}} = \tilde{\alpha}_{cm}y_3$ in the expression above. So, $\tau = -(\tilde{\alpha}_{cm} + \tilde{\beta}_{cm}) + \tilde{\alpha}_{cm}y_3 + \omega + (\tilde{\beta}_{cm} - \tilde{\alpha}_{cm})(x_3)$. Since x_3 and y_3 are the proportion of the population, they are small numbers. Thus $\tau < 0$. Also, $\tau^2 - 4\Delta > 0$. So the fixed point is a stable node .

- If $b < 0$ then $b - \sqrt{b^2 - 4\delta^2\tilde{\alpha}_{cm}\tilde{\beta}_{cm}} < 0$. Hence, $\Delta < 0$. This may suggest that the fixed point is a Saddle (see Figure 3.1). So there must be a bifurcation happening at $b = 0$.

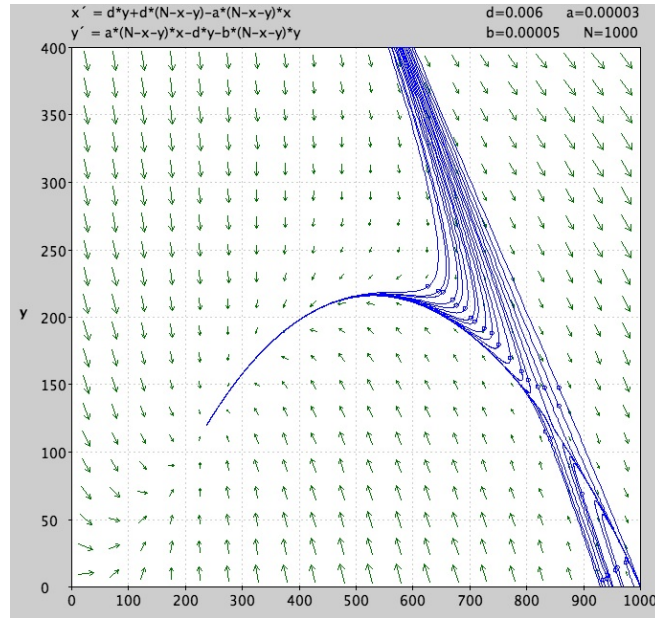


Figure 6.2: The Phase Portrait of the System

6.6.4 Phase Plane of the System

Sometimes we are interested in quantitative aspect of the fixed points. The fixed points can be represented numerically using the appropriate parameters. For a better visualization and representation of the fixed points in Figures (6.2,6.3,6.4), we use equation (6.10) where the parameter are not scaled.

The parameters estimated for this model were initially selected from Carla Rossi's paper in [5], where $\alpha_{cm} = 0.00003$, $\beta_{cm} = 0.00005$, $\delta = 0.006$ and $N = 1000$. The fixed points evaluated at the values are $[x_1 = 1000, y_1 = 0.]$, $[x_2 = 237, y_2 = 120]$, $[x_3 = 842, y_3 = 120]$. Recall that in Section 6.6 the linearization at these points predicts that the three fixed points are: degenerate node, stable node, and saddle node, respectively. Now because the two last fixed points are not borderline case, we can be certain that the fixed points for the full nonlinear system have been predicted correctly. We check our conclusion by deriving the phase plane portrait for the full nonlinear system:

Putting all this information together, we arrive at the phase portrait shown in Figure 6.2.

6.7 Bifurcations

The dynamics of vector fields on the line is very limited : all solutions either settle down to equilibrium or head out to $+\infty$ or $-\infty$. Given the triviality of dynamics sometimes, what is most interesting about the system is its dependency on the parameters. The qualitative structure of the flow can change as parameter are varied. In particular, fixed points can be created or destroyed, or their stability can change. These qualitative change in the dynamics are called *bifurcation*, and the parameter values at which they occur are called *bifurcation points*. Bifurcations are important scientifically— in this model as they provide useful information on the transitions and instabilities of the fixed points as some control parameter in the model are varied.

6.7.1 Saddle Node Bifurcation when $\tilde{\alpha}_{cm}$ Varies

As we discussed in the pervious section, the solution of the system settles down to 3 equilibrium points (Fixed points). The trivial fixed point $[x = 1, y = 0]$ which characterizes a drug-free state, exists for all the values of a parameter and can never be destroyed. The two other fixed points can be created if $\tilde{\alpha}_{cm} > \tilde{\alpha}_{cm,1}$ or $\tilde{\alpha}_{cm} < \tilde{\alpha}_{cm,2}$ and annihilated if $\tilde{\alpha}_{cm,1} < \tilde{\alpha}_{cm} < \tilde{\alpha}_{cm,2}$. So the Saddle node bifurcations happens when $\tilde{\alpha}_{cm,1} < \tilde{\alpha}_{cm} < \tilde{\alpha}_{cm,2}$. The only fixed point left is the trivial fixed point $[x = 1, y = 0]$ and it is stable (see Figure 6.3).

In this model we vary $\tilde{\alpha}_{cm}$ (Influence of dealers on susceptible and light users) where the other parameters held fixed. As a result the a Saddle Bifurcation occurs at the Bifurcation range. This means that for the values in $\tilde{\alpha}_{cm,1} < \tilde{\alpha}_{cm} < \tilde{\alpha}_{cm,2}$ the drug use problem goes extinct (eliminate drug use) and for $\tilde{\alpha}_{cm} > \tilde{\alpha}_{cm,1}$ or $\tilde{\alpha}_{cm} < \tilde{\alpha}_{cm,2}$ becomes epidemic.

6.7.2 Transcritical Bifurcation when δ Varies

For $\delta > \delta_0$, there is an unstable fixed point at $[x_3 = \frac{a - \sqrt{a^2 - 4\tilde{\beta}_{cm}^2 \tilde{\alpha}_{cm} \delta}}{2\tilde{\beta}_{cm} \tilde{\alpha}_{cm}}, y_3 = \frac{\delta}{\tilde{\beta}_{cm}}]$ (third fixed point) and a stable fixed point at $[x_1 = 1, y_1 = 0]$. As δ decrease ($\delta \rightarrow 0$), the unstable fixed point approaches the trivial fixed point $[x_1 = 1, y_1 = 0]$ and coalesces with it when

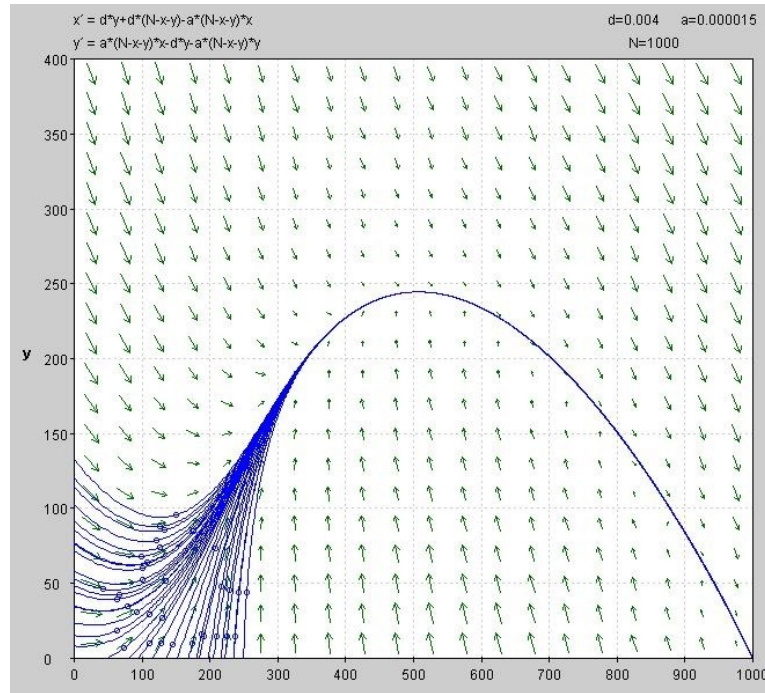


Figure 6.3: Saddle-node Bifurcation. Trivial fixed point is the only stable fixed point.

$\delta = \delta_0$. Finally $[x_1 = 1, y_1 = 0]$ has become unstable, and the nontrivial fixed point is stable. We arrive to this conclusion that the trivial fixed point has changed its stability and we numerically find the bifurcation value at $\delta_0 = 0.0000002$.

6.7.3 When $\delta = \delta_0 = 0$

Another interesting observation is when we set $\delta = 0$. The system has two completely different fixed points $[x_1 = 1 - y, y_1 = y]$ and $[x_2 = 0, y_2 = 0]$, where $x + y = 1$ is the unstable *line of fixed points* and $[x = 0, y = 0]$ is the stable fixed point (see Figure 6.4).

6.7.4 When b varies

In Section 6.6 we investigated the stability of the fixed points. We learned that the stability of the two nontrivial fixed points $[x_2, y_2]$ and $[x_3, y_3]$ is very dependent on positivity or negativity of $b = \tilde{\beta}_{cm}\tilde{\alpha}_{cm} - \delta\tilde{\alpha}_{cm} - \tilde{\beta}_{cm}\delta$. According to the classification of fixed points and our computations in Section 6.6,

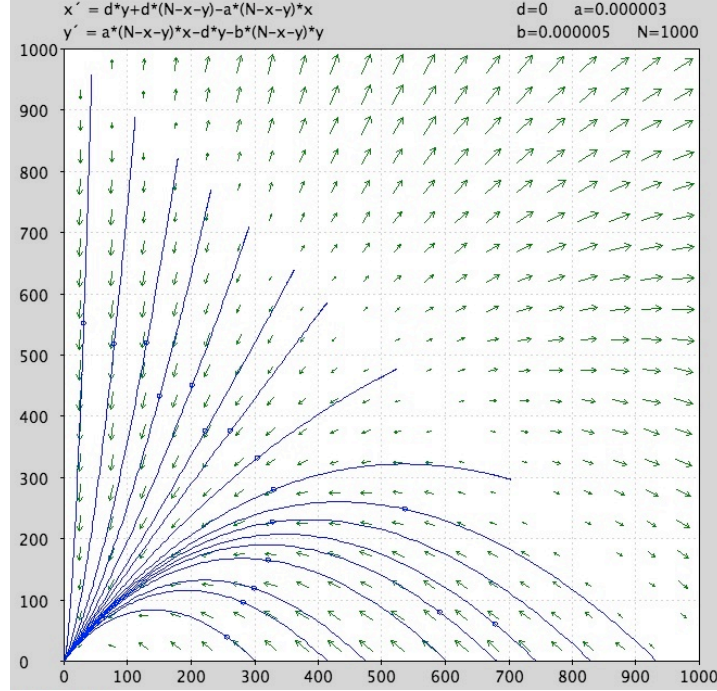


Figure 6.4: The fixed point $[x_2 = 0, y_2 = 0]$ is stable.

- if $b > 0$, that is $\tilde{\alpha}_{\text{cm}}(\tilde{\beta}_{\text{cm}} - \delta) > \tilde{\beta}_{\text{cm}}\delta$, then the second fixed point is saddle and a stable node, otherwise. So this situation occurs if $\tilde{\beta}_{\text{cm}} > \delta$.
- On the other hand, if $b < 0$, that is $\tilde{\alpha}_{\text{cm}}(\tilde{\beta}_{\text{cm}} - \delta) < \tilde{\beta}_{\text{cm}}\delta$, then the third fixed point is saddle and a stable node, So this situation occurs if $\tilde{\beta}_{\text{cm}} \leq \delta$.

Thus, there must be a bifurcation (see definition in Section 3.7.2) at $b = 0$ (see Figure 6.5 for the bifurcation curve).

We solve for $\tilde{\beta}_{\text{cm}}$ in $b = 0$ and obtain:

$$\tilde{\beta}_{\text{cm}} = \frac{\tilde{\alpha}_{\text{cm}}\delta}{-\delta + \tilde{\alpha}_{\text{cm}}}. \quad (6.20)$$

Note that bifurcation happens only at the points $(\tilde{\alpha}_{\text{cm},0}, \tilde{\beta}_{\text{cm},0})$ on the curve (6.20) and the points $(\tilde{\alpha}_{\text{cm},0}, \tilde{\beta}_{\text{cm},0})$ below the curve correspond to case when $b < 0$. Similarly the points above the curve correspond to $b > 0$. This means for those $(\tilde{\alpha}_{\text{cm},0}, \tilde{\beta}_{\text{cm},0})$ points below the curve, drug problem can be eliminated since the trivial fixed point $[x_1, y_1]$ is stable and

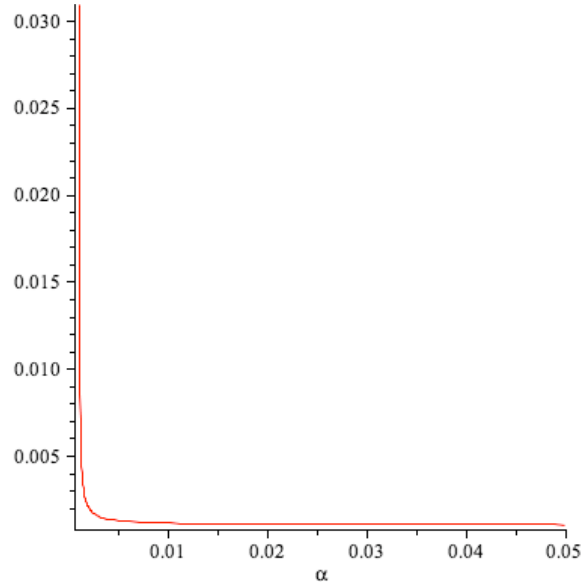


Figure 6.5: Bifurcation Curve

$[x_3, y_3]$ is an unstable fixed points.

6.8 Comparison Between Analytical Result and Simulation Result for the PCA model

We use the results of the Theorems 6.3.1 and 6.3.2 to compare the analytical result (MFA) and the simulation result for the PCA model.

Recall that the theorem for the 1-D CA stated that the compartmental model equations are the same as the mean field equations if we drop the 3rd or higher order terms and equate $\delta = \tilde{\delta}_{ca}$, $\tilde{\alpha}_{cm} = 2\alpha_{ca}(1 - \delta_{ca})$ and $\tilde{\beta}_{cm} = 2\beta_{ca}(1 - \delta_{ca})$. For the 2-D CA model, $\delta = \tilde{\delta}_{ca}$, $\tilde{\alpha}_{cm} = 4\alpha_{ca}(1 - \delta_{ca})$ and $\tilde{\beta}_{cm} = 4\beta_{ca}(1 - \delta_{ca})$.

Therefore, we substitute $\delta = \tilde{\delta}_{ca}$, $\alpha_{ca} = \frac{\tilde{\alpha}_{cm}}{2(1-\tilde{\delta}_{ca})}$ and $\beta_{ca} = \frac{\tilde{\beta}_{cm}}{2(1-\tilde{\delta}_{ca})}$ for the 1-D CA and $\delta = \tilde{\delta}_{ca}$, $\alpha_{ca} = \frac{\tilde{\alpha}_{cm}}{4(1-\tilde{\delta}_{ca})}$ and $\beta_{ca} = \frac{\tilde{\beta}_{cm}}{2(1-\tilde{\delta}_{ca})}$ for 2-D CA in the bifurcation curve equation (6.20), we obtained in Section 6.7.4.

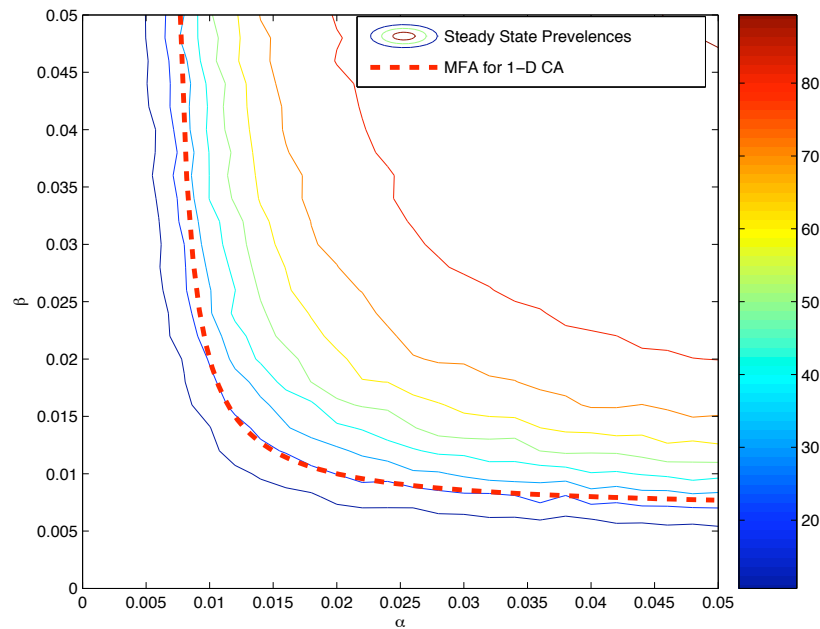


Figure 6.6: Simulation result and the mean field approximation (red dashed line) for 1-D PCA

The goal is to understand how well the compartmental model approximates the simulation result for different dimensions of the PCA model. Figure 6.6 and 6.7 show that the compartmental model generally gives a good approximation for the PCA model near the bifurcation. Note that the red dashed lines in these plots are matched with the curves in Figure 5.14 in Chapter 5.

6.9 Totalistic PCA

Recall the PCA model for the DTES where each cell can change its state with a given probability (see (5.1)). The probability of change for each cell is depend on the *Total* number of dealers in the neighborhood and the value of α_{ca} or β_{ca} . In next section we describe the *Totalistic PCA*. The plan is to use the totalistic PCA and perform the MFA for the neighborhood size of $N = n$ for the PCA model.

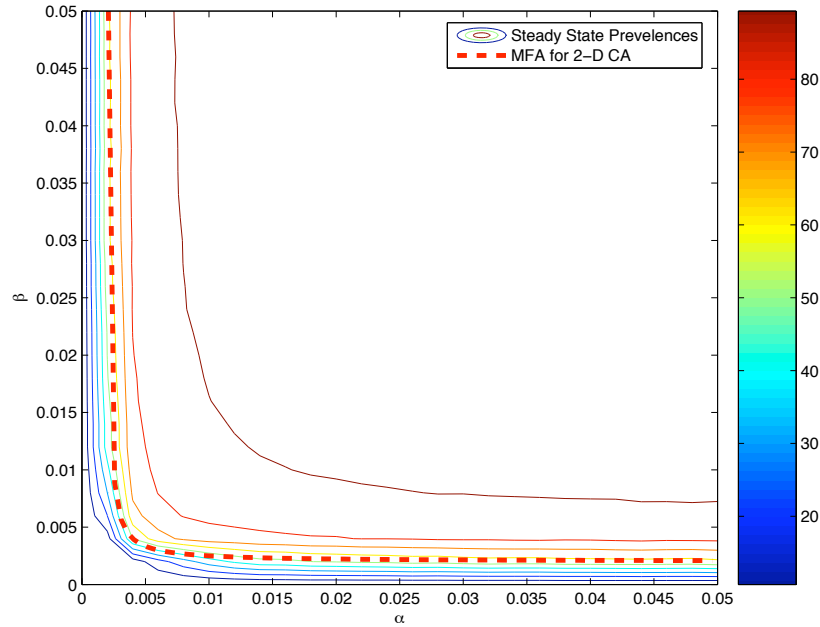


Figure 6.7: Simulation result and the mean field approximation (red dashed line) for 2-D PCA

The definition of the Totalistic PCA is based on the book by ‘*Andrew Ilachinski*’ in [24].

Consider the set of totalistic PCA, defined by the set of conditional probabilities $\{P_0, \dots, P_{|N|}\}$, $P_k = \mathbf{prob}(\sigma_i(t+1) = 1 | \sum_{j \in N_i} \sigma_j(t) = k)$ is the probability that a given site will have value ‘ a ’ at time $t+1$ given that the sum of its neighbors at time t equals k . Using $\rho_\sigma(t)$ to estimate the probability of finding value $\sigma = ‘a’$ at any site at time t , the probability that a given site has exactly k neighbors, $p_k(t)$, is given by:

$$p_k(t) = \binom{|N|}{k} [\rho_\sigma(t)]^k (1 - \rho_\sigma(t))^{|N|-k},$$

and , thus,

$$\rho_\sigma(t+1) = f[\rho_\sigma(t)] = \sum_{k=0}^{|N|} \binom{|N|}{k} [\rho_\sigma(t)]^k (1 - \rho_\sigma(t))^{|N|-k} \cdot (P_k), \quad (6.21)$$

Where $f(x)$ is the *iterative* function.

The possible asymptotic, or equilibrium, value of the density $\rho_\sigma^* \equiv \lim_{t \rightarrow \infty} \rho_\sigma(t)$ are obtained by solving for the stable fixed points of the equation $\rho_\sigma = f(\rho_\sigma)$. A given solution ρ_σ is stable if $|f'(\rho_\sigma)| < 1$ [24].

6.10 Generalized Mean Field Approximation for the PCA

We performed the mean field approximation for 1-D PCA model for DTES in section 6.1. Here, we use the totalistic PCA method (described in Section 6.9) to perform the MFA with neighborhood sizes of $N = n$ for PCA model. We consider the PCA with three states, $k = 3$, radius neighborhood of $r = 1$ and neighborhood size of $N = n$. Again we let q , p and $(1 - p - q)$ be the probability that of a given site being in state 0, 1 and 2, respectively. The average densities of zero, ones and twos are given by of μ , ρ and ζ under the PCA transition rules (see Section 5.4). The time evolution of μ , ρ are:

$$\begin{aligned}\frac{d\mu}{dt} &= (f_{1 \rightarrow 0} + f_{2 \rightarrow 0}) - (f_{0 \rightarrow 1}) \\ \frac{d\rho}{dt} &= (f_{0 \rightarrow 1}) - (f_{1 \rightarrow 0} + f_{1 \rightarrow 2})\end{aligned}$$

So we seek to find the probability transitions ($f_{i \rightarrow j}$) of sites whose values changes from $\sigma = i$ to $\sigma = j$. Our goal is to approximate the system's behavior, given the number of dealer neighbors in the neighborhood.

We let $p_n(t)$ be the probability that a given site has exactly n dealer neighbors where $|N|$ is the neighborhood size. So this probability is given by:

$$p_n = \binom{|N|}{n} [(1 - p - q)]^n (p + q)^{|N| - n},$$

We define $z = |\{j \in N_i | \sigma_j(t) = 2\}|$ be the number of dealers (type '2') in the neighborhood and let $P_n = \mathbf{prob}(\sigma_i(t+1) = 1 | z = n)$ be the probability that a given site which has value '0' will have value '1' at time $t + 1$ under the influence of n dealer neighbors. In another words P_n is the probability transiting from susceptible to light users under the influence of dealers. So, the probability that a susceptible become a drug users under the influence of at least one dealer neighbor is given by:

$$P_n = 1 - (1 - \alpha_{ca})^n q.$$

Thus, $\rho(t+1)$ is the probability of finding $\sigma = '1'$ at time $(t+1)$ and is given by (see the definition (6.21)):

$$\rho(t+1) = f[\rho(t)] = \sum_{n=1}^{|N|} \binom{|N|}{n} [(1-p-q)]^n (p+q)^{|N|-n} 1 - (1 - \alpha_{ca})^n q.$$

It follows that $\rho(t+1) \cdot (1 - \delta_{ca})$ is the probability transitioning from state '0' to '1', when there are n dealer neighbors in the neighborhood.

$$f_{0 \rightarrow 1} = (1 - \delta_{ca}) \left(\sum_{n=1}^{|N|} \binom{|N|}{n} [(1-p-q)]^n (p+q)^{|N|-n} 1 - (1 - \alpha_{ca})^n q \right). \quad (6.22)$$

This sum can be evaluated using the *Binomial theorem*:

6.10.1 Binomial Theorem

Recall the binomial Theorem:

$$(x+y)^n = \sum_{k=0}^n \binom{n}{k} x^k y^{n-k},$$

for any real numbers x, y and any positive integer n . Here, $\binom{n}{k} = \frac{n!}{k!(n-k)!}$. Now we have the following:

$$\begin{aligned}
f_{0 \rightarrow 1} &= q(1 - \delta_{ca}) \left[\sum_{n=1}^{|N|} \binom{|N|}{n} (1-p-q)^n (p+q)^{|N|-n} [1 - (1 - \alpha_{ca})^n] \right] \\
&= q(1 - \delta_{ca}) \left[\sum_{n=1}^{|N|} \binom{|N|}{n} (1-p-q)^n (p+q)^{|N|-n} - \right. \\
&\quad \left. \sum_{n=1}^{|N|} \binom{|N|}{n} (1-p-q)^n (p+q)^{|N|-n} (1 - \alpha_{ca})^n \right] \\
&= q(1 - \delta_{ca}) \left((1 - (p+q)^{|N|}) - \left(((1-p-q)(1 - \alpha_{ca}) + (p+q))^{|N|} - (p+q)^{|N|} \right) \right) \\
&= q(1 - \delta_{ca}) \left(1 - ((1-p-q)(1 - \alpha_{ca}) + (p+q))^{|N|} \right) \\
&= q(1 - \delta_{ca}) \left(1 - (1 - \alpha_{ca}(1-p-q))^{|N|} \right) \tag{6.23}
\end{aligned}$$

Since:

$$\begin{aligned}
(1 - \alpha_{ca}(1-p-q))^{|N|} &= \sum_{i=0}^{|N|} \binom{|N|}{i} (1)^{|N|-i} (-\alpha_{ca}(1-p-q))^i \\
&= 1 - N\alpha_{ca}(1-p-q) + \dots
\end{aligned}$$

Thus, the equation in (6.23) becomes:

$$f_{0 \rightarrow 1} = Nq\alpha_{ca}(1 - \delta_{ca})(1-p-q)$$

Similarly, we consider $z = |\{j \in N_i | \sigma_j(t) = 2\}|$ be the number of dealers (type ‘2’) in the neighborhood. We let $P_n = \mathbf{prob}(\sigma_i(t+1) = 2 | z = n)$ be the probability that a given site which has value ‘1’ will have value ‘2’ at time $t+1$. In another words P_n is the probability transiting from light users to dealers under the influence of dealers. So, the probability that a light user becomes a dealer under the influence of at least one dealer neighbor is:

$$P_n = 1 - (1 - \beta_{ca})^n p.$$

Thus, $\zeta(t+1)$ is the probability of finding $\sigma = \text{‘2’}$ at time $(t+1)$ is given by:

$$\zeta(t+1) = f[\zeta(t)] = \sum_{n=1}^{|N|} \binom{|N|}{n} [(1-p-q)^n (p+q)^{|N|-n} 1 - (1 - \alpha_{ca})^n] q.$$

It follows that $\zeta(t+1) \cdot (1 - \delta_{ca})$ is the probability transitioning from state '1' to '2' at time $(t+1)$, when there are n dealer neighbors in the neighborhood.

$$f_{1 \rightarrow 2} = (1 - \delta_{ca})p \sum_{n=1}^{|N|} \binom{|N|}{n} [(1-p-q)]^n (p+q)^{|N|-n} [1 - (1 - \beta_{ca})^n].$$

So, we evaluate this sum using the binomial theorem in 6.10.1:

$$\begin{aligned} f_{1 \rightarrow 2} &= p(1 - \delta_{ca}) \left[\sum_{n=1}^{|N|} \binom{|N|}{n} (1-p-q)^n (p+q)^{|N|-n} [1 - (1 - \beta_{ca})^n] \right] \\ &= p(1 - \delta_{ca}) \left[\sum_{n=1}^{|N|} \binom{|N|}{n} (1-p-q)^n (p+q)^{|N|-n} - \right. \\ &\quad \left. \sum_{n=1}^{|N|} \binom{|N|}{n} (1-p-q)^n (p+q)^{|N|-n} (1 - \beta_{ca})^n \right] \\ &= p(1 - \delta_{ca}) \left((1 - (p+q)^{|N|}) - \left(((1-p-q)(1 - \beta_{ca}) + (p+q))^{|N|} - (p+q)^{|N|} \right) \right) \\ &= p(1 - \delta_{ca}) \left(1 - ((1-p-q)(1 - \beta_{ca}) + (p+q))^{|N|} \right) \\ &= p(1 - \delta_{ca}) \left(1 - (1 - \beta_{ca}(1-p-q))^{|N|} \right) \end{aligned} \tag{6.24}$$

Since:

$$\begin{aligned} (1 - \beta_{ca}(1-p-q))^{|N|} &= \sum_{i=0}^{|N|} \binom{|N|}{i} (1)^{|N|-i} (-\beta_{ca}(1-p-q))^i \\ &= 1 - N\beta_{ca}(1-p-q) + \dots \end{aligned}$$

Thus the equation in (6.24) becomes:

$$f_{1 \rightarrow 2} = Np\beta_{ca}(1 - \delta_{ca})(1 - p - q)$$

So we have:

$$f_{0 \rightarrow 1} = Nq\alpha_{ca}(1 - \delta_{ca})(1 - p - q), \quad f_{1 \rightarrow 2} = Np\beta_{ca}(1 - \delta_{ca})(1 - p - q)$$

We have computed the probability transitions $f_{0 \rightarrow 1}$ and $f_{1 \rightarrow 2}$. Note that the probability transitions of $f_{1 \rightarrow 0}$ and $f_{2 \rightarrow 0}$ are given by the equations (6.4) and (6.5). So we substitute them in to the following system of equations, which are the time evolution of densities:

$$\begin{aligned}\frac{d\mu}{dt} &= (f_{1 \rightarrow 0} + f_{2 \rightarrow 0}) - (f_{0 \rightarrow 1}) \\ \frac{d\rho}{dt} &= (f_{0 \rightarrow 1}) - (f_{1 \rightarrow 0} + f_{1 \rightarrow 2})\end{aligned}$$

$$\begin{aligned}\frac{d\mu}{dt} &= \delta_{ca}(1 - q) - Nq\alpha_{ca}(1 - \delta_{ca})(1 - p - q). \\ \frac{d\rho}{dt} &= N[q\alpha_{ca}(1 - \delta_{ca})(1 - p - q)] - \delta_{ca}p - N[p\beta_{ca}(1 - \delta_{ca})(1 - p - q)]\end{aligned}\quad (6.25)$$

The system of equations in (6.25) are the mean field approximation (MFA) for the n-D PCA model. We expand the equation and collect the terms:

$$\frac{d\mu}{dt} = \delta_{ca}(1 - q) - N[(1 - \delta_{ca})\alpha_{ca}q(1 - p - q)].\quad (6.26)$$

$$\frac{d\rho}{dt} = N[\alpha_{ca}(1 - \delta_{ca})(q - pq - q^2)] - \delta_{ca}p - N[\beta_{ca}(1 - \delta_{ca})(p - p^2 - pq)]\quad (6.27)$$

We collect the terms with q 's in 6.26 and 6.27 and we obtain the following system of equations:

$$\begin{aligned}\frac{d\mu}{dt} &= \delta_{ca} - [\delta_{ca} + N(1 - \delta_{ca})\alpha_{ca}]q + N[(1 - \delta_{ca})\alpha_{ca}]q^2 + N[(1 - \delta_{ca})\alpha_{ca}]pq. \\ \frac{d\rho}{dt} &= (-\delta_{ca} - N(\beta_{ca}(1 - \delta_{ca}))p + N[\alpha_{ca}(1 - \delta_{ca})]q - [N\alpha_{ca}(1 - \delta_{ca}) - N\beta_{ca}(1 - \delta_{ca})]pq \\ &\quad - N[\alpha_{ca}(1 - \delta_{ca})]q^2 + N[\beta_{ca}(1 - \delta_{ca})]p^2\end{aligned}\quad (6.28)$$

We let $\tilde{\delta}_{ca} = \delta_{ca}$, $\tilde{\alpha}_{ca} = N[\alpha_{ca}(1 - \delta_{ca})]$ and $\tilde{\beta}_{ca} = N[\beta_{ca}(1 - \delta_{ca})]$ in the equation (6.28). Now the system of equation becomes:

$$\begin{aligned}\frac{d\mu}{dt} &= \tilde{\delta}_{ca} - (\tilde{\delta}_{ca} + \tilde{\alpha}_{ca})q + \tilde{\alpha}_{ca}pq + \tilde{\alpha}_{ca}q^2 \\ \frac{d\rho}{dt} &= \tilde{\alpha}_{ca}q - (\tilde{\delta}_{ca} + \tilde{\beta}_{ca})p - \tilde{\alpha}_{ca}q^2 + \tilde{\beta}_{ca}p^2 + (\tilde{\beta}_{ca} - \tilde{\alpha}_{ca})pq\end{aligned}\tag{6.29}$$

Remark 2. *The compartmental model equations in (6.13) are the same as the mean field approximation equations in (6.29) provided that we drop third or higher order terms in densities. We then make the following identifications: $x \leftrightarrow \mu$, $y \leftrightarrow \rho$, $\delta = \delta_{ca}$, $\tilde{\alpha}_{cm} = N\alpha_{ca}(1 - \delta_{ca})$, and $\tilde{\beta}_{cm} = N\beta_{ca}(1 - \delta_{ca})$.*

Thus, we have proved the following theorem:

Theorem 6.10.1. *Compartmental model equations are corresponding to the mean field approximation for the CA model with n nearest neighbors if:*

- (i) *Drop terms of 3rd or higher order in densities.*
- (ii) *Equate the forms of the coefficients:*
 - $x \leftrightarrow \mu$, $y \leftrightarrow \rho$, and $\delta = \delta_{ca}$,
 - $\tilde{\alpha}_{cm} = n\alpha_{ca}(1 - \delta_{ca})$ and $\tilde{\beta}_{cm} = n\beta_{ca}(1 - \delta_{ca})$.

Remark 3. *Notice that the system of equations in (6.29) are the same as system of equations in (6.18) which we obtained from the MFA for 1-D CA model. So, the bifurcation theory and stability analysis for the fixed points, which we performed for the ODE model (6.13) in Section 6.6 works for the system equations in (6.29) as well.*

Next chapter is a summary of important findings of this project.

Chapter 7

Conclusion and Discussion

Our observations in this project show that the social influence can dramatically affect the spread of drug use in the community. We should point out here that our results not only come from cellular automata (CA) simulations, but also from a deterministic system which provides a good approximations for predicting drug use epidemic. By modeling the interaction among individuals, we are able to understand the role of social influence in this dynamics without the need for complex mathematical methods. Whether an individual can successfully be convinced to begin or persist dug use in the long term depends on the interactions that exist in the neighborhood. In the following, we identify the main result of this project.

To summarize, from simulating the interaction among individuals who are randomly distributed in a lattice, we identify different effects of the parameters in the model. Although the short term behavior of the model may depend on the lattice size and details of the spatial distribution, the long term behavior mainly depends on three parameters: the social influences of dealer on susceptibles (α_{ca}), on drug users (β_{ca}), and life expectancies (δ_{ca}).

We change parameters α_{ca} and β_{ca} , which we believe can affect the spread of drug use in the community. Reduction for α_{ca} can be viewed as the indirect strategy (health promotion) and reducing β_{ca} implies the direct strategy (police involvement). The bifurcation curve in Figure 7.1 demonstrates that reduction for α_{ca} and β_{ca} is effective on their own but reducing

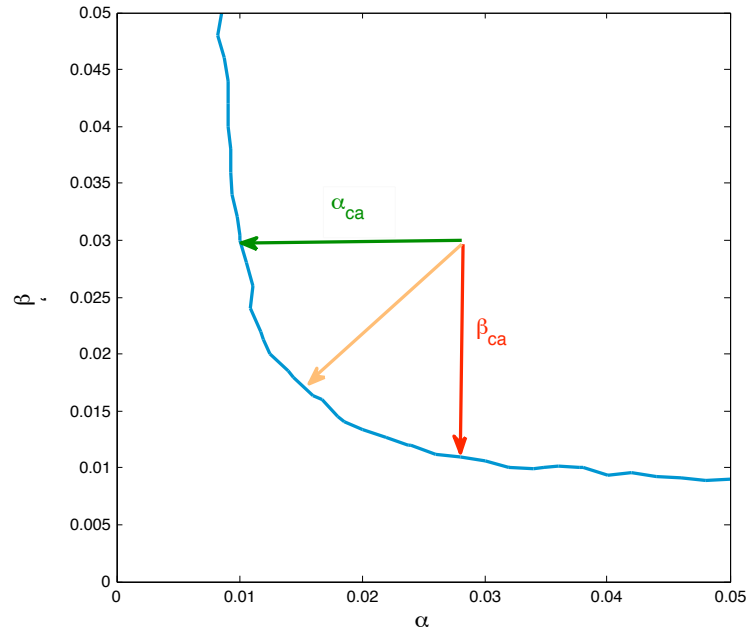


Figure 7.1: The effect of combined strategies

both simultaneously results in faster transitions to the drug free state. In other words the combination of the indirect and direct strategies are shown to be most effective (see Section 5.9 for more details).

The simulation results for 1-D and 2-D cellular automata corresponds to the input neighborhood sizes of $N = 2$ and $N = 4$, respectively. The comparison between the two CA models provide interesting results. It shows that an individual who has more number of dealers in the neighborhood is more likely to experiment drug use. We also compare the phase diagram and the time evolution plot of both 1-D and 2-D CA and conclude that the less social influences in smaller neighborhood will result in a lower need for intervention.

Inexact representation of something that is still close enough to be useful, is called an approximation [51]. If incomplete information prevents the use of exact representations then the approximations are used. Social issues are generally too complex to solve analytically. Thus, an approximation may yield a sufficiently accurate solution while reducing the complexity of the problem significantly.

Due to the complexity of the interactions among drug users, it is difficult to exactly analyze the impact of the social influences on drug use spread in the model. So an approximate solution is obtained by performing the mean field approximation (MFA) for the CA model. MFA results are used as a point of comparison for the CA model. The comparison is between the analytical results from the mean field analysis and simulation results for the CA model. We use the result of the theorems proved in this thesis to show that the MFA up to second degree in densities gives a good picture of CA model near the bifurcation.

Mean field approximation generally provides a good estimation on limiting densities and other properties of the cellular automata. The estimation for the limiting density is usually within 10 – 20% error. We found that the mean field approximation estimates the limiting density of a CA correctly with the general rules 4.5.1 and fails to do so with the asymmetric rules (see Section 4.10).

7.1 Future work

As mentioned in the introduction, in this project we have only considered three states which are susceptible, light user and dealer in the model. There are other states such as clients of the health care services, recidivist drug users and no users (temporary) that need to be taken in to account in order to accurately determine the prevalences. In addition to including these states, the transitions between these states also needs to be considered. Moreover, in this project, we assume that the rate of change in the population is zero to simplify the complexity. In the next phase of this project, we will consider a non constant population to make the model more realistic. Finally, we further need to investigate the policy by which the drug use interventions are applied to the communities and suggest policies based on our findings to authorities.

Appendix A

Cellular Automata and Elementary Rules

We have simulated and reproduced some of the one dimensional space-time pattern of a few elementary legal rules for $k = 2$, $r = 1$ in [24]. Some starting from an initial state consisting of a single nonzero value at the center site (see Figures A.1, A.2) and some with random initial condition (see Figure (A.3, A.4). By convention, the time axis runs from top to bottom and sites with value $\sigma_i = 1$ are colored white.

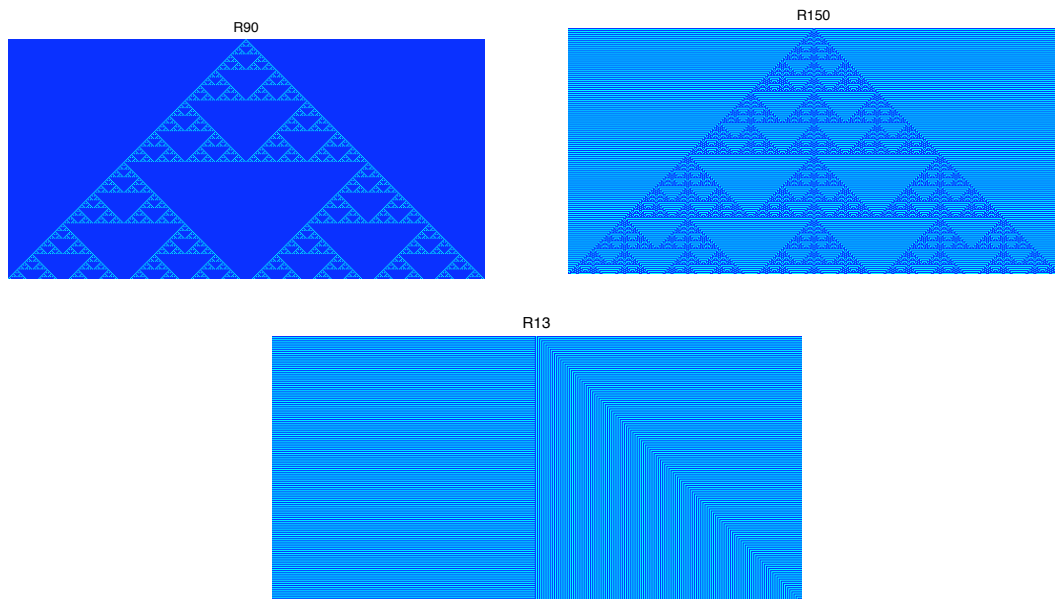


Figure A.1: Space-time pattern of a few elementary legal rules for $k = 2$, $r = 1$, an initial state with of a single nonzero value.

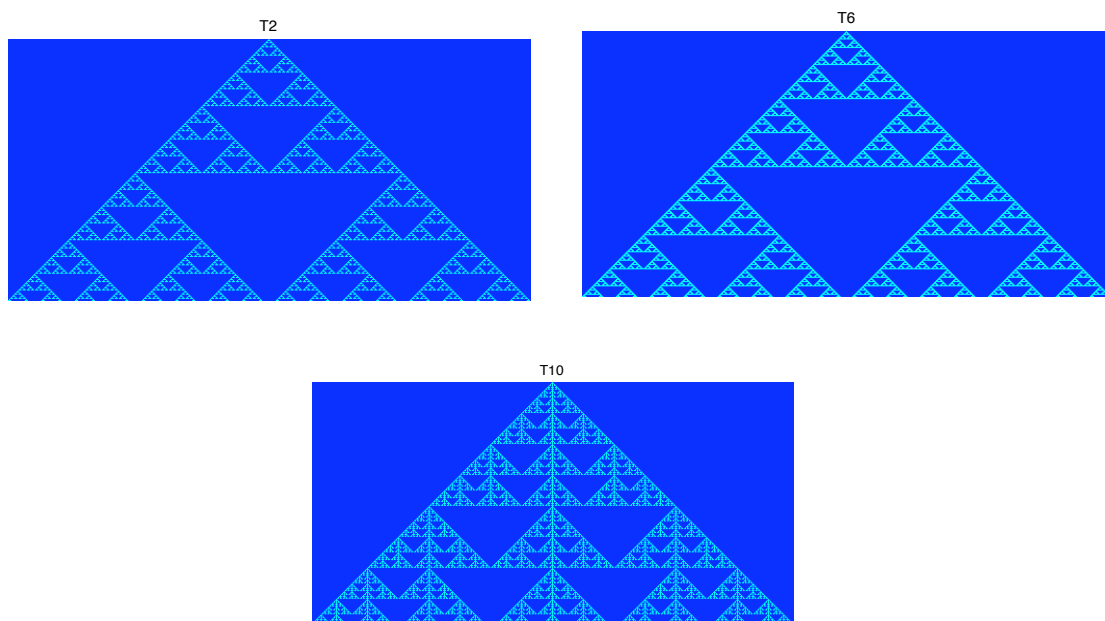


Figure A.2: Space-time pattern of a few totalistic rules for $k = 2$, $r = 1$, an initial state with of a single nonzero value.

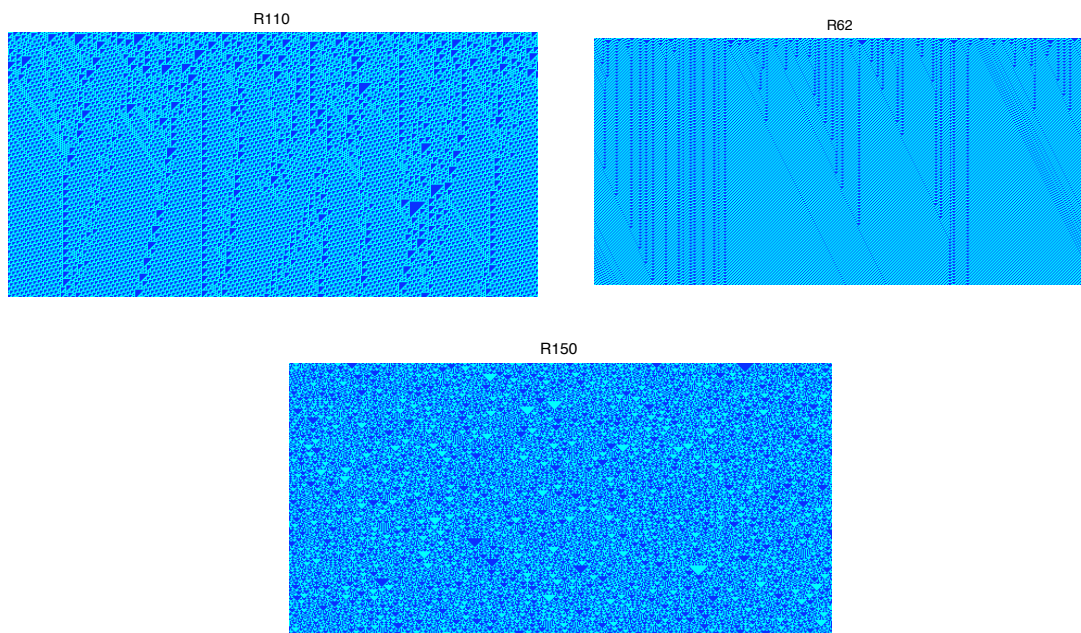


Figure A.3: Space-time pattern of a few elementary legal rules for $k = 2$, $r = 1$, with random initial condition.

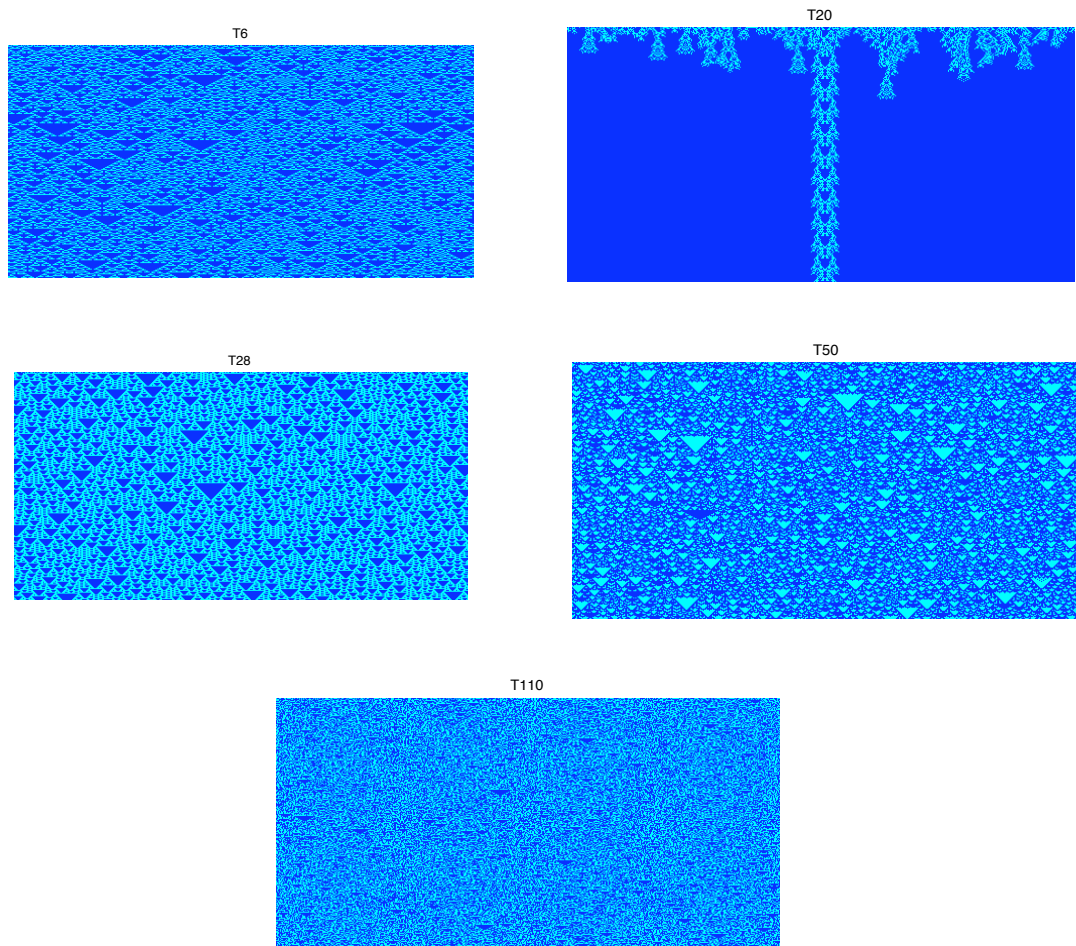


Figure A.4: Space-time pattern of a few totalistic rules for $k = 2$, $r = 2$, with random initial condition.

Bibliography

- [1] Shane PG. What about Americas Homeless Children? Hide and Seek. Thousand Oaks, CA: Sage, 1996.
- [2] Ringwalt CL, Greene JM, Robertson M, McPheeters M. The prevalence of home-lessness among adolescents in the United States. The *Am J Pub Health* (1998); 88: 1325.
- [3] Embalch H. A one-way street? A report on phase I of the street children project. Geneva, Switzerland: The *World Health Organization Program on Substance Abuse*, (1993).
- [4] Werb D, Kerr T, Li K, Montaner J, and Wood E. Risks surrounding drug trade involvement among street-involved youth, The *American Journal of Drug and Alcohol Abuse*, (2008); 34(6): 810-1820.
- [5] Carla Rossi, Operational models for epidemics of problematic drug use: the Mover-Stayer approach to heterogeneity, The *Socio-Economic Planning Sciences* 38 (2004) 73-90.
- [6] Hadeler KP. Modeling AIDS in structured populations. In: Proceedings of I.S.I. 47th Session. The *International Statistical Institute*, Paris, (1989). p. 83-99.
- [7] Jacquez JA, Simon CP, Koopman J, Sattenspiel L, Perry T. Modeling and analyzing HIV transmission: The *effect of contact patterns*. *Mathematical Biosciences* (1988);92:119-99.
- [8] Bailey NTJ. A revised assessment of the HIV/AIDS incubation period, assuming a very short early period of high infectivity and using only San Francisco public health data on prevalence and incidence. The *Statistics in Medicine*,(1997);16:2447-58.

- [9] Fischer B, Medved W, Kirst M, Rehm J, Gliksman L. Illicit opiates and crime: Results of an untreated user cohort study in Toronto. The *Can J Criminol/Rev Can Criminol* (2001); 43:197-217.
- [10] Sherman SG, Latkin CA. Drug users involvement in the drug economy: Implications for harm reduction and HIV prevention programs. The *J Urban Health* (2002); 79:266-277.
- [11] DeBeck K, Shannon K, Wood E, Li K, Montaner J, Kerr T. Income generating activities of people who inject drugs. The *Drug Alcohol Depend*, (2007); 91:50-56.
- [12] Hegselmann R and Flache A. Understanding complex social dynamics: a plea for Cellular automata based modeling. *Journal of Artificial Societies and social Simulation*(1998); 1(3).
- [13] Coobs R.W, Collier a.C, Allain J.P, Nikora B, Leuther M, Gjerset G. F, and Corey L. Plasma viremia in human immunodeficiency virus infection. *New England Journal of Medicine*(1989); 321: 1626-1631.
- [14] Dabbaghian V, Vasarhelyi K, Richardson N and Borwein P, Rutherford A.R. The Impact of Social Interactions on the Spread of HIV Infection among Injection Drug Users: A Cellular Automaton Model. *Advances in Complex Systems World Scientific Publishing Company*.
- [15] Dabbaghian V, Spicer V, Singh S.K, P Borwein, P Brantingham. The Social Impact on the Drug Crime Nexus: A Cellular Automata Model. *private communication*.
- [16] Chopard B, Luthi P.O, Queloz P-A. Cellular Automaton Model of Car Traffic in a two-dimensional Street Network. *Journal of Physics A: Mathematical and General*,(1996); 29:2325-2336.
- [17] Batty M. Cities and Complexity: Understanding Cities with Cellular Automata, Agent-Based Models, and Fractals. *Journal of Regional Science*,(2007), 4 no 3;624-627.
- [18] Manzoni P, Fisher B, Rehm J, Local drug crime dynamics in a Canadian multi site sample of untreated opioid users, *it Canadian Journal of Criminology and Criminal Justice* (2007);49 no 3: 341-373.

- [19] Van Ballegooijen W.M and Boerlijst M.C, Emergent trade-offs and selection for outbreak frequency in spatial epidemics. *Proc. Nat. Acad. Sci.* (2004); USA 101,18246.
- [20] Liu Q.X, Wang R and Jin Z. Persistence, extinction and spatio-temporal synchronization of SIRS spatial models. *Journal of Statistical Mechanics: Theory and Experiment*; (2009)- p.7007.
- [21] Benyoussef A, El HafidAllah N, ElKenz A, Ez-Zahraouy H, M. Loulidi. Dynamics of HIV infection on $2D$ cellular automata. *PhysicaA*; (2003), 322, 506-520.
- [22] Eslahchi C, Pezeshk H, Sadeghi M and Dabbaghian V. A probabilistic Model for the Spread of HIV Infection among Injection Drug Users.
- [23] Perko L. Differential Equation and Dynamical System: *Springer-Vellag, New york, Inc.* (2001); 3rd. ed.
- [24] Ilachinski A. Cellular Automata. Discrete Universe ,River Edge, NJ: *World Scientific Publishing co., Inc*; (2001).
- [25] Wolfram S. A New Kind of Science. *Champaign, IL: Wolfram Media*; (2002).
- [26] Strogatz S.H, Nonlinear Dynamics and Chaos. with application to physics, biology, chemistry, and Engineering. *Perseus Books Publishing, LLC*; (1994).
- [27] Bronson R & Naadimuthu G, Operations Research. The McGraw-Hill companies, Inc; (1997).
- [28] Hegselmann R. and Flache A. Understanding Complex Social Dynamics: A Plea For Cellular Automata Based Modelling. *Journal of Artificial Societies and Social Simulation*, (1998); vol. 1, no. 3.
- [29] Boccara, N., and Cheong, K. Critical behaviour of a probabilistic automata network SIS model for the spread of an infectious disease in a population of moving individuals. *Journal of Physics A: Mathematical and General.* 26, 5 (1993), 3707-3717.
- [30] Boccara, N, Cheong, K., and Oram, M. A probabilistic automata network epidemic model with births and deaths exhibiting cyclic behaviour. *Journal of Physics A: Mathematical and General.* 27 (1994), 1585-1597.

- [31] Duryea, M, Caraco, T., Gardner, G., Maniatty, W., and Szymanski, B. K. Population dispersion and equilibrium infection frequency in a spatial epidemic. *Physica D* 132, 4 (1999), 511-519.
- [32] Kleczkowski A, and Grenfell, B. T. Mean-eld-type equations for spread of epidemics: The small world model. *Physica A*. 274, 1-2 (1999), 355-360.
- [33] S Jenkins, An Introduction to Solid State Many-Body Theory. *The Many Body Problem and Density Functional*.
- [34] Fu S, Modeling Epidemic Spread using Cellular Automata , *A report submitted for the Department of Computer Science and Software Engineering, The University of Western Australia*; (2002).
- [35] Stewart J, Calculus, Brooks/Cole: *A Division of Thomson Learning, Inc.* (2003).
- [36] Modelling of Complex Social Systems. Mocssy, IRMACS center. Simon Fraser University.
- [37] United Nations World Drug Report *An In-Depth Look into Global Drug Trends*, VIENNA, 25 June (2004).
- [38] Riley D, Drugs and Drug Policy in Canada: A Brief Review & Commentary *Canadian Foundation for Drug Policy & International Harm Reduction Association*.
- [39] Desrochesm F, Research on upped-level drug trafficking: A review, *Journal of Drug Issues*, vol 37 no 4 (2007), 827-844.
- [40] Kertzschar M and Wiessing L. G. Modeling the spread of HIV in social networks of injection drug users. *AIDS*, (1998);12:801-811.
- [41] Taylor A, Frischer M, Covell R. Reduction in needle sharing among injection drug users. *International conference AIDS* (1992); Jul 19-24.
- [42] Mathers B. M, Degenhardt L, Phillips B, Wiessing L, Hickman M, Strathdee S.A, Wodak A, Panda S, Tyndall M, Touk A, Mattick R. P, Global epidemiology of injecting drug use and HIV among people who inject drugs: a systematic review. *for the 2007 Reference Group to the UN on HIV and Injecting Drug Use: www.thelancet.com.* (2008); vol 372, November 15.

- [43] Des Jarlais D.C. Preventing HIV infection among injection drug users: Intuitive and counter- intuitive findings. *Applied & Preventive Psychology*, (1999); 8:63-70.
- [44] Maas B, Fairbairn N, Kerr T, Li K, Montaner J and Wood E. Neighborhood and HIV infection among IDU: place of residence independently predicts HIV infection among a cohort of injection drug users. *Health & Place* (2007);13, 432-439.
- [45] Christoff S & Kalache S, The Poorest Postal Code *The Dominion news from the grass-roots*. <http://www.dominionpaper.ca/articles/909>.
- [46] Packard N.H. Lattice Models for Solidication and Aggregation. *In First International Symposium for Science on Form*, (1986).
- [47] Schonsch B. Propagation of Fronts in Cellular Automata. *Physica D*, (2002); 80:433-450.
- [48] Galam S. Spontaneous Coalition Forming. Why Some are Stable. *In Proc. of Fifth International Conference on Cellular Automata for Research and Industry*, ACRI 2002, Switzerland,1-9, October (2002).
- [49] Hare W. L, Alimadad A, Dodd H, Ferguson R, & Rutherford A. A Deterministic Model of Home and Community Care Client Counts in British Columbia. *Health Care Management Science* (2009); 12(1), 80-99.
- [50] Tasoti V. Enhancement of environmental security by mathematical modelling and simulations of processes. *Strategies to Enhance Environmental Security in Transition Countries*, R. N. Hull et al. (eds.), 47-56. (2007) Springer.
- [51] Golub H.G & Charles F V. L. Matrix Computations - Third Edition. Baltimore: *The Johns Hopkins University Press* (1996). pp. 53. ISBN 0-8018-5413-X.
- [52] Berlekamp E. R, Conway J.H, Guy R.K, (2001-2004) *Winning Ways for your Mathematical Plays* (2nd ed.), *A K Peters Ltd*, ISBN 978-1-56881-130-7; ISBN 156881142X; ISBN 1568811438; ISBN 1568811446